Criticality Analyses of the Used and Spent Fuel Storage Facility of the 400 MW_{th} PBMR Plant

Anand Kaisavelu

Dissertation submitted in partial fulfilment of the requirements for the degree of M.Sc. in Nuclear Engineering at the Post-Graduate School of Nuclear Science and Engineering (Potchefstroom Campus)

Supervisor: Dr Hans Gougar

Centurion, August 2009

ABSTRACT

The development of the Pebble Bed Modular Reactor entails the design of numerous systems for various purposes. One such system of significant importance is the Sphere Storage System (a subsystem of the Fuel Handling and Storage system) where fuel spheres that are unloaded from the core will be stored until approximately eighty years after the power plant has been decommissioned.

Over and above the normal conventional safety analyses that one expects to be performed for any new system being designed, in the case of the Sphere Storage System a detailed Criticality Safety Analysis must be performed. The universally accepted Effective Neutron Multiplication Factor, k_{eff}, was used to indicate the margins of subcriticality for all the conditions modelled.

Since this Used and Spent Fuel storage facility is a Critical Safety-relevant system that will store nuclear fuel for a long time, it is required by regulation that the Criticality Safety Analyses be performed to verify whether this system will always remain “critical safe” (k_{eff} < 0.95) under all plausible conditions.

This study covers a variety of tasks, from the modelling of a single fuel sphere to modelling of the entire Sphere Storage System for the normal and various off-normal conditions, and for the determination of k_{eff} values for the system under these conditions. Additional models were also created to investigate the phenomena of clustering of low burnup fuel spheres and the effects of graphite spheres being mixed with the fuel spheres in the storage containers.

The entire study was done using the SCALE 5.1 computer code package. SCALE 5.1 is licensed by the United States Nuclear Regulatory Commission (US NRC) and is a package that is widely used in the US and around the world to perform criticality safety analyses as well as other nuclear-related calculations. For this study the control module CSAS6 was specifically used to develop the appropriate models because of its suitability for the modelling of pebble fuel and its advanced geometric modelling capabilities. It also automatically invokes the specific functional modules using the sequence CSAS26 in order to obtain the appropriate information as required by another functional module KENO-VI, which calculates k_{eff} for the specified input models.

The results from the models for the various scenarios representing normal and off-normal conditions show that the design of the proposed current design of the Sphere Storage System remains critical safe (k_{eff} < 0.95) for all the plausible scenarios considered. Any change to the current design requires new Criticality Safety Analyses to be performed. However, the methodology developed in this study can be used as a guide for future studies.

Declaration

I, the undersigned, hereby declare that the work contained in this project is my own original work.

_____

Anand Kaisavelu

Date: 14 August 2009

Centurion

Dedication

To the people from the community of Phoenix (in Durban, Kwa-Zulu Natal), where I grew up, it is my sincere hope and wish that you would achieve great things for yourselves, the community and our country

14 August 2009

Acknowledgments

My sincere thanks go out to the following people and organisations:

Dr Hans Gougar, my dissertation supervisor, for his patience, understanding and guidance during the duration of this study.

To all my friends, colleagues and family (especially my mum and dad), for their support whilst I was engaged in this task.

Mrs Sandra van der Merwe, who agreed to edit the dissertation on such short notice.

Mr Sanjay Premraj and Mr Vinnesh Singh for their assistance with drawing of the diagrams.

Pebble Bed Modular Reactor (Pty) Ltd, for presenting this opportunity to further my studies in terms of sponsorship and the use of their resources.

University of North-West (Potchefstroom), for their assistance during my studies and in developing an excellent, masters programme in Nuclear Engineering.

CONTENTS

ABBREVIATIONS **11**

1. INTRODUCTION **13**

1.1 BACKGROUND 13
1.2 GENERAL DESCRIPTION OF THE PBMR OPERATION AND SPHERE STORAGE SYSTEM [3] 15
1.3 MOTIVATION FOR THIS STUDY AND THE INTENDED OUTCOMES 20
1.4 LAYOUT OF THE DISSERTATION 22

2. SCALE 5.1 COMPUTER CODE PACKAGE [10] **23**

2.1 BRIEF HISTORY 23
2.2 CONTROL MODULE CSAS6 23
2.2.1 Purpose and Description 23
2.2.2 Implementation of the Criticality Safety Analyses Sequence 25
2.3 FUNCTIONAL MODULE KENO-VI 30
Purpose and Description 30
2.3.1 30
2.3.2 Theory: Monte Carlo Three-dimensional Multigroup Transport Equations 30

3. RESEARCH METHODOLOGY **37**

RESEARCH DESIGN 37
3.1 37
3.2 MODELLING ASSUMPTIONS 39
3.3 PROCESS AND FLOW OF THE MODELS 42

4. DEVELOPMENT OF THE MODELS USING CSAS6 ..... **49**

4.1 PROCEDURE TO MODEL FUEL SPHERES 49
4.2 PROCEDURE TO MODEL FUEL STORAGE CONTAINERS AND THE SPHERE STORAGE SYSTEM 51
4.3 INCORPORATION OF NORMAL AND OFF-NORMAL CONDITIONS INTO THE MODELS 55
4.4 MODIFICATION OF THE MOST CONSERVATIVE MODEL 57
4.4.1 Fresh Fuel (4.2 Weight Percent-Enriched) 57
4.4.2 Clustering 57
4.4.3 Failure of the Storage Containers 60
4.4.4 Inclusion of Graphite Spheres into the Fresh Fuel Model 60

5. RESULTS **61**

5.1 PRESENTATION OF THE RESULTS 61
5.1.1 Dry Storage Cells 61
5.1.2 Optimum Moderation of the Model (2 Dry Storage Cells at temperature 300 K with Packing Fraction of 0.66) with the largest k_{eff} 63
5.1.3 Wet Cell Storage 64
5.1.4 Optimum Moderation of the Model (1 Wet Storage Cell at Temperature 300 K with Packing Fraction of 0.66) with the Largest k_{eff} 66
5.1.5 1 Dry Storage Cell Adjacent to a Wet Storage Cell 67
5.1.6 Optimum Moderation of the Model (Wet-Dry Cell at temperature 300 K with Packing Fraction of 0.66) with the largest k_{eff} 69
5.1.7 Whole Model 70
5.1.8 Optimum Moderation of the Whole Model (All Cells at temperature 300 K with Packing Fraction of 0.66) with the largest k_{eff} 72
5.1.9 Fresh Fuel Spheres (4.2 w/o Enriched) 75
Graphite Spheres interspersed within Fresh Fuel Spheres (4.2 w/o enriched) 76
5.1.10 76
5.1.11 Graphite Spheres interspersed within Used Fuel Spheres from the Most Reactive Core 77
5.1.12 Optimum Moderation of the Low Burnup Cluster Model 78

5.2 DISCUSSION OF THE RESULTS 80

6. CONCLUSION 83

7. BIBLIOGRAPHY 84

8. APPENDIX: INPUT FOR THE SPHERE STORAGE SYSTEM (WHOLE MODEL AT TEMPERATURE OF 300 K WITH A PACKING FRACTION OF 0.61. WATER IS PRESENT ONLY IN THE WET CELLS, AIR IN THE DRY CELLS AND BETWEEN ALL THE FUEL SPHERES) 85

FIGURES

Figure 1: A TRISO Particle 16
Figure 2: A Fuel Sphere [4] 16
Figure 3: UFC in the Wet Storage Cell 18
Figure 4: SFC in the Dry Storage Cell 19
Figure 5: Steps for CSAS6 shown graphically 29
Figure 6: Actual Physical Layout of the SSS 41
Figure 7: Model of SSS using SCALE 5.1 41
Figure 8: Model of Wet Storage Cell 42
Figure 9: Model of Dry Storage Cell 43
Figure 10: Model of Low Burnup Fuel Clusters in UFC 46
Figure 11: Fuel Spheres being packed into the Storage Containers 52
Figure 12: Clusters of 6 Low Burnup Fuel Spheres 59
Figure 13: k_{eff} for Varying Water Densities showing Optimum Moderation (2 Dry Storage Cells) 63
Figure 14: k_{eff} for Varying Water Densities showing Optimum Moderation (2 Wet Storage Cells) 66
Figure 15: k_{eff} for Varying Water Densities showing Optimum Moderation (Wet-Dry Cell) 69
Figure 16: k_{eff} for Varying Water Densities showing Optimum Moderation (Whole Model) 72
Figure 17: k_{eff} Values for the Most Reactive Configuration of each Model Type 73
Figure 18: k_{eff} Values at Optimum Moderation for the Most Reactive Configuration of each Model Type 73
Figure 19: Maximum k_{eff} obtained at each Temperature Analysed 74
Figure 20: Maximum k_{eff} obtained for each Packing Fraction Analysed 74
Figure 21: Maximum k_{eff} obtained for Most Reactive Configuration of each type of Model when filled with 4.2 w/o Enriched Fresh Fuel 75
Figure 22: k_{eff} for Different Percentages of Graphite Spheres 77
Figure 23: k_{eff} for the Clusters in the Most Reactive Model Configuration at Varying Water Densities 78
Figure 24: k_{eff} of Fuel Spheres in a Storage Cell from 6 Burst Storage Containers at Varying Water Densities (Temperature of 300 K and a Packing Fraction of 0.61) 79

TABLES

Table 1: Functional Modules with Related Functions 24
Table 2: Normal and Off-Normal Events Modelled 47
Table 3: TRISO Particle Input Data 50
Table 4: Fuel Sphere Input Data 50
Table 5: Input Data used for Modelling Storage Containers 53
Table 6: Input Data used for modelling Sphere Storage System 54
Table 7: Number of Clusters of 1st Cycle Fuel Spheres for a given type of Cluster 58
Table 8: k_{eff} of Dry Storage Cells with Packing Fraction of 0.61 at Different Temperatures 61
Table 9: k_{eff} of Dry Storage Cells with Packing Fraction of 0.64 at Different Temperatures 62
Table 10: k_{eff} of Dry Storage Cells with Packing Fraction of 0.66 at Different Temperatures 62
Table 11: k_{eff} for Varying Water Densities (inside Containers) showing Optimum Moderation (2 Dry Storage Cells) 63
Table 12: k_{eff} of Wet Storage Cells with Packing Fraction of 0.61 at Different Temperatures 64
Table 13: k_{eff} of Wet Storage Cells with Packing Fraction of 0.64 at Different Temperatures 64
Table 14: k_{eff} of Wet Storage Cells with Packing Fraction of 0.66 at Different Temperatures 65
Table 15: k_{eff} for Varying Water Densities (inside containers) showing Optimum Moderation (1 Wet Storage Cell) 66
Table 16: k_{eff} of Wet-Dry Storage Cells with Packing Fraction of 0.61 at Different Temperatures 67
Table 17: k_{eff} of Wet-Dry Storage Cells with Packing Fraction of 0.64 at Different Temperatures 67
Table 18: k_{eff} of Wet-Dry Storage Cells with Packing Fraction of 0.66 at Different Temperatures 68
Table 19: k_{eff} for Varying Water Densities (inside containers) showing Optimum Moderation (Wet-Dry Cell) 69

Table 20: k_{eff} of Whole Model with Packing Fraction of 0.61 at Different Temperatures 70
Table 21: k_{eff} of Whole Model with Packing Fraction of 0.64 at Different Temperatures 70
Table 22: k_{eff} of Whole Model with Packing Fraction of 0.66 at Different Temperatures 71
Table 23: $k_{\mathbf{eff}}$ for Varying Water Densities (inside containers) showing Optimum Moderation (Whole Model) 72
Table 24: $k_{\mathbf{eff}}$ for the Most Reactive Configuration of Each Model Type when containing 4.2 w/o enriched Fresh Fuel 75
Table 25: $k_{\mathbf{eff}}$ for Different Percentages of Graphite Spheres amongst 4.2 w/o enriched Fresh Fuel .. 76
Table 26: $k_{\mathbf{eff}}$ for Different Percentages of Graphite Spheres amongst Fuel Spheres from the Most Reactive Core 77
Table 27: $k_{\mathbf{eff}}$ for the Clusters in the Most Reactive Model Configuration at Varying Water Densities inside Containers (Temperature at 300 K and Packing Fraction at 0.66) 78
Table 28: $k_{\mathbf{eff}}$ of Fuel Spheres in a Storage Cell from 6 Burst Storage Containers at Varying Water Densities (Temperature of 300 K and a Packing Fraction of 0.61) 79

ABBREVIATIONS

This list contains the abbreviations used in this document.

Abbreviation or Acronym	Definition
AVR	Arbeitsgemeinschaft Versuchsreaktor (German for *Jointly-Operated Prototype Reactor*)
BUMS	Burnup Measurement System
CSAS	Criticality Safety Analyses Sequence Control Module
CSAS6	Criticality Safety Analyses Sequence Control Module 6
CSAS26	Criticality Safety Analyses Sequence 26 used by CSAS6
DPP	Demonstration Power Plant
Eq	Equation
FHSS	Fuel Handling and Storage System
HTR	High Temperature Reactor
k_{eff}	Effective Neutron Multiplication Factor
KENO-VI	A functional module of CSAS6 using Monte Carlo methods for Calculation of the Effective Neutron Multiplication Factor, k_{eff}
Kernel	Ceramic Uranium Dioxide Fuel Particle
LWR	Light Water Reactor
MW_{th}	Megawatt Thermal (Unit of Power)
MWd/tU	Megawatt Days per Ton of Uranium (Indication of fuel burnup)
MPa	MegaPascal (Unit of Pressure)
n/a	not applicable
NaCl	Sodium Chloride
NNR	National Nuclear Regulator (RSA)
NSR	Nuclear Safety Relevant
ORNL	Oak Ridge National Laboratory
PBMR	Pebble Bed Modular Reactor
PBMR (Pty) Ltd	Pebble Bed Modular Reactor (Proprietary) Limited
PWR	Pressurised Water Reactor
RSICC	Radiation Safety Information Computational Center
SCALE	Standardized Computer Analyses for Licensing Evaluation
SF	Spent Fuel
SFC	Spent Fuel Container
SGGP	Scale Generalized Geometry Package
SiC	Silicon Carbide
SS304	Stainless Steel of Type 304
SSS	Sphere Storage System
THTR	Thorium High-Temperature Reactor

Abbreviation or Acronym	Definition
TRISO	Fuel Particle (kernel) enclosed by 3 layers of coating material
UFC	Used Fuel Container
UF	Used Fuel
US DOE	United States Department of Energy
US NRC	United States National Regulatory Commission
U-238	Uranium Isotope 238
VSOP	Very Sophisticated Old Program
w/o	Weight percent

DEFINITIONS

Term	Definition
Off-normal	Not normal or an accident
Under-moderated	A system is said to be under-moderated if the addition of a moderator adds positive reactivity
Load-shedding	The systematic switching off of electricity to predetermined areas and businesses during times when electricity supply is in shortfall
Common mode failure	It is assumed that all components/equipment of the same design and specifications fails simultaneously due to an event or fault

1. INTRODUCTION

1.1 BACKGROUND

South Africa is currently experiencing a shortage in electricity capacity as demand has grown much faster than generating capacity due to economic growth. Currently in South Africa, approximately ninety percent (90%) of the electricity is generated by coal-fired power stations. Hydroelectric dams, some with pumped storage facilities, 2 nuclear units, and open cycle gas turbines provide most of the remainder of the electricity quota. Electricity from wind turbines and solar cells is minimal. Although many desire that more of our electricity should be generated utilising renewable energy sources such as wind and solar energy, these technologies have limited generating capacity and are too unreliable to sustain a modern industrial economy. Currently wind, and especially solar-generated electricity, is much more expensive than other methods of electricity generation. Open cycle gas turbines are also very expensive to run and are only operated during periods of peak electricity demand when there is a shortage of electricity on the national grid.

The severe reduction in generating margin has resulted in frequent electricity load-shedding around the country and a reduction in industrial growth that is likely to have a devastating effect on the economy [1]. This has led government to take the decision to increase the electricity generating capacity in South Africa. The state-owned electricity provider, Eskom, is pursuing a rigorous new-build program, which ranges from the construction of conventional coal power stations all the way to nuclear power stations [2]. The nuclear new-build portion will consist of nuclear power stations procured from overseas suppliers (the forerunners being Areva and Westinghouse) and the local development of a high temperature gas reactor. The locally developed 400 MW_{th} high temperature gas reactor is known as the Pebble Bed Modular Reactor (PBMR). This reactor is being designed by the South African company Pebble Bed Modular Reactor (Pty) Ltd and is based on the design of the German Arbeitsgemeinschaft Versuchsreaktor (AVR) and Thorium High-Temperature Reactor (THTR) high temperature gas reactors.

It is hoped that the development of the PBMR will bolster South Africa's electricity supplies as the PBMR (Pty) Ltd Company intends to initially supply Eskom and then international markets with the PBMR technology. It is also anticipated that this nuclear power technology will have enormous economic benefits for South Africa over and above electricity production. It is estimated that the development and operation of the PBMR in South Africa will generate approximately 50 000 jobs directly and indirectly in the nuclear industry. It also has the

potential to generate billions of rands from foreign sales of the plant and from providing auxiliary and support services. It is hoped that pebble-bed HTR technology will boost the now developing South African nuclear industry to new heights, creating capabilities in terms of design and manufacturing of systems, structures and components for HTR. The fuel manufacturing capabilities that South Africa had will also be revived but it will now be directed to developing pebble bed fuel. The government is hoping that the impetus will continue to a stage where South Africa will develop a complete nuclear fuel cycle that creates even more jobs and drives further economic development. This is truly achievable as South Africa is currently one of the major producers of refined uranium with large reserves of natural uranium still available. The only part of the fuel cycle that provides a challenge is the development of new enrichment technology as the technology developed previously may not be economically viable.

The PBMR has the added advantage of high outlet temperatures, which makes it a prime candidate for the provision of process heat services to a variety of industries. Currently companies like Sasol and the Canadian Oil Sands have shown an interest in implementing this technology. Sasol currently burns fossil fuels to provide heat for its refining and liquid fuels manufacturing processes. To extend its supplies and to reduce emissions, it may now consider the PBMR as the source of this process heat.

The PBMR can also provide heat for desalination in arid or semi-arid regions that are blessed with neither an abundance of rainfall nor indigenous energy supplies. International pressure to reduce carbon dioxide emissions along with dwindling reserves of fossil fuels is generating interest in alternative fuels for heating and transportation. The PBMR with its high outlet temperatures makes it a potential candidate for emission-free hydrogen production. The procurement of PMBR technology by industries that rely heavily on coal utilisation for process heat and electricity will allow these companies to reduce their carbon footprint while still enjoying reliable and inexpensive energy supplies. In the long run, carbon credits accumulated can be a source of revenue for these companies if their credits are sold to other companies that are not doing well in terms of reducing carbon dioxide emissions.

Proponents of PBMR technology anticipate shorter construction times compared to Light Water Reactors (LWRs). Along with a smaller power output, the PBMR may be better suited for the smaller grids and growing markets of developing nations. Its modular nature allows more modules to be added to the initial one as the demand for electricity or process heat increases. Unlike coal-fired power stations that must be built close to the coal mines or next to dedicated railway lines that can continuously supply large amounts of fuel, the PBMR can be built closer to the large cities and industries where the load is really required. Light Water

Reactors (LWRs) also have limitations in terms of location because of the need for ample supplies of cooling water.

However, the main benefit that the PBMR has over other conventional nuclear reactor designs is that it is inherently safe when it comes to design-based accidents. Inherently safe refers to the ability of the reactor to shut down and reject excess heat passively without active safety systems or operator intervention. The PBMR is designed so that fuel temperatures cannot reach levels at which the fuel elements start to degrade and release harmful amounts of their radiological inventory. This very feature of inherent safety is what makes the PBMR technology so different from other reactors, especially PWRs, which require the use of redundant active safety systems to prevent a fuel meltdown even for design basis accidents. Passive safety will contribute to greater public acceptance of nuclear technology as well as reducing the capital costs of nuclear plants.

1.2 GENERAL DESCRIPTION OF THE PBMR OPERATION AND SPHERE STORAGE SYSTEM [3]

The key to the safety characteristics of the PBMR are the spherical fuel elements, each with a radius of 3 cm. These fuel spheres will consist of approximately 15 000 TRISO particles distributed randomly in a graphite matrix in a region with a radius of 2.5 cm and coated by a layer of graphite 0.5 cm thick. Each TRISO particle will consist of a uranium dioxide kernel enclosed by the following layers: the Buffer, followed by the Inner Pyrolytic Carbon, then the Silicon Carbide and lastly the Outer Pyrolytic Carbon layer. The Buffer layer, which is relatively soft compared to the other layers, is there to accommodate the changes in dimension of the kernel during the operation of the reactor and to absorb fission products. The dimensional changes result from expansion due to the swelling of the kernel by the high temperatures and the accumulation of fission products during reactor operation. The Inner Pyrolytic Carbon is used to prevent the release of most fission products. The Silicon Carbide is the layer that stops virtually all fission products and gases from leaving the TRISO particle. The Outer Pyrolytic Carbon serves as the final barrier should the Silicon Carbide protective layer fail.

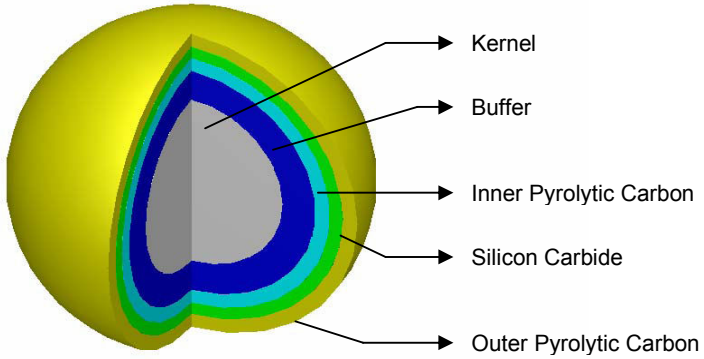

Figure 1: A TRISO Particle

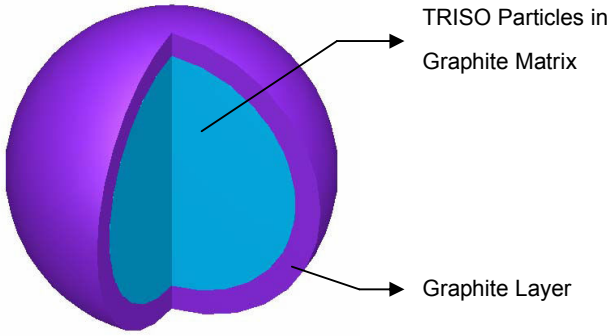

Figure 2: A Fuel Sphere [4]

During the initial start-up of the PBMR, the core will be filled with graphite spheres only. As the graphite spheres are removed from the bottom of the core, 4.2 w/o enriched Uranium-235 (U-235) fuel spheres will be added from the top. The reactor would be made critical and operate with an increasing number of these start-up fuel spheres as they are burned. Eventually the start-up fuel spheres will be replaced by 9.6 w/o enriched U-235 fuel spheres. Eventually all of the graphite and 4.2 w/o fuel will be replaced with 9.6 w/o spheres and the core power profile will achieve a state of equilibrium. From then on only 9.6 w/o enriched U-235 fuel spheres will be used to the end of life of the plant. Approximately 450 000 fuel spheres will be required to fill the core. Each fuel pebble will pass through the reactor approximately 6 times until it reaches the desired discharge burnup. The burnup of the fuel spheres coming out the core are estimated by performing spectrometric analyses of the fission product nuclides in the 500 to 700 keV energy regions by using the Burnup Measurement System (BUMS).

If the burnup of the fuel coming out of the core is approximately equal to the discharge burnup of 90 000 MWd/tU, it is discharged as Spent Fuel (SF). If the fuel spheres have not reached the desired burnup it is returned to the reactor to be re-circulated through the core. This process continues until the desired burnup is reached. However, all fuel that needs to be stored would not only be SF. Instances may arise during start-up or during steady state operation where the core may need to be unloaded. The fuel being unloaded will have a range of burnup, ranging from almost fresh to near the required discharge burnup. Hence, all fuel being unloaded from the core which has not reached the desired Spent Fuel burnup of approximately 90 000 MWd/tU is known as Used Fuel (UF).

The Sphere Storage System (SSS) forms part of the larger Fuel Handling and Storage System (FHSS) and fuel will be stored in the SSS during the life of the plant plus a further 80 years. The SSS is divided into two parts: the wet storage and the dry storage sections [5]. The wet storage section consists of two storage cells where the storage containers (Used Fuel Container) in each cell are stored in a three-by-two array under water. The dry storage section consists of 4 storage cells where the storage containers (Spent Fuel Containers) are also stored in a three-by-two array in each cell under normal atmospheric conditions. The dimensions and the material composition of the Spent Fuel Container (SFC) are exactly the same as the Used Fuel Container (UFC). Only the UFC from the wet storage section can be connected to the fuel handling system, which is under helium pressure during unload or reload operations. The pressure may range from 0.1 MPa to 1 MPa. In order to maintain balance of pressure, the UFCs are also under helium pressure. The fuel from the reactor cannot be directly unloaded into the SFC in the dry storage section. The SFC can only be filled from the UFC. The SFC is sealed in nitrogen gas at 0.1 MPa to preserve them by inhibiting corrosion.

As a result, all fuel spheres (Used and Spent Fuel) that come out of the core and that are diverted to the SSS will first be housed in the UFC which are under water in the wet storage section. All fuel coming out of the core will be producing large amounts of decay heat, which necessitates removal by the cooling water in the wet storage section and by a heat exchanger. Once the SF has lost most of its decay heat after about five or six years it will be transferred to the dry storage section for long term storage. The UF will always remain in the UFC in the Wet Storage Section for the life of the plant. In the dry fuel storage section, the storage containers are cooled by natural convection. The dry cells are designed in such a way that cooling by convection is enhanced by means of the ‘chimney effect’. After about five or six years the SF is transferred from the UFC to SFC. By this time the decay heat released by the spent fuel is low enough so that cooling by natural convection would be sufficient.

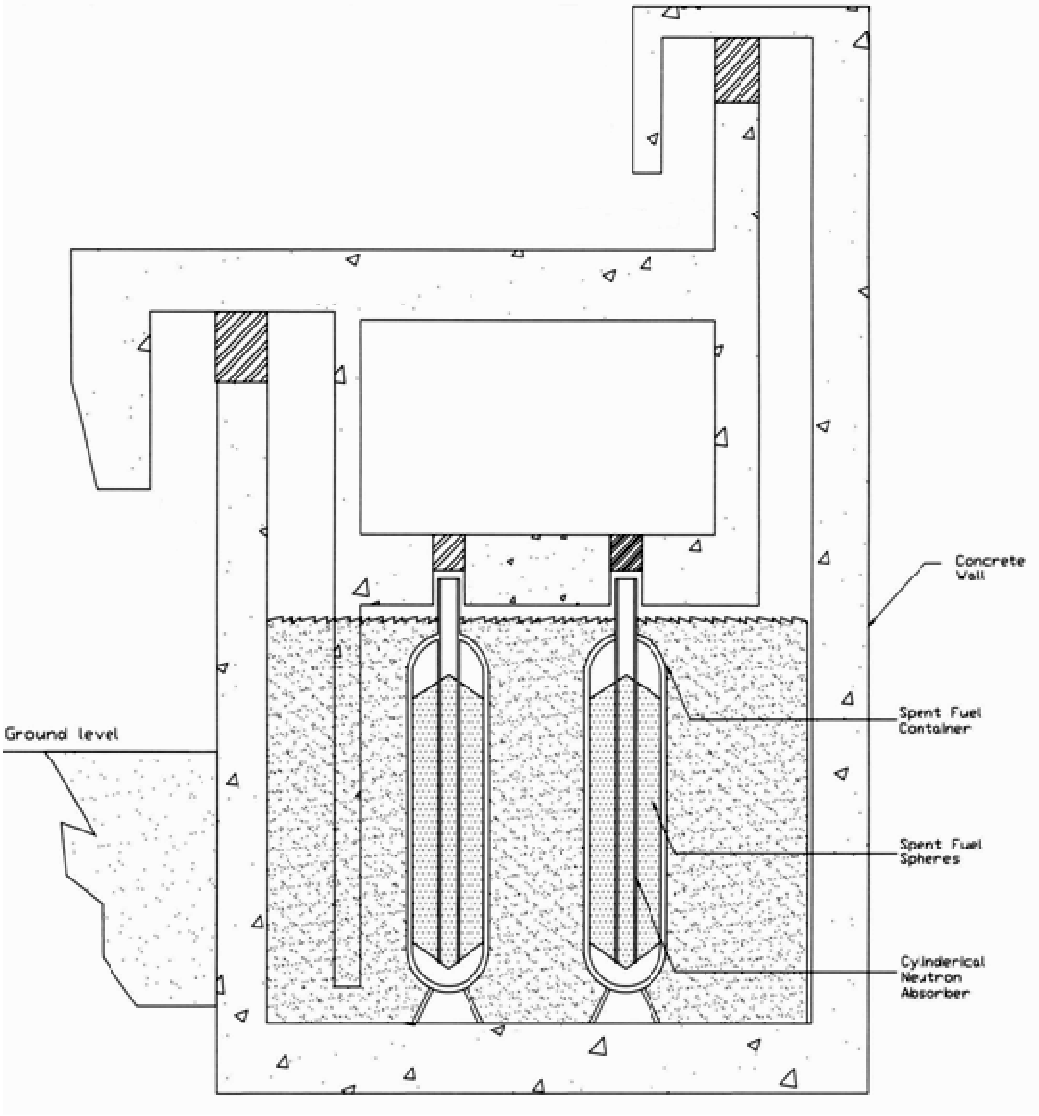

Figure 3: UFC in the Wet Storage Cell

Approximately five to six years after the power plant final shutdown the wet fuel storage cells would be converted to dry storage cells as there would be no further need for wet storage cooling. The fuel in the UFC will now be cooled by natural convection like the SFC.

Currently the fate of this fuel after about 80 years from the plant final shutdown is still undecided. Long-term disposal and reprocessing are under consideration for ultimate disposition. Reprocessing technology is a subject of significant research and much more development is expected to occur in the next hundred years. However, the decision to reprocess or to store the Used and Spent Fuel in an underground repository still needs to be determined by the relevant governmental and nuclear authorities.

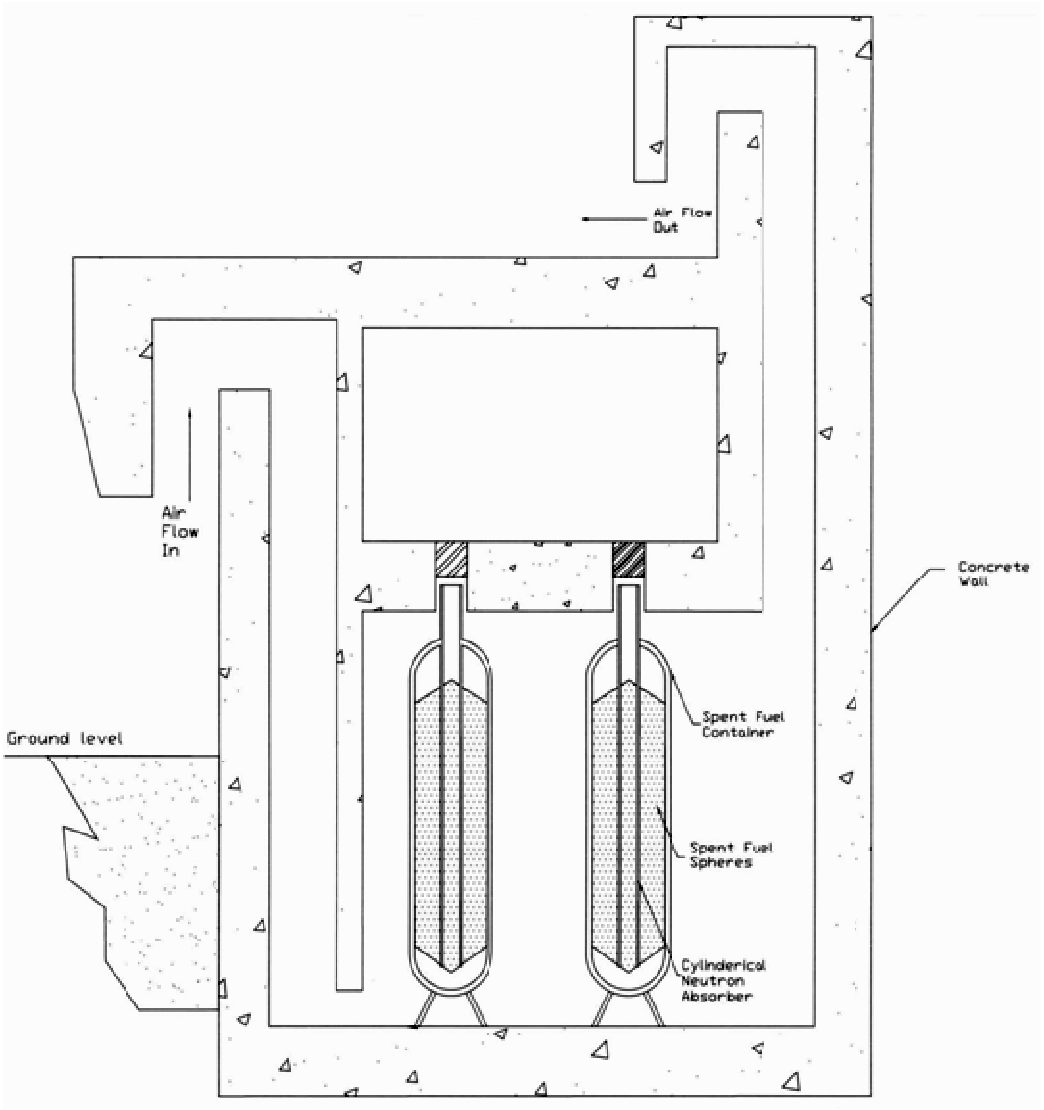

Figure 4: SFC in the Dry Storage Cell

The fuel storage facility will be situated along the interior circumferential wall of the PBMR building and it would consist of storage cells (six containers per storage cell) separated by concrete walls. At one end there would be the two cells containing the UFC and on the other, four storage cells containing the SFC. This results in 12 UFCs and 24 SFCs in total. Each container can hold as much as 175 000 fuel spheres. The FHSS (which includes SSS) of the PBMR reactor power plant is classified as an NSR system.

1.3 MOTIVATION FOR THIS STUDY AND THE INTENDED OUTCOMES

It is imperative from a nuclear safety point of view to ensure that all fissile material goes critical only in the reactor core in a controlled fashion. Fissile material (nuclear fuel) must be maintained critical safe ($k_{eff} \leq 0.95$) at all times and under all plausible conditions outside the core (including the SSS). It is important to note that any criticality event outside the core at a nuclear facility (including the SSS) is classified as a nuclear accident of variable degree according to the International Nuclear and Radiological Event Scale (INES) [6].

The current design of the SSS is intended for the use of storing fuel from the PBMR Demonstration Power Plant (DPP) that is planned at the Koeberg site in the Western Cape. In order for the SSS to be used for the storage of Used and Spent Fuel, it is imperative to provide proof that this system remains critical safe under all postulated scenarios that may arise during the period of fuel storage at this facility. It is also a regulatory requirement that a criticality safety analysis be done for all fuel storage facilities to determine the margins of subcriticality for licensing purposes. A study has not been done for the current design of the PBMR SSS before; therefore, the results of this study will contribute to the Safety Analyses Report.

Version 5.1 of the SCALE code has additional functionalities geared towards HTR compared to previous versions [7]. One such functionality is the ability to incorporate the heterogeneous structure of the fuel sphere during modelling. This results in more accurate modelling of the system and when combined with 3-dimensional analyses, provides more accurate results.

In addition to this, the effects of sphere clustering in the storage containers have also not been investigated for the current design of the SSS by PBMR, much less its international collaborators. The stochastic nature of pebble fuel loading and unloading into the storage containers allows for the possibility of clustering of fuel pebbles with low burnup (thus resulting in higher reactivity). The increase in reactivity impacts on criticality safety and is therefore an important phenomenon that requires investigation [8].

This study will range from the modelling of one fuel sphere to the entire storage facility and will include the performance of criticality analyses on these models for normal and off-normal conditions. There is much detail explaining how the models were set up, the assumptions made in the modelling, the conservatism built into the models and the reasoning behind the

choice of the off-normal scenarios chosen. The study develops a methodology illustrating how a criticality safety analysis can be performed for a spent fuel storage facility of an HTR in general, and the process that needs to be followed.

The more studies done to prove that the PBMR is safe in all respects will greatly enhance the licensability and financial viability of this new reactor type by gaining the acceptance of the public, government and investors. This growing acceptance will encourage government and investors to divert more capital into the project and increase the likelihood of success.

However, the ultimate aim of this study is to provide verification as to whether the fuel that has been through the core at least once is critical safe under normal and off-normal conditions when stored in the SSS of the PBMR [9]. If this is the case then the design would be considered safe to use in the construction of the PBMR DPP. If not, it would be clearly stated that the design is not critical safe under certain conditions and that it needs to be redesigned.

1.4 LAYOUT OF THE DISSERTATION

This dissertation consists of eight sections with the first section being the Introduction and the last section ending as the Appendix.

Section 1 briefly describes the current sources of electricity supply in South Africa and the need to increase power generating capacity due to growing demand. The PBMR is then introduced as a possible option for power generation with a general description given on its operation, type of fuel to be utilised and the design of the proposed Used and Spent Fuel storage system. The section ends by stating South Africa's intention to develop this technology and how a criticality safety analysis of the Used and Spent Fuel storage facility will contribute to the licensability of the PBMR in South Africa.

Section 2 provides information about the computer package SCALE 5.1 that was used for the study. It explains the capabilities of the code, the advantages it has over other versions, its appropriateness to pebble fuel modelling and the basic reactor theory used in the analyses.

Section 3 contains information about the different models of the SSS that need to be developed in order to complete the study and the reasoning behind the choice of these models. It also describes the assumptions that were made during the modelling process and the impact on the criticality safety analyses to be performed.

Section 4 provides a detailed description of how the various components that makes up the SSS were actually modelled using SCALE 5.1. It describes how the separately modelled components were assimilated to develop the whole model of SSS.

Section 5 is where all the results of the criticality safety analyses are presented for all the models developed during the study. It contains information about trends observed and comparisons made between the results of the various models analysed.

Section 6 contains summaries of the results and demonstrates that the proposed Used and Spent Fuel storage facility of the PBMR is critical safe under all plausible scenarios. It also contains suggestions for further work that may be undertaken.

2. SCALE 5.1 COMPUTER CODE PACKAGE [10]

2.1 BRIEF HISTORY

The involvement of ORNL with the development and maintenance of SCALE started off initially by providing staff at the US Department of Energy (DOE) with support in criticality and shielding analyses. The US DOE staffs was then transferred to the US NRC and they found that occasional use of those calculation codes made it difficult to become proficient in them as required in order to perform calculations for independent reviews. The US NRC then tasked ORNL to incorporate the individual codes that they were using into an easy-to-use analysis system comprising of control and functional modules. This was achieved by developing an input format, using well-established codes and data libraries and creating control modules (standard analysis sequences) that would automatically use functional modules (multiple codes) and other data to do system analyses. This resulted in the birth of the SCALE computer code package. The RSICC department within ORNL is currently responsible for further development and maintenance of SCALE.

2.2 CONTROL MODULE CSAS6

2.2.1 Purpose and Description

Although SCALE 5.1 has numerous control modules, only the control module CSAS6 was used for all the modelling and analyses in this study. CSAS6 was specifically developed for the functional module KENO-VI because of conflict that exists due to differences in the geometry package of KENO-VI and the other CSAS control modules available. As CSAS6 is the latest in the series of CSAS control modules, it has additional functionalities such as automatic problem-dependent cross-section processing, modelling of complex geometries and the capability to perform three-dimensional Monte Carlo analyses to obtain the Effective Neutron Multiplication Factor, k_{eff}, for a given system using the functional module KENO-VI.

CSAS6 provides the platform that allows the user to model the entire system under consideration and then performs the criticality calculation to determine k_{eff}. The functional modules with their related functions are listed in Table 1 below:

Table 1: Functional Modules with Related Functions

Functional Modules	Functions
BONAMI	Resonance self-shielding calculations (for nuclides with Bondarenko data related to their cross-sections)
NITAWL	Nordheim resonance self-shielding correction. (Applied to the nuclides that have resonance parameters)
WORKER	Creates an AMPX working format library from the master format library
CENTRM	Creates a pointwise continuous flux spectrum by using the pointwise continuous cross-section library and a cell description
PMC	Collapses pointwise continuous cross sections to a set of multigroup cross sections by using the pointwise continuous flux spectrum created in CENTRM
XSDRNPM	Calculates cell-weighted cross-sections for a specified cell. It can also calculate Effective Multiplication Factor, k_{eff}, for a 1-dimensional system
ICE	Creates a mixed cross-section library in the Monte Carlo format for use by KENO-VI
CHOPS	Creates homogenized point cross sections by computing pointwise flux disadvantage factors
CAJUN	Combines homogenized point cross-section libraries
WAX	Creates a combined working library of the homogenized cross sections
AJAX	Removes unused mixtures from the final master library
KENO-VI	Uses the Monte Carlo method to calculate k-effective of a three-dimensional system

The fuel sphere in this study is modelled as a double-heterogeneous cell. The first level of heterogeneity is the kernels in the graphite matrix and the second level of heterogeneity the pebbles in the container.

2.2.2 Implementation of the Criticality Safety Analyses Sequence

CSAS6 uses the following steps to determine the cross-sections for a double-heterogeneous cell as defined in an input:

1. First the unit cell information is read. Then input files are created for the modules that will be used for resonance processing and the rest of the analyses. The modules used to generate resonance-corrected cross-sections for double heterogeneous cells are: BONAMI, CENTRM, CHOPS, CAJUN, PMC, WORKER, AJAX and XSDRNPM. WAX. These will also be used if cell-weighted cross-sections are required.

2. CSAS06 then determines all the nuclides that exist in all the unit cells (this includes the nuclides that will be treated as an infinite homogeneous medium by default). Next it creates a short master multigroup cross-section library and a short point cross-section library with the latter library thinned and interpolated to the temperature of the corresponding mixture.

3. BONAMI (code used to perform Bondarenko calculations for resonance self-shielding) is executed and it performs resonance correction for the unresolved energy range of the multigroup master library cross sections. It then creates a new master cross-section library.

4. WORKER is executed, converting the master multigroup library into a working multigroup library.

5. CENTRM is executed for the first level cell. It utilizes the working multigroup library from step 4 and the point cross-section library from step 2 to determine the flux spectrum throughout the cell.

6. CHOPS is executed and it calculates the cell-averaged fluxes and the corresponding flux disadvantage factors. The flux disadvantage factors are used to calculate homogenized cell-averaged microscopic cross sections. Then a new point library containing only homogenized cross sections is created.

$$\Phi_{cell,E} = \frac{\sum_z \Phi_{z,E}.V_z}{\sum_z V_z}$$

$$f_{z,E} = \frac{\Phi_{z,E}}{\Phi_{cell,E}}$$

$$\sigma^j_{cell,x,E} = \frac{\sum_z f_{z,E}.N^j_z.\sigma^j_{z,x,E}}{\sum_z N^j_z}$$

where,

$\Phi_{cell,E}$ = cell-averaged flux at energy point E;

$\Phi_{z,E}$ = flux for *z* and energy point E;

V_z = volume of zone z*;*

$f_{z,E}$ = flux disadvantage factor for zone *z* and energy point E;

$\sigma^j_{cell,x,E}$ = cell-averaged microscopic cross section of nuclide j, reaction x at energy point E;

$\sigma^j_{z,x,E}$ = microscopic cross section for nuclide j in zone z, reaction *x* at energy point E;

N^j_z = number density of nuclide j in zone z;

7. PMC is executed, this results in the fluxes from step 5, and the homogenized and cell-averaged point cross sections from step 6 being used to modify the multigroup master cross-section library for the first level cell.

8. WORKER is executed, this converts the master multigroup library into a working multigroup library.

9. XSDRNPM (the 1-Dimensional discrete ordinates transport code) is executed, to determine the multiplication factor k_{inf} of the first level cell. This step is not really required for the proper treatment of the double heterogeneity, however, it provides insight into the nuclear properties of the first level cell.

10. Depending on the number of different first level cells (types of kernel in the fuel region) steps 5 through to 9 will be repeated for each unique kernel type. Once this step has been completed, there is one master multigroup library and a number of point-wise cross-section libraries (same as the number of are first level cells within the second level cell) that are being processed. This is in addition to the original thinned and short point cross-section library. In the case of the PBMR fuel there is only one type of kernel, hence there is only one first level cell within the second level cell.

11. CAJUN is then executed; it combines the original point cross-section library from step 2 with the homogenized point cross-section libraries (created for each first level cell in the same second level cell) in step 6 to form a new point library.

12. CENTRM is executed for the second level cell (the pebble fuel element) to determine the flux spectrum throughout the cell by the use of the point cross-section library from step 11 and the working multigroup library from step 8.

13. PMC is executed to modify the multigroup master cross-section library from step 7 for the second level cell. It does this by using the point cross sections from step 11 and the fluxes from step 12. This results in the multigroup cross sections ending up, zone-weighted and resonance-corrected for double heterogeneity.

14. The execution of WORKER converts the master multigroup library from the previous step into a working multigroup library.

15. XSDRNPM is then executed to obtain the k_{inf} of the second level cell. This step is not really required for the treatment of double heterogeneity. It provides additional information with respect to the nuclear properties of the fuel element (fuel sphere). The cell-weighted nuclide cross sections will also be created in this step for the second level cell if required.

16. AJAX is executed in order to remove all extra nuclides from the master multigroup library. This step is not necessary but it was implemented since the mixtures used in the kernels are homogenized into a single fuel region mixture and are not needed or used in any of the modules after the resonance-corrected cross sections are generated.

17. WORKER is executed and it converts the final master multigroup library into a working multigroup library.

18. If cell-weighted cross sections were opted for in step 15 then WAX is executed to combine the final multigroup working library and these cross sections.

The above sequence of steps is then followed by the analysis module KENO-VI.

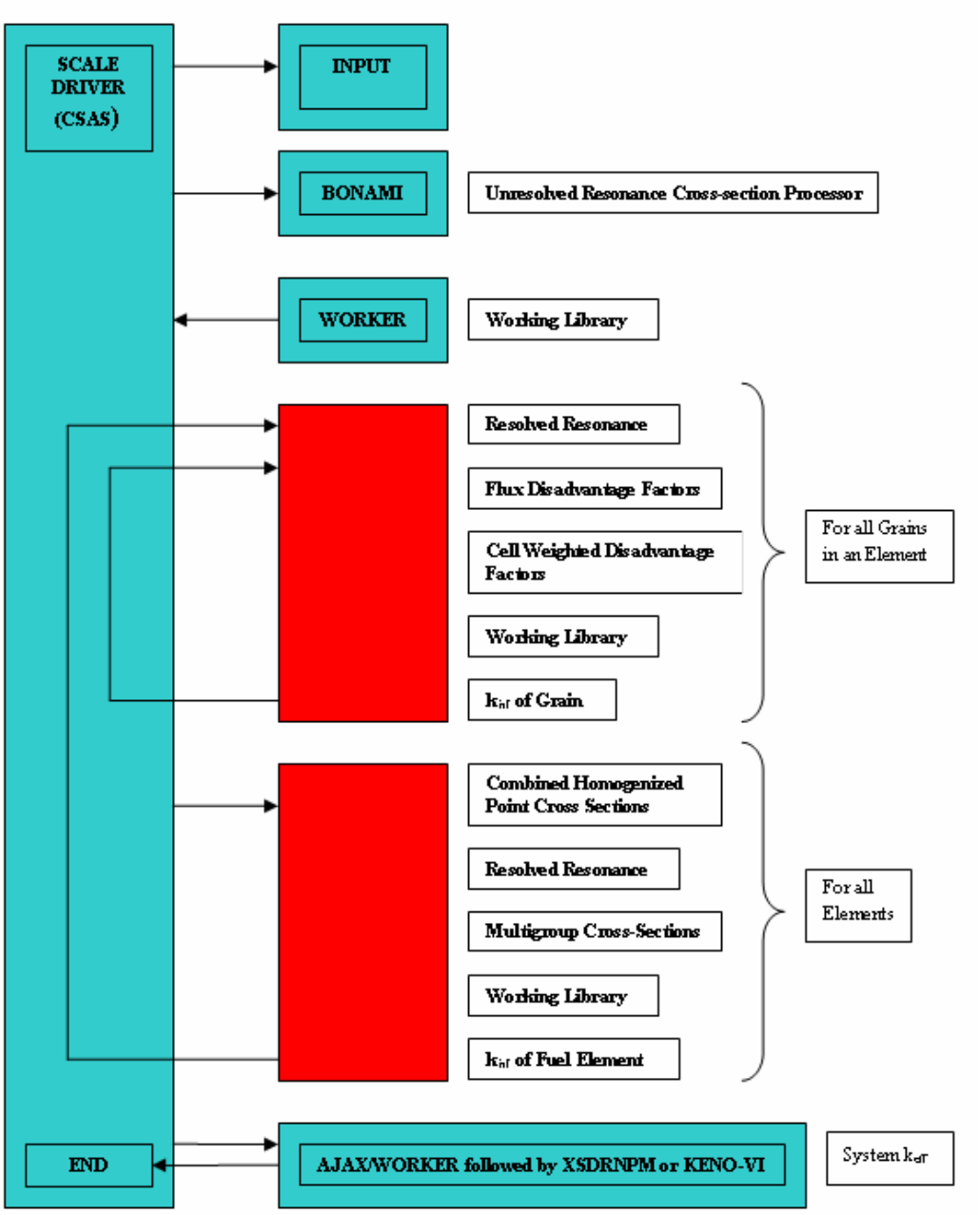

Figure 5: Steps for CSAS6 shown graphically

2.3 FUNCTIONAL MODULE KENO-VI

2.3.1 Purpose and Description

KENO-VI is the functional module that is invoked as part of the CSAS26 sequence after the relevant problem-dependent cross-section libraries have been created to specifically calculate the Effective Neutron Multiplication Factor, k_{eff}, of the system under investigation. It is a three-dimensional analysis code that allows for relatively accurate analysis of complex geometry using Monte Carlo Methods.

2.3.2 Theory: Monte Carlo Three-dimensional Multigroup Transport Equations

The equation that KENO-VI solves in order to obtain the Multiplication Factor, k_{eff}, for a given system is derived in the following manner. We start with the Boltzmann neutron transport equation which is written in the following form.

$$\begin{aligned}&\frac{1}{v}\frac{\partial\Phi}{\partial t}\left(X,E,\Omega,t\right)+\Omega.\nabla\Phi\left(X,E,\Omega,t\right)+\sum\nolimits_{t}\left(X,E,\Omega,t\right)\Phi\left(X,E,\Omega,t\right)\\&=S\left(X,E,\Omega,t\right)+\int_{E'}\int_{\Omega'}\sum\nolimits_{s}\left(X,E'\rightarrow E,\Omega'\rightarrow\Omega,t\right)\Phi\left(X,E',\Omega',t\right)d\Omega'dE'\end{aligned} \qquad (1)$$

where,

$\Phi\left(X,E,\Omega,t\right)$ = neutron flux (neutrons/cm^2/s) per unit energy at energy E per steradian about direction Ω at position X at time t moving at speed v corresponding to E.

$\sum_{t}\left(X,E,\Omega,t\right)$ = macroscopic total cross section of the media (cm^{-1}) at position X, energy E, direction Ω and time t.

$\sum_{s}\left(X,E'\rightarrow E,\Omega'\rightarrow\Omega,t\right)$ = macroscopic differential cross section of the media (cm^{-1}) per unit energy at energy E′ per steradian about direction Ω′ at position X, and time t, for scattering to energy E and direction Ω.

$S(X,E,\Omega,t)$ = neutrons/cm^3/s born at position X and time t per unit energy at energy E per steradian about direction Ω (excludes scatter source).

Next we define $q(X,E,\Omega,t)$ as the total source. It is a combination of the external source, scattering, fission and all other contributions that may exist. The relationship can be written as:

$$q(X,E,\Omega,t) = S(X,E,\Omega,t) + \int_{E'}\int_{\Omega'} \sum_s (X,E' \to E,\Omega' \to \Omega,t)\Phi(X,E',\Omega',t)d\Omega' dE' \quad (2)$$

The following assumptions are then made:

- The media is isotropic
- The cross sections are time independent

Combining Eqs. (1) and (2), and converting the equation to a multigroup form, yields:

$$\frac{1}{v_g}\frac{\partial \Phi_g}{\partial t}(X,\Omega,t) + \Omega.\nabla\Phi_g(X,\Omega,t) + \sum_{tg}(X)\Phi_g(X,\Omega,t) = q_g(X,\Omega,t) \quad (3)$$

where,

g is the energy group of interest,

v_g is the average velocity of the neutrons in group g,

$\Phi_g(X,\Omega,t)$ is the angular flux of neutrons having their energies in group g, at position X and time t,

$\sum_{tg}(X)$ is the macroscopic total cross section of the media at position X for group g.

$\sum_{tg}(X)$ is defined in the following way:

$$\sum_{tg}(X)=\frac{\int_{\Delta E_g}\sum_t(X,E)\Phi(X,E,\Omega,t)\,dE}{\int_{\Delta E_g}\Phi(X,E,\Omega,t)\,dE}$$

where,

ΔE_g defines energy group g,

$q_g(X,\Omega,t)$ is the total source contributing to energy group g at position X and time t in direction Ω.

In this step the relationship $X'=X-R\Omega$ is used. The problem is defined to be time-independent. An integrating factor on both sides of Eq. (3) and $T(R)$ is defined as follows:

$$T(R)=\int_0^R\sum_{tg}(X-R'\Omega)dR',$$

The following equation can be obtained:

$$\Phi_g(X,\Omega)=\int_0^\infty q_g(X-R\Omega,\Omega)e^{-T(R)}dR \qquad (4)$$

At this stage, the problem becomes an eigenvalue problem. In the absence of an external source, the source term may be defined as:

$$q_g(X,\Omega)=\sum_{g'}\int d\Omega'\Phi_{g'}(X,\Omega')\sum_s(X,g'\to g,\Omega'.\Omega)+\frac{1}{k}Q'_g(X,\Omega) \qquad (5)$$

where,

k is the largest eigenvalue of the integral equation,

$Q'_g(X,\Omega)$ is the fission source at position X for energy group g and direction Ω (all fission contributions to group g from all energy groups in the previous generation),

$\sum_s(X, g' \to g, \Omega'.\Omega)$ is the scattering cross section for scattering at position X from group g' and direction Ω' to group g and direction Ω.

The scatter cross-section can be defined in terms of energy as follows:

$$\sum_s(X, g' \to g, \Omega'.\Omega) = \frac{\int_{\Delta E_g}\int_{\Delta E_{g'}} \sum_s(X, E' \to E, \Omega'.\Omega)\Phi(X, E', \Omega')dE'dE}{\int_{\Delta E_{g'}} \Phi(X, E', \Omega')dE'} \quad (6)$$

where,

ΔE_g is the energy range defining energy group g

$\Delta E_{g'}$ is the energy range defining energy group g′.

The fission neutrons are assumed to be isotropic so that the fission source $Q'_g(X,\Omega)$ can be written as:

$$Q'_g(X,\Omega) = \frac{1}{4\pi}\sum_{g'}\int_{\Omega'} d\Omega'\Phi_{g'}(X,\Omega')\chi(X, g' \to g)\upsilon_{g'}(X)\sum_{fg'}(X) \quad (7)$$

where,

$\chi\left(X, g' \rightarrow g\right)$ is the fraction of neutrons born in energy group g from fission in energy group g' in the media at position X,

$\upsilon_{g'}\left(X\right)$ is the number of neutrons resulting from fission in group g' at position X,

$\sum_{fg'}\left(X\right)$ is the macroscopic fission cross section of the material at position X for a neutron in energy group g'.

Eq. (5) is substituted into Eq. (4) to yield the following equation:

$$\Phi_g\left(X,\Omega\right)=\int_0^\infty d\,Re^{-T(R)}\left\{\frac{1}{k}Q'_g\left(X-R\Omega,\Omega\right)+\sum_{g'}\left[\int_{\Omega'}d\Omega'\Phi_{g'}\left(X-R\Omega,\Omega'\right)\sum_s\left(X-R\Omega,g'\rightarrow g,\Omega'.\Omega\right)\right]\right\} \tag{8}$$

k_{eff} may be defined as the ratio of the number of neutrons in the (n + 1)th generation to the number of neutrons in the nth generation or the largest eigenvalue of the integral equation.

By using Eq. (7), Eq. (8) can be written as follows:

$$\Phi_g\left(X,\Omega\right)=\int_0^\infty d\,Re^{-T(R)}\left\{\sum_{g'}\frac{1}{k}\int_{\Omega'}\upsilon_{g'}\left(X-R\Omega\right)\sum_{fg'}\left(X-R\Omega\right)\chi\left(X-R\Omega,g'\rightarrow g\right)\Phi_{g'}\left(X-R\Omega,\Omega'\right)\frac{d\Omega'}{4\pi}+\sum_{g'}\left[\int_{\Omega'}d\Omega'\Phi_{g'}\left(X-R\Omega,\Omega'\right)\sum_s\left(X-R\Omega,g'\rightarrow g,\Omega'.\Omega\right)\right]\right\} \tag{9}$$

Eq. (9) is now written in the “generation notation”. Certain terms are multiplied and divided by $\sum_t\left(X\right)$ and then Eq. (9) is multiplied on both sides by $\upsilon_g\left(X\right)\sum_{fg}\left(X\right)$ yields the following equation which is solved by KENO-VI.

$$\frac{\upsilon_g(X)\sum_{fg}(X)}{\sum_{tg}(X)}\sum_{tg}(X)\Phi_{g,n}(X,\Omega)=\frac{\upsilon_g(X)\sum_{fg}(X)}{\sum_{tg}(X)}\sum_{tg}(X)\int_0^{\infty}d\,Re^{-T(R)}$$
$$\left\{\frac{1}{k_{eff}}\sum_{g'}\int_{\Omega'}\frac{\upsilon_{g'}(X-R\Omega)\sum_{fg'}(X-R\Omega)}{\sum_{tg'}(X-R\Omega)}\chi(X-R\Omega,g'\to g)\sum_{tg'}(X-R\Omega)\phi_{g',n-1}(X-R\Omega,\Omega')\right.$$
$$\left.\frac{d\Omega'}{4\pi}+\sum_{g'}\int_{\Omega'}\frac{\sum_s(X-R\Omega,g'\to g,\Omega'.\Omega)}{\sum_{tg'}(X-R\Omega)}\sum_{tg'}(X-R\Omega)\phi_{g',n}(X-R\Omega,\Omega')d\Omega'\right\}$$

(10)

where

n indicates the nth generation

n–1 is the (n–1)th generation.

The left-hand side of the above equation, $\upsilon_g(X)\sum_{fg}(X)\Phi_{g,n}(X,\Omega)$, is the fission production for the nth generation.

KENO-VI uses an iterative procedure as the solution strategy to solve Eq. (10). The fission production, normalized to the system multiplication at point X in energy group g due to neutrons in the (n–1)th generation is as follows:

$$\frac{1}{k_{eff}}\sum_{g'}\int_{\Omega'}\frac{\upsilon_{g'}(X)\sum_{fg'}(X)}{\sum_{tg'}(X)}\chi(X,g'\to g)\sum_{tg'}(X)\Phi_{g',n-1}(X,\Omega')\frac{d\Omega'}{4\pi}$$

KENO-VI uses collision points that are chosen by selecting path lengths from the following distribution:

$$e^{-T(R)}$$

This is actually the probability of transport from any position $X-R\Omega$ to position X.

The first collision density of neutrons in group g per unit solid angle about Ω resulting from the fission source produced by the (n–1) generation, normalized to the system multiplication, is as follows:

$$\sum_{tg}(X)\int_0^{\infty} d\,Re^{-T(R)}\frac{1}{k}\int_{\Omega'}\sum_{g'}\frac{\upsilon_{g'}(X-R\Omega)\sum_{fg'}(X-R\Omega)}{\sum_{tg'}(X-R\Omega)}$$
$$\chi\left(X-R\Omega,g'\rightarrow g\right)\sum_{tg'}(X-R\Omega)\Phi_{g',n-1}\left(X-R\Omega,\Omega'\right)\frac{d\Omega'}{4\pi}$$

The scattering source at position X emerging in group g and direction Ω resulting from previous collisions in the same generation is as follows:

$$\sum_{g'}\int_{\Omega'}\frac{\sum_s\left(X,g'\rightarrow g,\Omega'.\Omega\right)}{\sum_{tg'}(X)}\sum_{tg'}(X)\Phi_{g',n}(X,\Omega)\,d\Omega'$$

The collision density in group g, per solid angle about Ω is:

$$\sum_{tg}\int_0^{\infty} d\,Re^{-T(R)}\sum_{g'}\int_{\Omega'}\frac{\sum_s\left(X-R\Omega,g'\rightarrow g,\Omega'.\Omega\right)}{\sum_{tg'}(X-R\Omega)}\sum_{tg'}(X-R\Omega)\Phi_{g',n}\left(X-R\Omega,\Omega'\right)d\Omega'$$

The total collision density times $\frac{\upsilon_g(X)\sum_{fg}(X)}{\sum_{tg}(X)}$ is the relationship from which

KENO-VI picks the source points for the next generation.

3. RESEARCH METHODOLOGY

3.1 RESEARCH DESIGN

The study is subdivided into the following stages:

Stage 1

- Collect and read all existing information on criticality safety analyses based on the previous designs of the used and spent fuel containers.

Stage 2

- Obtain the detailed design of the current Used and Spent Fuel Storage Containers and the storage facility (SSS) from the system and design engineers [5].
- Obtain core average fuel isotopic number densities for the most reactive core during the operation cycle from a VSOP99 calculation.

Stage 3

- Develop a SCALE 5.1 model of the whole SSS using the average fuel isotopic number densities for the most reactive core for normal operating conditions by utilizing the control sequence CSAS6.
- Develop the following SCALE 5.1 sub-models of the SSS using the average fuel isotopic number densities for the most reactive core for normal operating conditions by utilizing the control sequence CSAS6:
    - 1 Storage Cell
    - 2 Storage Cells
    - 1 Dry Storage Cell and 1 Wet Storage Cell
- Develop the following SCALE 5.1 sub-models of the SSS using the average fuel isotopic number densities for the most reactive core for off-normal operating conditions by utilizing the control sequence CSAS6:
    - 1 Storage Cubicle
    - 2 Storage Cubicles
    - 1 Dry Storage Cell and 1 Wet Storage Cell
- Perform the criticality analyses on all of the models (for normal and off-normal conditions) using functional module KENO-VI by CSAS6 from the SCALE 5.1 code package.
- Determine the most conservative model from all the scenarios analyzed. The largest Multiplication Factor, k_{eff}, will be used as the determining factor in choosing the most conservative model.

Stage 4

- After the most conservative model has been determined, as explained in stage 2, the model would then be modified by inserting fresh 4.2 w/o enriched Uranium-235 fuel into the storage containers.
- A criticality analysis will be performed on this model using the functional module KENO-VI that is invoked by the control module CSAS06 of the SCALE 5.1 code to determine k_{eff}.

Stage 5

- The most conservative model as determined in stage 2 will once again be modified to incorporate the clustering affects. Fresh, 9.6 w/o enriched Uranium-235 fuel spheres will be used for the clusters against the background of fuel spheres containing average fuel isotopic number densities for the most reactive core. A model with a general clustering scenario will be considered in this study.
- An additional model with all the fuel spheres lying in the storage cubicle will also be modelled to investigate the effect of the spheres falling onto the floor of the storage cubicle in the case of structural failure of the storage containers.
- Criticality analyses will be also be performed on these models using the functional module KENO-VI by CSAS6 from the SCALE 5.1 code to determine k_{eff}.

Stage 6

The value of k_{eff}, is influenced by a number of factors within a model. Some of these factors are:

- The isotopic number densities of the nuclides in the fuel (influences burnup)
- Fission and transmutated products (influences burnup credit)
- Fuel and cooling water temperatures
- Composition of material used for the containers and storage area and their geometries
- The fuel sphere packing fractions in the storage containers

The variation of some of these parameters and their effects on k_{eff} could also be investigated by making changes to the models. However, the fundamental aim of this study is to determine the margins of subcriticality of the SSS for normal and off-normal conditions. The fundamental parameter indicating the margins of subcritical for the models developed is the value of the Effective Neutron Multiplication Factor, k_{eff} [11]. The, k_{eff} obtained from all the models will be checked against the nuclear industry norm of

0.95 for critical safe systems. If the values are equal to or less than 0.95 then the SSS will remain critical safe for scenarios modelled.

3.2 MODELLING ASSUMPTIONS

All models were developed to insure that as much conservatism as possible had been introduced from a criticality perspective, i.e. wherever possible more than the expected positive reactivity and less than the expected negative reactivity was introduced. One of the many instances where more than the expected positive reactivity was introduced was to model the UF sphere to contain the average isotopic composition of the fuel when the reactor core was at its most reactive stage during the operating cycle [12]. Furthermore, all the isotopes were not included in the fuel sphere model and all the isotopes with distinctive absorption properties were excluded, thus reducing the negative reactivity contributions (no burnup credit was assumed). The spent fuel spheres were also modelled using the average fuel isotopic compositions of the most reactive core even though in practice its reactivity will be very low as it is only sent to storage when it has reached the average discharge burnup of approximately 90 000 MWd/tU.

The packing fraction of the stored spheres is expected to be 0.61. Additional models with packing fractions of 0.64 and 0.66 were included to investigate the sensitivity of keff to increased packing fractions [8]. The higher packing fractions also increase the density of the fuel spheres in the container allowing a larger quantity of fuel to be incorporated into the storage containers, which adds conservatism to the model. The containers were also filled to the top while in practice the fuel would be filled to a level of 18 m from the bottom of the storage container. Furthermore, certain components of the fuel loading/unloading mechanisms inside the container were excluded from the model as they would serve as neutron absorbers and would also take up space, resulting in fewer fuel spheres being incorporated into the containers. The section that was included, which form a hollow cylinder inside the storage containers, was also modelled in a way that added further conservatism. In reality, the absorber cylinder has holes of 20 cm in diameter spaced 40 cm apart and each alternate hole is at 90˚ to the previous one. In the model entire 20 cm long sections of the absorber were excluded at the heights where these holes were positioned to reduce the quantity of absorber material in the models. Less absorber material implies that there are more neutrons available for multiplication. This results in more positive reactivity and adds further conservatism to the models used in the analyses.

The following approximations were made in terms of the geometric layout of the SSS and the positioning of the storage containers in the storage cells. According to the layout of the PBMR building plans, the FHSS will be positioned at the circumference of the reactor building with the storage cells adjacent to each other. Due to the large radius from the centre of the reactor building, the curvature at the circumference where the FHSS (which includes the SSS) is located is quite small. It was decided that the modelling of the SSS in a straight line with the storage cells adjacent to each was a good approximation because of the small curvature and as coupling effects between the cells at the extreme ends is unlikely at such large distances. However, the coupling effects were still investigated by first developing a model of the entire SSS system and then sub-models (just 1 dry and 1 wet storage cell, 2 wet storage cells, 2 dry storage cells and a combination of 1 dry and 1 wet storage cell adjacent to each other) and then comparing the calculated k_{eff} values. This investigation had a twofold benefit. The first being that the coupling between the storage cells could be studied and secondly it allowed for the determination of the most penalizing model in terms of criticality.

In addition the positioning of the SSS along a curvature in the design meant that adjacent containers on the inside were positioned closer to each when compared to adjacent containers on the outside for given radial directions. The containers adjacent to the separating wall on the inside were also closer than the containers on the outside because of the curved layout. To be conservative, the shortest separating distance between adjacent containers were used when the SSS was modelled in the straight-line layout.

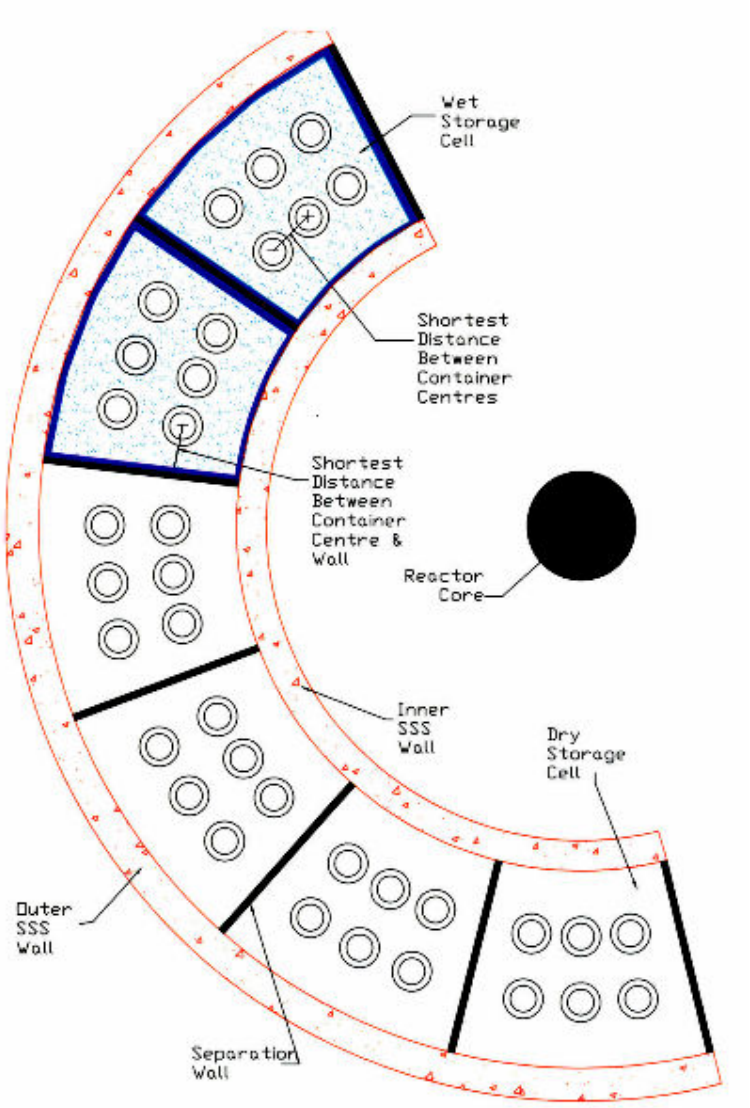

Figure 6: Actual Physical Layout of the SSS

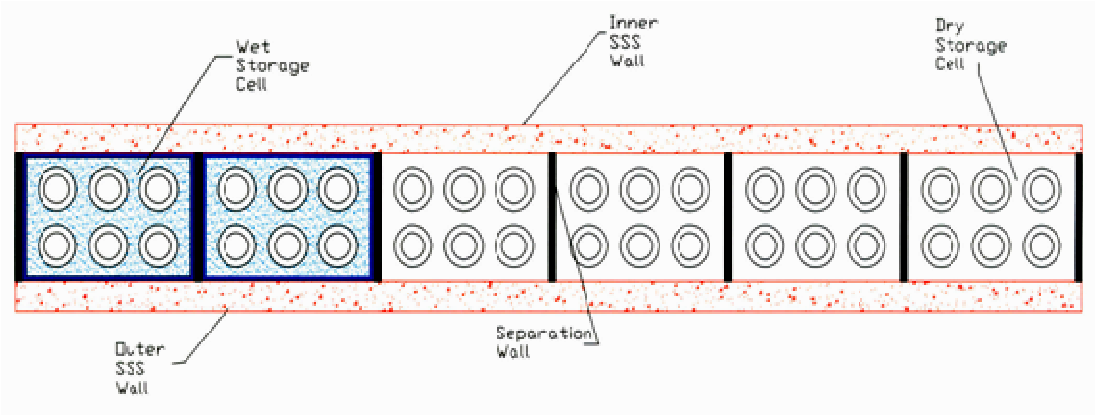

Figure 7: Model of SSS using SCALE 5.1

3.3 PROCESS AND FLOW OF THE MODELS

The whole SSS consists of two wet and four dry storage cells, as explained previously. It is a large system relative to the volume of the reactor, especially in terms of length. It was decided to investigate the coupling effects of the storage cells and at the same time to obtain the most reactive combination of storage cells. The idea was to create models at normal and off-normal conditions for the whole model, and sub-models. The sub-models considered were as follows:

- 1 dry and 1 wet storage cell separately
- 2 wet storage cells
- 2 dry storage cells
- 1 wet storage cell adjacent to 1 dry storage cell

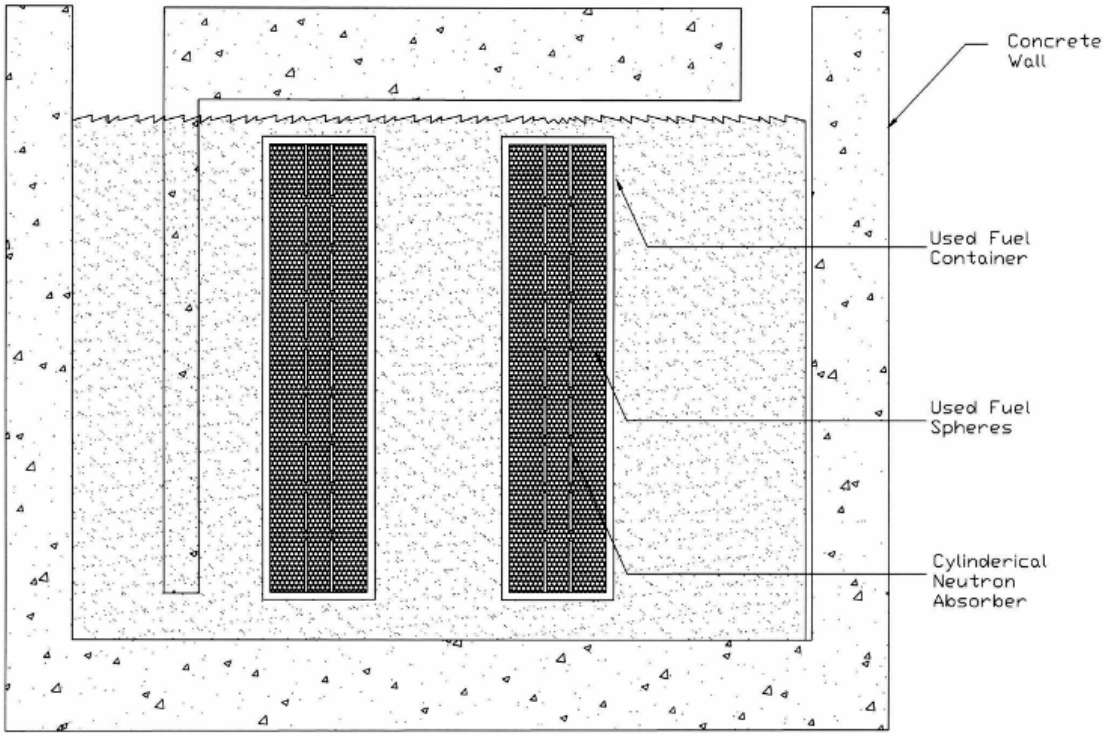

Figure 8: Model of Wet Storage Cell

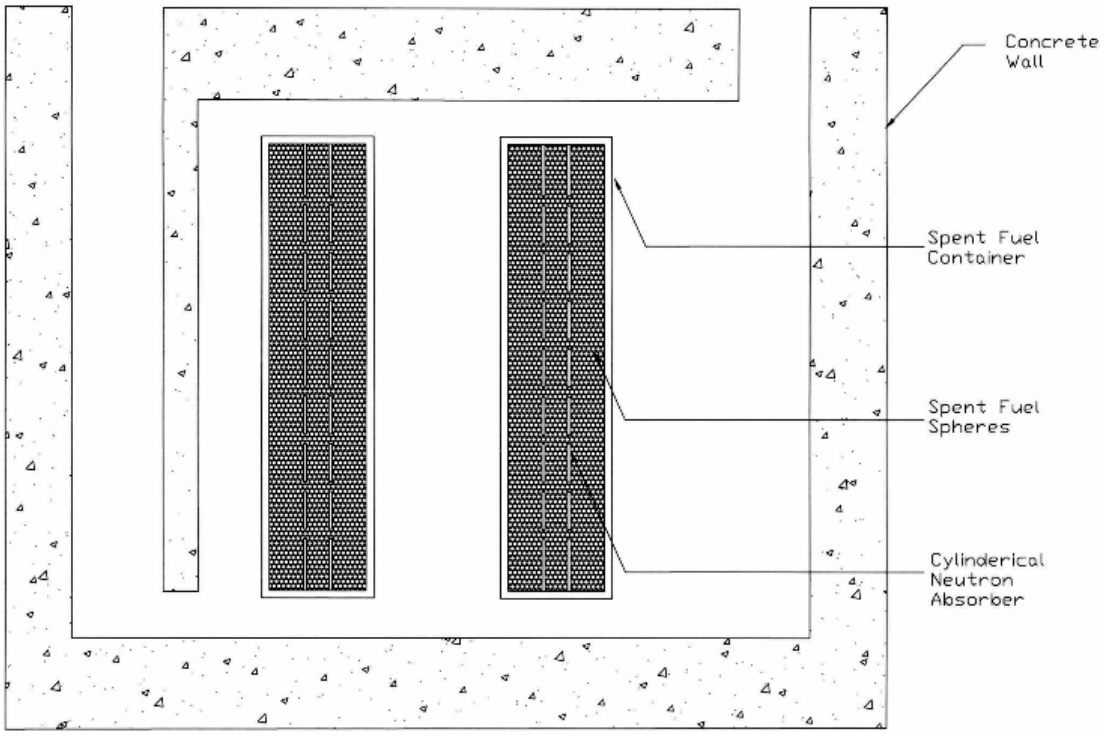

Figure 9: Model of Dry Storage Cell

Generally, off-normal conditions can cover a vast range of scenarios ranging from high probability (highly likely) to low probability (highly unlikely) events. Therefore, it was important in this study to choose off-normal events that are realistic and that had a reasonably high probability of occurring. The off-normal events were chosen based on the following information:

- The intended location of the demonstration plant in South Africa
- The layout of the SSS within the PBMR demonstration plant
- The material composition of the storage containers
- The stochastic movement of fuel spheres through the core and resulting unloading of it to the SSS
- The length of time the fuel spheres are going to be stored in the SSS.

Although the necessary precautions would be taken to prevent the following events, the fact that the PBMR demonstration plant is planned to be built on the shores of the Atlantic Ocean (at the Koeberg Nuclear Power site) and that the SSS will be situated below ground level, the probability of flooding of the SSS cannot be ruled out. The event of flooding thus constitutes

a realistic and highly likely possible off-normal condition. The flooding events considered for analyses were as follows [9]:

- The flooding of the dry storage cells only (the wet storage cells contain water as per normal operation)
- The ingress of water into both the Used and Spent Fuel Containers (breech of the containers or lids) with the dry storage cells flooded (the wet storage cells contain water as per normal operation)
- The ingress of water into both the Used and Spent Fuel Containers with no water in either the dry or wet storage cells (breech in the storage cell structure after the flooding event)

The above analyses will be for performed for a range of temperatures from 27˚C to 97˚C. This range starts from the ambient region right up to close to the boiling point of water. This allows us to investigate the effect of temperature changes on the storage facility. However over this range the density of water was kept at its nominal density. The effects of a changing water density was analysed separately by varying the water density inside the containers from 0.001 g/cm^3 to 0.9982 g/cm^3. Since the pebble bed fuel are under-moderated the analyses also yields the water density at optimum moderation conditions. Though the plant is planned to be built close to the Atlantic Ocean, the material composition of the water used during the modelling of the scenarios was that of normal water. Sea water, which has high concentrations of NaCl and other impurities, was not used. It is accepted that disregarding the impurities reduces the absorption characteristics of the water while maintaining its moderation characteristics making more neutrons available for fission, which makes for conservative analyses.

The primary system of the Koeberg Nuclear Power Plant (which consists of the reactor pressure vessel, primary coolant pumps, piping and the steam generators) is built on a platform that sits on thousands of stilts with seismic bearings. The purpose of these is to absorb seismic movement occurring off the west coast of South Africa. The design of the platform with the stilts is intended to keep the primary system intact during a seismic event. In the case of the SSS of the PBMR, seismic events could shake the fuel storage containers causing stored fuel to pack into much higher density than normal, resulting in packing fractions higher than 0.61. The intention to store the fuel for a long period in the SSS may result in corrosion of the storage containers that will weaken their structure and a seismic event could cause the containers to fail resulting in all fuel spheres falling into the storage

cells. Additional higher-than-normal fuel sphere packing fractions (> 0.61) and the event of fuel spheres filling the storage cells were modelled for investigation.

The stochastic nature of loading fuel spheres into the UFC from the core allows for the possibility of the clustering of spheres with low burnup in these storage containers. This may result in a higher reactivity in the UFC, an important phenomenon that was modelled for investigation. The clustering scenarios considered were the low but non-negligible probability of a gathering of low burnup fuel spheres in the UFC. In theory, the lowest possible burnup of fuel is actually fuel with no burnup at all (fresh fuel). The fresh fuel spheres were used in the models to form the clusters against the background of fuel having the average isotopic composition from the most reactive core in the cycle.

The probabilities of low burnup clustering are extremely small and get even smaller as the number of fuel spheres per cluster increases. Only clusters ranging from two to six low burnup fuel spheres (in our case fresh) per cluster were considered for analyses. The reason for this is explained by a statistical evaluation in section 4.4.2. Each container can hold as much as 175 000 randomly loaded fuel spheres usually partitioned into six burnup classes. The clustering of low burnup pebbles is not only possible but the approximate number of such clusters can be predicted using basic probability theory. The distribution of these clusters is also spatially random, thus a large number of clustering scenarios can occur for a given number of clusters per cluster type (number of spheres per cluster) especially for the type with two spheres per cluster. It is clear that modelling every possible clustering scenario is virtually impossible. Hence, for the sake of this study all the clusters from all the cluster types would be incorporated into one model. This study will also be done for a higher packing fraction as this could possibly occur during a seismic event. The use of fresh fuel spheres for the clusters and the use of higher-than-normal packing fractions also add conservatism to the analyses.

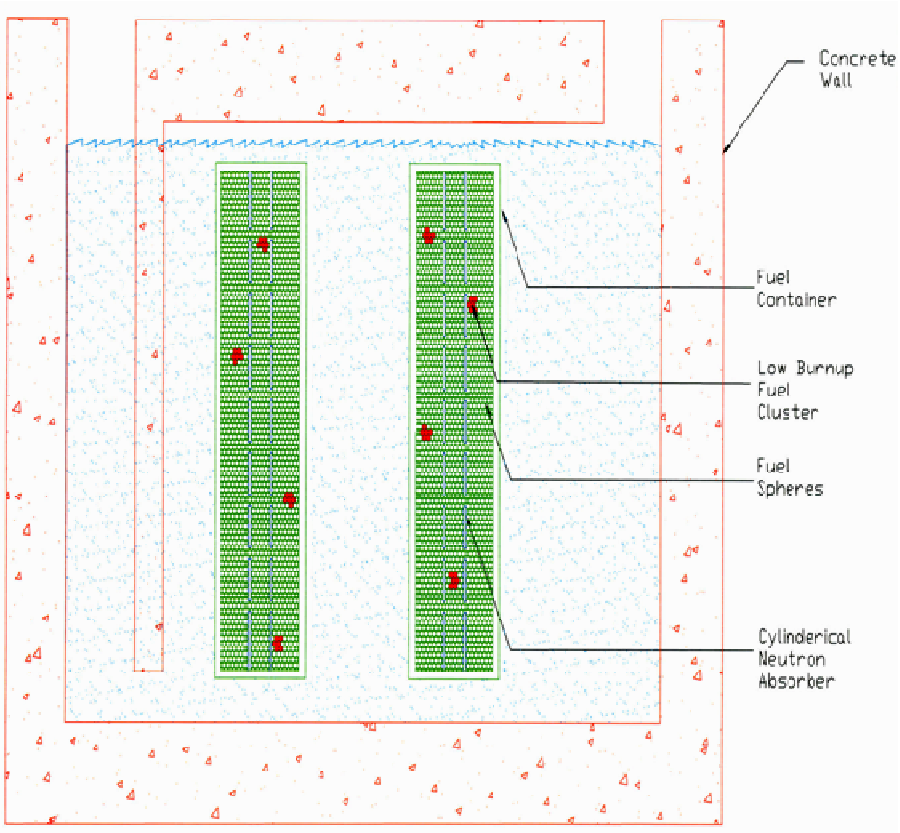

Figure 10: Model of Low Burnup Fuel Clusters in UFC

The fuel of the PBMR is under-moderated; so the addition of a moderator (in the form of water) adds reactivity. It is important to investigate the conditions under which optimal moderation occurs. There is a probability of water ingress into the storage containers and depending on the amount, it may increase or decrease the reactivity of the filled storage cell, depending upon the relative change in rates of absorption and moderation. If the right amount of water ingress into the containers occurs, a condition of optimal moderation may occur with an attendant peak in the multiplication factor. The SSS must accommodate this configuration so it must be included in this analysis. Therefore, the water density was varied to determine its sensitivity on k_{eff} and to determine the density of water that gives the optimum moderation.

The models developed for the normal and off-normal events for the whole models and sub-models listed in Table 2 below:

Table 2: Normal and Off-Normal Events Modelled

Scenarios	Wet Storage Cells	Dry Storage Cells	Both Wet and Dry Storage Cells	Whole SSS
Normal Conditions				
1 Storage Cell	Yes	Yes	N/A	N/A
2 Storage Cells	Yes	Yes	N/A	N/A
1 Dry and 1 Wet	N/A	N/A	Yes	N/A
All Cell (2 Wet and 4 Dry)	N/A	N/A	N/A	Yes
Off-Normal Conditions				
1 Storage Cell (Water Outside Containers)	N/A	Yes	N/A	N/A
2 Storage Cells (Water Outside Containers)	N/A	Yes	N/A	N/A
1 Dry and 1 Wet (Water Outside Containers)	N/A	N/A	Yes	N/A
All Cell (Water outside Containers)	N/A	N/A	N/A	Yes
1 Storage Cell (Water inside and outside Containers)	Yes	Yes	N/A	N/A
2 Storage Cells (Water inside and outside Containers)	Yes	Yes	N/A	N/A
1 Dry and 1 Wet (Water inside and outside Containers)	N/A	N/A	Yes	N/A
All Cell (Water inside and outside Containers)	N/A	N/A	N/A	Yes
1 Storage Cell (No Water inside and outside Containers)	Yes	N/A	N/A	N/A
2 Storage Cells (No Water inside and outside Containers)	Yes	N/A	N/A	N/A
1 Dry and 1 Wet (No Water inside and outside Containers)	N/A	N/A	Yes	N/A
All Cell (No Water inside and outside Containers)	N/A	N/A	N/A	Yes

Two additional models with fresh fuel spheres stored in the UFC were also developed. The first model took into consideration only the 4.2 weight percent enriched fresh fuel spheres for the following reason. During initial start-up of the reactor when graphite spheres are being replaced by 4.2 percent weight enriched fuel, unforeseen circumstances may arise that require the unloading of the core into the UFC. In such a case most of the fuel will have burnup that is extremely low, to almost zero. All fresh 4.2 weight percent-enriched fuel was used in the model in order to obtain a bounding model.

In the second model, a small number of pure graphite spheres were interspersed randomly amongst the 4.2 weight percent-enriched fresh fuel spheres in the UFC. The reason for modelling this event was to investigate the outcome of a small number of pure graphite spheres that may find their way into the UFC due to equipment malfunction.

All the events modelled for the off-normal conditions were done by assuming common mode failure. The reasoning behind this is twofold; this restricts the number of models that needed to be developed and it results in the most penalizing model for a given scenario. For example in the burst storage container scenario it is assumed that all the containers in the model failed instead of considering that just a few might fail and the others may remain intact. Similarly it was assumed that during a seismic event, the packing fraction in all the containers increased to a higher value instead of taking into account that in some containers the packing fraction may have not changed much.

4. DEVELOPMENT OF THE MODELS USING CSAS6

CSAS26 is the only control sequence that can be utilized by CSAS6. CSAS26 performs a sequence of operations on a specified system in order to obtain the final result, i.e. the Effective Neutron Multiplication Factor, k_{eff}, for the system. However, every system is different in terms of material composition, geometry, required operating conditions and modelling assumptions that may be used. This results in the modelling technique being unique depending on the system parameters and the way in which the user goes about setting up the models for the system. As a result, it is important to discuss how the user went about setting up the models in order to ensure that the most conservative configuration is captured.

The methodology followed in this study entailed the development of models for the smallest unit (fuel spheres), then the larger units (the UFC and SFC) and then the wet and dry storage cells. The fuel spheres were placed into the UFC and SFC and these containers were then placed into the Wet and Dry Storage cells. Lastly the required numbers of Wet and Dry Storage cells were combined to form the required model for the SSS. In all the analyses the V6-238 cross section library was used with the white boundary condition defined on the outer boundary of the concrete cells for all the models.

The methodology used to model the entire SSS encompasses a number of steps, as will be described below:

4.1 PROCEDURE TO MODEL FUEL SPHERES

The main reason for using CSAS6 is that it has the functionality that allows users to model HTR pebble fuel heterogeneously. The material composition of the fuel is specified in the composition specification of the input. The fuel sphere modelling is carried out in the ‘celldata’ section of the input. The input for the ‘celldata’ section consists of the grain (TRISO particle) parameters and the fuel sphere parameters.

The grain input data required are as follows:

- The radius and material composition of the kernel (Uranium Dioxide fuel), Buffer (1st coating layer), Inner Pyrolytic Carbon (2nd coating layer), SiC (3rd coating layer) and Outer Pyrolytic Carbon (4th coating layer).
- The number of TRISO particles that will be in the fuel region of the fuel sphere.
- The composition of the matrix that occurs between the TRISO particles.

The input data for the TRISO particles is listed in Table 3 [13]:

Table 3: TRISO Particle Input Data

Grain (TRISO Particle)		
	Radii (cm)	Material Composition
Kernel	0.025	Uranium Dioxide
Buffer Layer	0.0345	Graphite
Inner Pyrolytic Carbon Layer	0.0385	Pyrolytic Carbon
SiC Layer	0.042	Silicon Carbide
Outer Pyrolytic Carbon Layer	0.046	Pyrolytic Carbon
Number of TRISO particles in the fuel region of the sphere: 15 000		
Matrix composition: Graphite		

The fuel sphere input data are listed in Table 4 [13]:

Table 4: Fuel Sphere Input Data

Fuel Sphere	
	Radii (cm)
Fuel Region	2.5
Cladding Radius	3
Type of Lattice: Triangular-Pitched Dodecahedral Lattice (SPHTRIANGP)	

The geometry specification of the fuel sphere was done within a unit cell. The unit cell used was a rhombic dodecahedron (a 12-sided polyhedron with each surface being a rhombus) [14]. This geometry was especially chosen as it allows for spheres to be packed during modelling in a way that is close to the manner in which they would actually be packed naturally.

4.2 PROCEDURE TO MODEL FUEL STORAGE CONTAINERS AND THE SPHERE STORAGE SYSTEM

The storage containers and storage cells of the SSS were modelled in the last geometric unit known as the global unit. The next step involved the filling the storage tanks with the fuel spheres. The storage tanks were then placed at the appropriate locations within the storage cells of the SSS. This completed the modelling of the whole SSS.

The Spent and Used Fuel containers have the same dimensions (inner and outer radii and heights) with cylindrical load/unload mechanism (also serve as neutron absorbers) placed inside them. The modelling of the load/unload mechanism formed the next two geometric units in the input. The absorber was modelled as cylindrical rings stacked vertically at 20 cm intervals. The reason for this was explained in section 4.2. Both the fuel containers and the load/unload mechanism, which have regular cylindrical geometries, were modelled using the available geometries in the SGGP.

In the case of the SSS the boundary walls were modelled by first creating 2 cuboids, one was placed inside the other. The inner cuboid formed the inner surface while the outer cuboid formed the outer surface of the boundary walls. The separation distances between the cuboids were the same thickness as the boundary walls. Next, cuboids with the dimensions of the wet and dry storage cells where created. These cuboids where then placed in the correct positions within the boundary walls of the SSS. The spaces between the all the cuboids were filled with material that had the composition of concrete, thus forming the separation walls between the storage cells and the boundary walls of the SSS. All the modelling was done with respect to a chosen reference point in the Cartesian coordinate system.

The next task involved positioning the UFC and SFC into the wet and dry storage cells of the SSS. The containers were positioned in the desired positions by stipulating their position with respect to the above-mentioned reference point.

In order to fill the storage containers with the fuel spheres, the fuel spheres were placed into a three-dimensional dodecahedron array. The three-dimensional dodecahedron array allows for the storage of dodecahedron units. Since the fuel spheres where modelled into dodecahedral unit cells, this allowed for their storage in the array. Entire arrays of fuel

spheres where placed into the containers that were already positioned in the storage cells. The arrays were positioned in the containers by stipulating their positions with respect to the reference point as well. The inner surfaces of the storage containers formed the array boundaries, allowing the arrays to fill the cylindrical volumes. However, this resulted in fuel spheres being cut-off at the array boundary (the storage container inner surface). This phenomenon allows for a larger volume of fuel to be packed into a storage container during modelling than would actually occur in reality. This may result in further conservatism being built into the models depending on how the moderator to fuel ratio is affected.

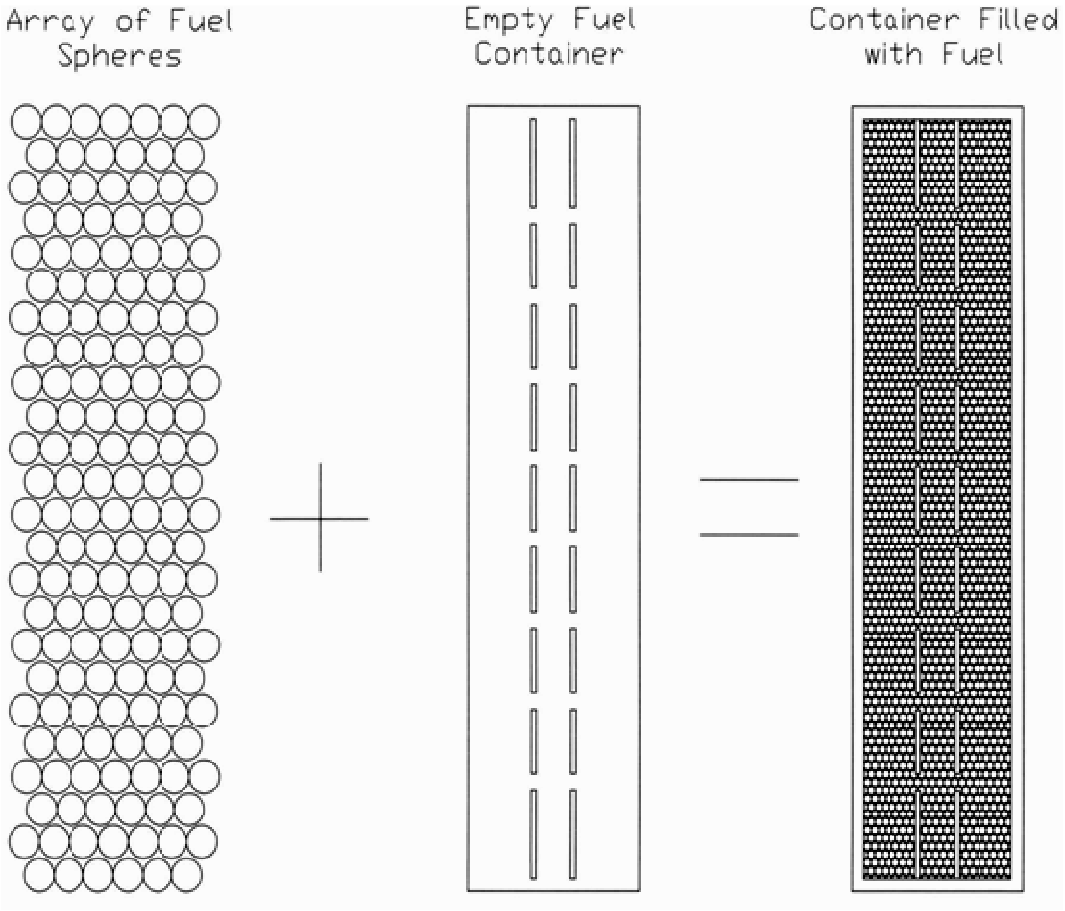

Figure 11: Fuel Spheres being packed into the Storage Containers

Finally, the volume in-between the fuel spheres in the containers were filled with air and the volume in-between the storage containers were filled with water or air, depending on whether the containers were in the wet storage section or the dry storage section of the SSS.

The input data used in the modelling of the storage containers are listed in Table 5:

Table 5: Input Data used for Modelling Storage Containers

Used and Spent Fuel Storage Containers	
UFC and SFC (Same Dimensions)	Dimensions (cm)
Inner Container Radius	84.0
Outer Container Radius	85.6
Container Thickness	1.6
Inner Container Height	1976.8
Outer Height	1980.0
Lid and base thickness	1.6
Neutron Absorber	
Inner Radius of Absorber	44.0
Outer Radius of Absorber	46.0
Absorber Height	1976.8
The material used for both the storage tanks and the neutron absorber is SS304	

Table 6 lists the input data used that was current at the time of modelling the SSS:

Table 6: Input Data used for modelling Sphere Storage System

Sphere Storage System	
Wet Storage Cell	Dimensions (cm)
Inner Length	867.2
Inner Width	850.0
Inner Height	2344.0
Inner Length (Wall Liner)	865.2
Outer Length (Wall Liner)	867.2
Inner Width (Wall Liner)	848.0
Outer Width (Wall Liner)	850.0
Inner Height (Wall Liner)	2343
Outer Height (Wall Liner)	2344
Wall Liner Thickness	1.0
Hanging Wall Length	787.2
Hanging Wall Width	50.0
Hanging Wall Height	2244.0
Dry Storage Cell	
Inner Length	807.2
Inner Width	850.0
Inner Height	2344.0
Hanging Wall Length	807.2
Hanging Wall Width	50.0
Hanging Wall Height	2244.0
Whole Storage System	
Inner Length	5338.2
Outer Length	5488.2
Inner Wall Width	850.0
Outer Wall Width	1150.0
Inner Wall Height	2344.0
Outer Wall Height	2644
Floor Thickness	150.0
Roof Thickness	150.0
Cell separation wall thickness	75.0
The entire structure of the SSS apart from the wet storage cell inner wall liner is made of Regular Concrete	
The material used for the wet storage cell inner wall liner is SS304	

4.3 INCORPORATION OF NORMAL AND OFF-NORMAL CONDITIONS INTO THE MODELS

Once the models were developed for the normal operating conditions it made sense to modify the same models to incorporate the off-normal events as the fuel sphere, storage containers and SSS geometric structure remains the same. It was just a matter of changing certain parameters in order to obtain the required models, as explained below.

The ingress of water into the containers required changing the material that was in-between the fuel spheres from air to water. Similarly, the flooding of the dry storage cells required the material medium in-between the SFC to be changed from air to water. Lastly, the loss of cooling water from the wet storage cells meant just changing the material medium between the UFC containers from water to air.

As discussed in section 3.3 there is a possibility of the stored spheres ending up in a much denser packed configuration than normal. Physically this translated to an increase in the packing fraction of the fuel spheres in the storage containers. The change of the packing fraction of the stored fuel spheres in the models was addressed in the following manner:

The packing fraction is given by the following equation:

$$PF = \frac{Vs}{V_c}$$

where,

Vs is the fuel sphere volume

Vc is the dodecahedron cell volume

PF is the packing fraction

This equation indicates that in order to change the packing fraction either Vs or Vc must change. In this study the volume of the fuel sphere (V_s) is constant and it is assumed that it remains unchanged. The only quantity that can change is the dodecahedron cell volume (V_c). In the code, the input to define a dodecahedron cell volume is a radius (R), defined as the shortest distance from the centre of the dodecahedron to an inner surface.

The radius (R) was obtained in the following manner:

For a given packing fraction (PF) and the known V_s, V_c is obtained as follows:

$$V_c = \frac{V_s}{PF}$$

$$R = \frac{(V_c)^{\frac{1}{3}}}{(3.07920144)^{\frac{1}{3}}}\left(\frac{2}{3}\right)^{\frac{1}{2}}$$

So, the dodecahedron volume is obtained by specifying the packing fraction that is needed for the analyses. This is used in the above equation to obtain the dodecahedron cell radius (R) which is used in the code input to specify the volume of the dodecahedron cell and this result in the fuel spheres being packed into the storage containers at the required packing fraction.

The off-normal condition of water ingress into the containers also requires further investigation in terms of the water density that results in the optimal moderation condition. This was investigated by varying the water density of the model from very low densities (close to 0 g/cm^3) to that of water at normal atmospheric conditions (close to 1 g/cm^3). The water density that yields the largest Effective Multiplication Factor, k_{eff}, is the optimal moderation water density.

4.4 MODIFICATION OF THE MOST CONSERVATIVE MODEL

Once all the models for normal and off-normal conditions were modelled and the k_{eff} values obtained, the most conservative model with respect to k_{eff} was chosen for further investigations.

4.4.1 Fresh Fuel (4.2 Weight Percent-Enriched)

The most conservative model was first modified so that fresh 4.2 w/o enriched fuel was stored in the containers. The reason, as explained in section 3.3, covers the possible scenario of fresh fuel 4.2 w/o enriched being unloaded into the UFC during the start-up.

From the modelling side, this entailed only changing the fuel composition from the average isotopic composition of the most reactive core to that of 4.2 w/o U-235 and 95.8 w/o U-238 for fresh fuel.

4.4.2 Clustering

The most reactive model was then modified to incorporate the various possible clustering scenarios. A new fuel type in the form of 9.6 w/o enrichment fresh fuel spheres was defined in the code input in addition to the type defined for the most reactive core. The clusters were developed using the fresh 9.6 w/o enriched fuel spheres against the background of the fuel from the most reactive core, as explained previously. The modelling of the cluster sizes from two to nine fresh fuel spheres per cluster was achieved by placing the groups of fresh fuel spheres at adjacent positions in the dodecahedron array. Similar groups were also placed at different positions in the array, so this manifested itself as similar clusters at different positions within the storage containers. As explained previously, there are too many combinations of clustering within a container for a particular type of cluster to model all the combinations. The positions of the clusters in the dodecahedron array for all the cluster types (from two to nine fresh fuels spheres per cluster) for this study were chosen randomly. This was considered sufficient for the purpose of this study. The largest cluster size considered was a group of nine fresh fuel spheres adjacent to each other. The reason for this is illustrated by a simple statistical formulation as shown below:

Assume that the fuel spheres are randomly loaded and re-circulated into the core during operation. Within a few years, the core will reach an equilibrium burnup state at which it will

remain for the remainder of the operating life of the core. In the event that the entire core is off-loaded, approximately 175 000 partial burned fuel spheres will end up in a particular UFC of which 1/6 are 1st cycle fuel spheres. Except for ones located near the vessel walls, each fuel sphere will have, on average, 12 other fuel spheres in contact or very close in proximity. Therefore the fuel spheres stored in the storage containers can be considered as being stored as clusters of fuel where each cluster contains 13 fuel spheres. By using statistical combinations the number of clusters of a certain type containing 1st cycle fuel spheres in the storage containers can be obtained.

The following statistical formulation illustrates how the number of 1st cycle fuel spheres that are in clusters of 2 was obtained:

$$\frac{\binom{\text{No. of 1st cycle spheres in the container}}{\text{No. of 1st cycle spheres in the clusters}}\binom{\text{No. of spheres in the container besides 1st cycle ones}}{\text{No. of fuel spheres remaining in the cluster besides 1st cycle ones}}}{\binom{\text{Total no. of fuel spheres in the container}}{\text{Total no. of fuel spheres in a cluster}}}$$

Similarly the number of the other cluster types that occur in the container can be obtained.

Table 7 lists the estimated number of clusters of a particular type containing 1st cycle fuel spheres that could possibility occur in each storage container:

Table 7: Number of Clusters of 1st Cycle Fuel Spheres for a given type of Cluster

Types of Fuel Sphere Clusters	Probability of the 1st Cycle Fuel Spheres occurring in the Cluster	Number of Clusters of a certain type containing 1st Cycle Fuel Spheres in the storage Containers
2	0.291596638	3926
3	0.213833135	2879
4	0.106909969	1440
5	0.03848363	518
6	0.010260823	139
7	0.002051785	28
8	0.000307698	5
9	3.41795E-05	1

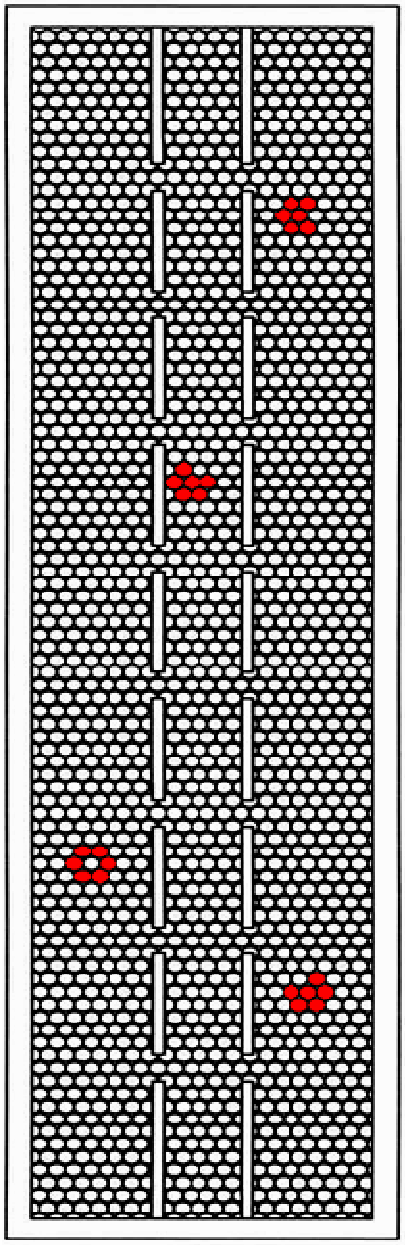

Figure 12: Clusters of 6 Low Burnup Fuel Spheres

4.4.3 Failure of the Storage Containers

In this last case, the most conservative model was modified to investigate the failure of all the storage containers within a particular storage cell. It was assumed that due to the common mode failure of all the containers the total number of fuel spheres from all six containers drop onto the floor of the storage cell.

This was modelled by storing the total number of fuel spheres that would drop onto the floor into a three-dimensional dodecahedral array. The array was then positioned in the storage cell. The storage containers were left at their original positions but were only filled with fuel spheres to the same height as the rest of the cell thus leaving the major portion of the containers empty.

4.4.4 Inclusion of Graphite Spheres into the Fresh Fuel Model

If a core unload has to occur during the start-up of the PBMR, as explained in section 3.3 where 4.2 w/o enriched fuel spheres will be unloaded into the UFC, there is a possibility that graphite spheres may also end up in the UFC. Although the intention is to separate the graphite spheres from the fuel during unloading, equipment failure or any other unforeseen circumstance may allow a small number of graphite spheres into the UFC.

The graphite spheres were incorporated into the model in exactly the same way as the clustering was done. The only difference in this model is that the 4.2 w/o enriched fuel formed the background and the pure graphite spheres were positioned in the dodecahedron array at random positions. This translated to a small number of pure graphite spheres occurring at random positions within the UFC.

5. RESULTS

5.1 PRESENTATION OF THE RESULTS

The results of the criticality analyses done on all the models are presented in this section. First the results obtained for the submodels will be presented, followed by the whole model then for the 4.2 w/o fresh fuel and lastly for the clustering scenarios.

These results are presented in the form of tables (the uncertainties are in brackets) as well as graphs in order to illustrate the sensitivity of k_{eff} to the various models and the changes of certain parameters within these models.

5.1.1 Dry Storage Cells

Table 8: k_{eff} of Dry Storage Cells with Packing Fraction of 0.61 at Different Temperatures

Packing Fraction: 0.61				
Storage Cell Types	Normal (no H_2O inside and outside containers)	H_2O inside containers only	H_2O inside and outside all containers	H_2O outside containers only
Models at 300 K				
1 Dry Cell	0.5596 (0.0013)	0.5993 (0.0010)	0.60085 (0.00092)	0.5237 (0.0017)
2 Dry Cells	0.5583 (0.0013)	0.60276 (0.00072)	0.60273 (0.00098)	0.5234 (0.0012)
Models at 335 K				
1 Dry Cell	0.5538 (0.0014)	0.59895 (0.00073)	0.5978 (0.0011)	0.5167 (0.0013)
2 Dry Cells	0.5523 (0.0013)	0.60027 (0.00096)	0.59732 (0.00073)	0.5169 (0.0017)
Models at 370 K				
1 Dry Cell	0.5454 (0.0014)	0.5991 (0.0010)	0.5974 (0.0010)	0.5123 (0.0015)
2 Dry Cells	0.5474 (0.0014)	0.59524 (0.00096)	0.5970 (0.0011)	0.5089 (0.0012)

Table 9: k_{eff} of Dry Storage Cells with Packing Fraction of 0.64 at Different Temperatures

Packing Fraction: 0.64				
Storage Cell Types	Normal (no H_2O inside and outside containers	H_2O inside containers only	H_2O inside and outside all containers	H_2O outside containers only
Models at 300 K				
1 Dry Cell	0.5936 (0.0016)	0.6401 (0.0011)	0.6392 (0.0010)	0.5571 (0.0015)
2 Dry Cells	0.5932 (0.0015)	0.64130 (0.00089)	0.6397 (0.0010)	0.5591 (0.0014)
Models at 335 K				
1 Dry Cell	0.5854 (0.0015)	0.64003 (0.00091)	0.6363 (0.0010)	0.5519 (0.0015)
2 Dry Cells	0.5837 (0.0012)	0.6382 (0.0010)	0.63864 (0.00077)	0.5533 (0.0012)
Models at 370 K				
1 Dry Cell	0.5790 (0.0013)	0.63936 (0.00083)	0.6389 (0.0010)	0.5450 (0.0015)
2 Dry Cells	0.5787 (0.0012)	0.6389 (0.0011)	0.63431 (0.00092)	0.5441 (0.0017)

Table 10: k_{eff} of Dry Storage Cells with Packing Fraction of 0.66 at Different Temperatures

Packing Fraction: 0.66				
Storage Cell Types	Normal (no H_2O inside and outside containers	H_2O inside containers only	H_2O inside and outside all containers	H_2O outside containers only
Models at 300 K				
1 Dry Cell	0.6125 (0.0017)	0.6700 (0.0011)	0.6663 (0.0011)	0.5800 (0.0014)
2 Dry Cells	0.6126 (0.0015)	0.6706 (0.0012)	0.66710 (0.00088)	0.5822 (0.0014)
Models at 335 K				
1 Dry Cell	0.6037 (0.0016)	0.6646 (0.0010)	0.6651 (0.0013)	0.5732 (0.0016)
2 Dry Cells	0.6045 (0.0016)	0.6686 (0.0014)	0.6659 (0.0014)	0.5733 (0.0014)
Models at 370 K				
1 Dry Cell	0.6019 (0.0013)	0.6637 (0.0010)	0.6645 (0.0010)	0.5675 (0.0016)
2 Dry Cells	0.5991 (0.0015)	0.6607 (0.0011)	0.66428 (0.00093)	0.5682 (0.0020)

5.1.2 Optimum Moderation of the Model (2 Dry Storage Cells at temperature 300 K with Packing Fraction of 0.66) with the largest k_{eff}

Table 11: k_{eff} for Varying Water Densities (inside Containers) showing Optimum Moderation (2 Dry Storage Cells)

Water Density (g/cm^3)	k_{eff}
0.1	0.6170 (0.0017)
0.2	0.8226 (0.0017)
0.3	0.8772 (0.0013)
0.4	0.8552 (0.0013)
0.5	0.8239 (0.0013)
0.6	0.7928 (0.0011)
0.7	0.7595 (0.0013)
0.8	0.7251 (0.0016)
0.9	0.7022 (0.0015)
0.9982	0.6706 (0.0012)

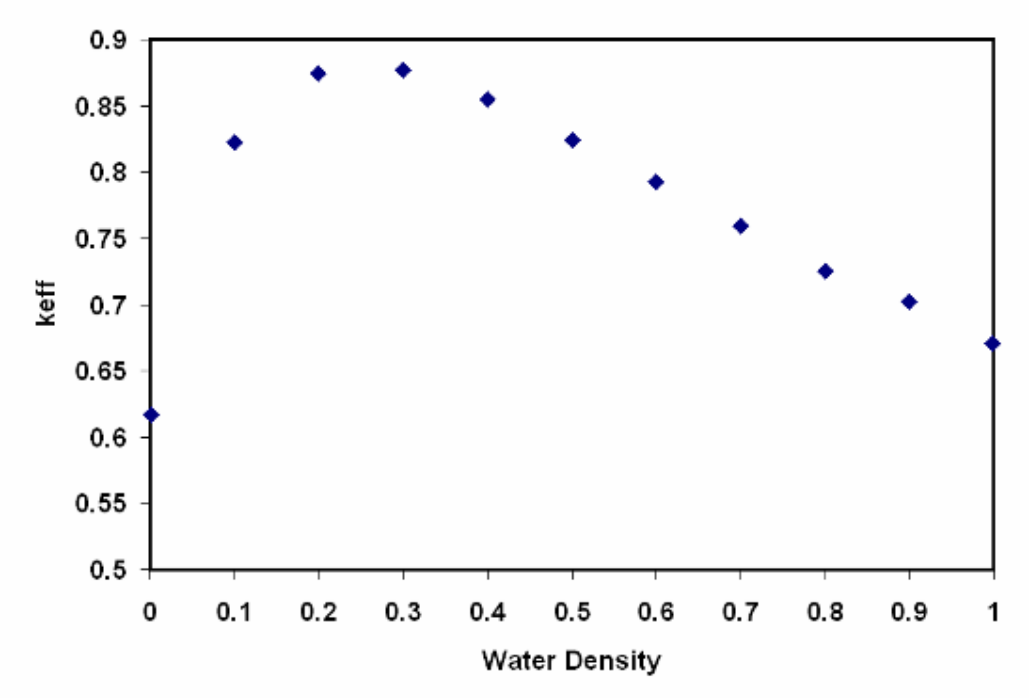

Figure 13: k_{eff} for Varying Water Densities showing Optimum Moderation (2 Dry Storage Cells)

5.1.3 Wet Cell Storage

Table 12: k_{eff} of Wet Storage Cells with Packing Fraction of 0.61 at Different Temperatures

Packing Fraction: 0.61				
Storage Cell Types	Normal (no H_2O on the inside, but only on the outside of containers)	No H_2O inside and outside containers	H_2O inside containers only	H_2O inside and outside all containers
Models at 300 K				
1 Wet Cell	0.5213 (0.0015)	0.5545 (0.0012)	0.59981 (0.00085)	0.59949 (0.00091)
2 Wet Cells	0.5196 (0.0012)	0.5563 (0.0013)	0.6030 (0.0011)	0.60104 (0.00093)
Models at 335 K				
1 Wet Cell	0.5156 (0.0019)	0.5467 (0.0013)	0.59990 (0.00089)	0.5968 (0.0015)
2 Wet Cells	0.5154 (0.0012)	0.5472 (0.0012)	0.59991 (0.00064)	0.59778 (0.00085)
Models at 370 K				
1 Wet Cell	0.5129 (0.0013)	0.5410 (0.0013)	0.5981 (0.0013)	0.5986 (0.0013)
2 Wet Cells	0.5133 (0.0014)	0.5417 (0.0012)	0.59826 (0.00082)	0.59739 (0.00094)

Table 13: k_{eff} of Wet Storage Cells with Packing Fraction of 0.64 at Different Temperatures

Packing Fraction: 0.64				
Storage Cell Types	Normal (no H_2O on the inside but only on the outside of containers)	No H_2O inside and outside containers	H_2O inside containers only	H_2O inside and outside all containers
Models at 300 K				
1 Wet Cell	0.5569 (0.0014)	0.5880 (0.0012)	0.64006 (0.00086)	0.64239 (0.00099)
2 Wet Cells	0.5580 (0.0012)	0.5860 (0.0013)	0.6417 (0.0011)	0.64169 (0.00079)
Models at 335 K				
1 Wet Cell	0.5523 (0.0013)	0.5798 (0.0014)	0.6393 (0.0011)	0.63516 (0.00086)
2 Wet Cells	0.5507 (0.0015)	0.5788 (0.0014)	0.6397 (0.0010)	0.6372 (0.0011)
Models at 370 K				
1 Wet Cell	0.5485 (0.0013)	0.5733 (0.0013)	0.63747 (0.00092)	0.6368 (0.0014)
2 Wet Cells	0.5458 (0.0015)	0.5741 (0.0013)	0.6357 (0.0012)	0.6343 (0.0014)

Table 14: k_{eff} of Wet Storage Cells with Packing Fraction of 0.66 at Different Temperatures

Packing Fraction: 0.66				
Storage Cell Types	Normal (no H_2O on the inside but only on the outside of containers)	No H_2O inside and outside containers	H_2O inside containers only	H_2O inside and outside all containers
Models at 300 K				
1 Wet Cell	0.5802 (0.0016)	0.6097 (0.0013)	0.6696 (0.0010)	0.67026 (0.00092)
2 Wet Cells	0.5804 (0.0016)	0.6090 (0.0015)	0.6688 (0.0010)	0.66870 (0.00089)
Models at 335 K				
1 Wet Cell	0.5725 (0.0020)	0.6009 (0.0013)	0.6641 (0.0011)	0.6661 (0.0011)
2 Wet Cells	0.5730 (0.0015)	0.6021 (0.0014)	0.66585 (0.00094)	0.6608 (0.0010)
Models at 370 K				
1 Wet Cell	0.5725 (0.0017)	0.5962 (0.0014)	0.66180 (0.00089)	0.66033 (0.00097)
2 Wet Cells	0.5668 (0.0013)	0.5947 (0.0015)	0.66475 (0.00075)	0.66409 (0.00098)

5.1.4 Optimum Moderation of the Model (1 Wet Storage Cell at Temperature 300 K with Packing Fraction of 0.66) with the Largest k_{eff}

Table 15: k_{eff} for Varying Water Densities (inside containers) showing Optimum Moderation (1 Wet Storage Cell)

Water Density (g/cm^3)	k_{eff}
0.001	0.5838 (0.0017)
0.1	0.7965 (0.0017)
0.2	0.8572 (0.0016)
0.3	0.8610 (0.0013)
0.4	0.8443 (0.0019)
0.5	0.8195 (0.0012)
0.6	0.7886 (0.0016)
0.7	0.7567 (0.0010)
0.8	0.7260 (0.0013)
0.9	0.6957 (0.0014)
0.9982	0.6664 (0.001)

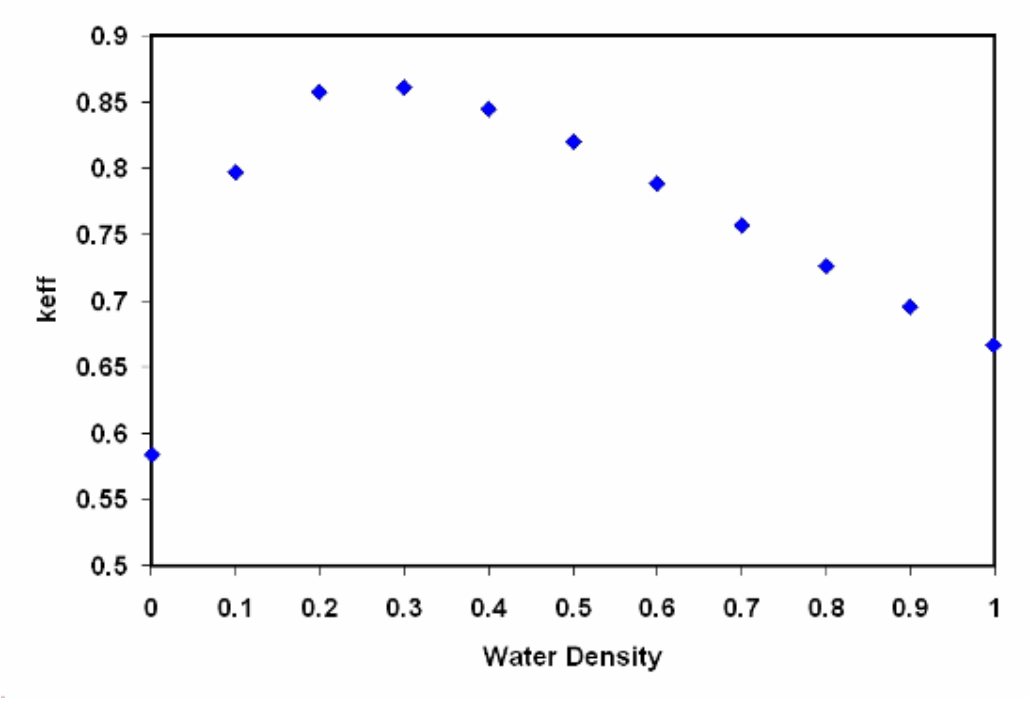

Figure 14: k_{eff} for Varying Water Densities showing Optimum Moderation (2 Wet Storage Cells)

5.1.5 1 Dry Storage Cell Adjacent to a Wet Storage Cell

Table 16: k_{eff} of Wet-Dry Storage Cells with Packing Fraction of 0.61 at Different Temperatures

Packing Fraction: 0.61					
Storage Cell Type	Normal (no H_2O on the inside of containers for both cells, but only on the outside of the wet storage containers)	No H_2O inside and outside containers	H_2O inside containers only	H_2O inside and outside all containers	H_2O outside containers only
Models at 300 K					
Wet-Dry Cell	0.5576 (0.0013)	0.5539 (0.0012)	0.60024 (0.00078)	0.6015 (0.0011)	0.5220 (0.0014)
Models at 335 K					
Wet-Dry Cell	0.5546 (0.0016)	0.5499 (0.0017)	0.5995 (0.0010)	0.59821 (0.00092)	0.5166 (0.0013)
Models at 370 K					
Wet-Dry Cell	0.5462 (0.0013)	0.5429 (0.0012)	0.60012 (0.00072)	0.5947 (0.0014)	0.5107 (0.0018)

Table 17: k_{eff} of Wet-Dry Storage Cells with Packing Fraction of 0.64 at Different Temperatures

Packing Fraction: 0.64					
Storage Cell Type	Normal (no H_2O on the inside of containers for both cells, but only on the outside of the wet storage containers)	No H_2O inside and outside containers	H_2O inside containers only	H_2O inside and outside all containers	H_2O outside containers only
Models at 300 K					
Wet-Dry Cell	0.5910 (0.0017)	0.5925 (0.0020)	0.6424 (0.0011)	0.64175 (0.00081)	0.5572 (0.0013)
Models at 335 K					
Wet-Dry Cell	0.5836 (0.0014)	0.5832 (0.0011)	0.63633 (0.00095)	0.6380 (0.0010)	0.5512 (0.0015)
Models at 370 K					
Wet-Dry Cell	0.5773 (0.0013)	0.5767 (0.0013)	0.6405 (0.0013)	0.63532 (0.000840	0.5457 (0.0015)

Table 18: k_{eff} of Wet-Dry Storage Cells with Packing Fraction of 0.66 at Different Temperatures

Packing Fraction: 0.66					
Storage Cell Type	Normal (no H_2O on the inside of containers for both cells, but only on the outside of the wet storage containers)	No H_2O inside and outside containers	H_2O inside containers only	H_2O inside and outside all containers	H_2O outside containers only
Models at 300 K					
Wet-Dry Cell	0.6149 (0.0021)	0.6102 (0.0013)	0.6706 (0.0011)	0.6665 (0.0013)	0.5810 (0.0014)
Models at 335 K					
Wet-Dry Cell	0.6033 (0.0013)	0.6071 (0.0013)	0.66657 (0.00098)	0.66651 (0.00084)	0.5764 (0.0015)
Models at 370 K					
Wet-Dry Cell	0.5985 (0.0014)	0.5975 (0.0017)	0.6647 (0.0012)	0.6622 (0.0010)	0.5664 (0.0016)

5.1.6 Optimum Moderation of the Model (Wet-Dry Cell at temperature 300 K with Packing Fraction of 0.66) with the largest k_{eff}

Table 19: k_{eff} for Varying Water Densities (inside containers) showing Optimum Moderation (Wet-Dry Cell)

Water Density (g/cm^3)	k_{eff}
0.001	0.6194 (0.0016)
0.1	0.6194 (0.0016)
0.2	0.8206 (0.0017)
0.3	0.8731 (0.0013)
0.4	0.8537 (0.0013)
0.5	0.8273 (0.0012)
0.6	0.7925 (0.0014)
0.7	0.7616 (0.0018)
0.8	0.72721 (0.00085)
0.9	0.6983 (0.0011)
0.9982	0.6706 (0.0011)

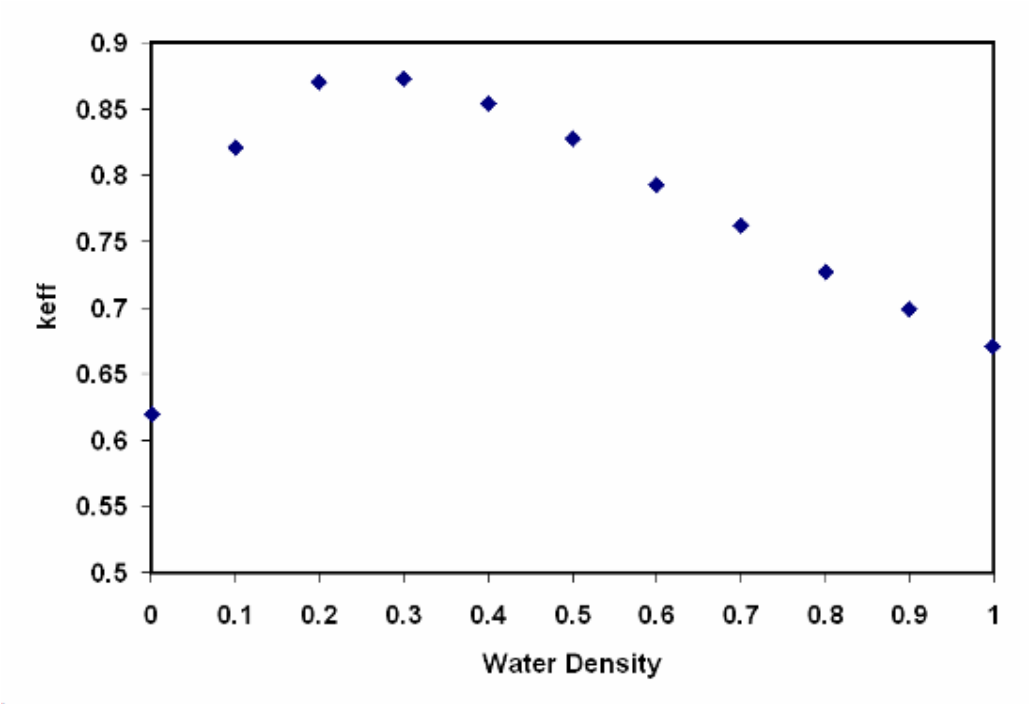

Figure 15: k_{eff} for Varying Water Densities showing Optimum Moderation (Wet-Dry Cell)

5.1.7 Whole Model

Table 20: k_{eff} of Whole Model with Packing Fraction of 0.61 at Different Temperatures

Packing Fraction: 0.61					
Storage Cell Type	Normal (no H_2O on the inside of containers for both cells, but only on the outside of the wet storage containers)	No H_2O inside and outside containers	H_2O inside containers only	H_2O inside and outside all containers	H_2O outside containers only
Models at 300 K					
All Storage Cells	0.5597 (0.0013)	0.5564 (0.0015)	0.5991 (0.0011)	0.59976 (0.00083)	0.5237 (0.0011)
Models at 335 K					
All Storage Cells	0.5496 (0.0015)	0.5512 (0.0014)	0.59773 (0.00078)	0.59933 (0.00087)	0.5187 (0.0015)
Models at 370 K					
All Storage Cells	0.5442 (0.0014)	0.5453 (0.0012)	0.5948 (0.0013)	0.5985 (0.0014)	0.5101 (0.0012)

Table 21: k_{eff} of Whole Model with Packing Fraction of 0.64 at Different Temperatures

Packing Fraction: 0.64					
Storage Cell Type	Normal (no H_2O on the inside of containers for both cells, but only on the outside of the wet storage containers)	No H_2O inside and outside containers	H_2O inside containers only	H_2O inside and outside all containers	H_2O outside containers only
Models at 300 K					
All Storage Cells	0.5925 (0.0013)	0.5927 (0.0015)	0.6414 (0.0011)	0.6395 (0.0011)	0.5569 (0.0014)
Models at 335 K					
All Storage Cells	0.5846 (0.0012)	0.5834 (0.0014)	0.6381 (0.0010)	0.63772 (0.00088)	0.5523 (0.0018)
Models at 370 K					
All Storage Cells	0.5766 (0.0015)	0.5769 (0.0014)	0.6344 (0.0012)	0.63567 (0.00098)	0.5439 (0.0015)

Table 22: k_{eff} of Whole Model with Packing Fraction of 0.66 at Different Temperatures

Packing Fraction: 0.66					
Storage Cell Type	Normal (no H_2O on the inside of containers for both cells, but only on the outside of the wet storage containers)	No H_2O inside and outside containers	H_2O inside containers only	H_2O inside and outside all containers	H_2O outside containers only
Models at 300 K					
All Storage Cells	0.6112 (0.0014)	0.6125 (0.0014)	0.66876 (0.0009)	0.66758 (0.00083)	0.5808 (0.0013)
Models at 335 K					
All Storage Cells	0.6052 (0.0013)	0.6044 (0.0013)	0.66540 (0.00082)	0.6654 (0.0011)	0.5745 (0.0015)
Models at 370 K					
All Storage Cells	0.5980 (0.0015)	0.6002 (0.0015)	0.6621 (0.0010)	0.6632 (0.0010)	0.5684 (0.0018)

5.1.8 Optimum Moderation of the Whole Model (All Cells at temperature 300 K with Packing Fraction of 0.66) with the largest k_{eff}

Table 23: k_{eff} for Varying Water Densities (inside containers) showing Optimum Moderation (Whole Model)

Water Density (g/cm^3)	k_{eff}
0.001	0.6187 (0.0013)
0.1	0.6187 (0.0013)
0.2	0.8209 (0.0018)
0.3	0.8718 (0.0015)
0.4	0.8532 (0.0011)
0.5	0.8229 (0.0014)
0.6	0.7910 (0.0013)
0.7	0.7604 (0.0012)
0.8	0.7245 (0.0012)
0.9	0.6955 (0.0011)
0.9982	0.66876 (0.0009)

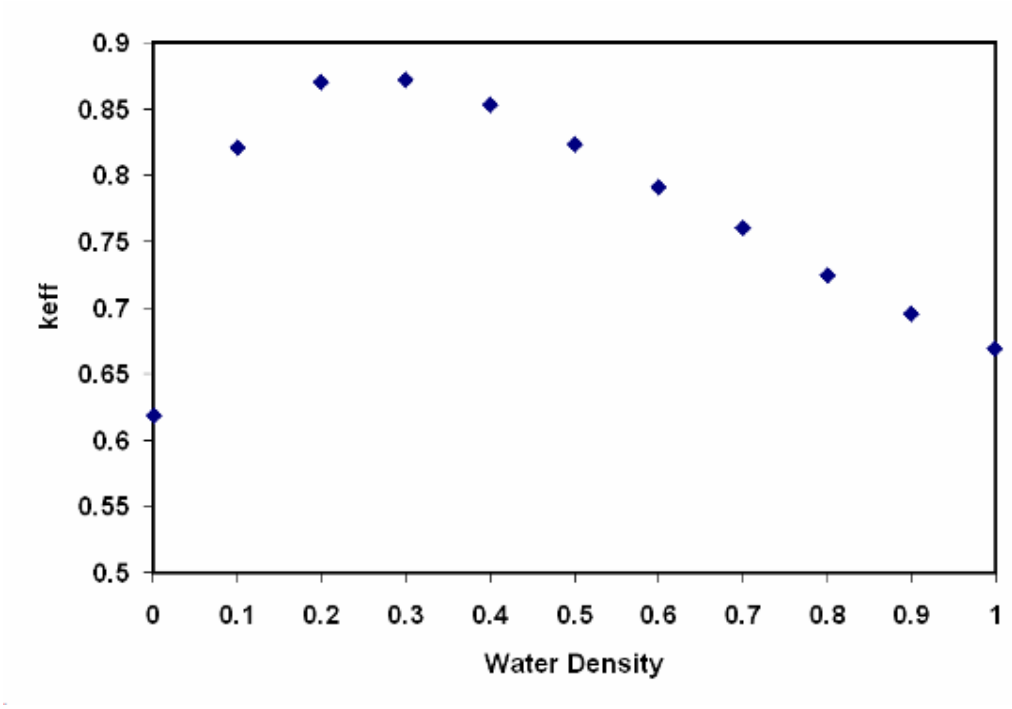

Figure 16: k_{eff} for Varying Water Densities showing Optimum Moderation (Whole Model)

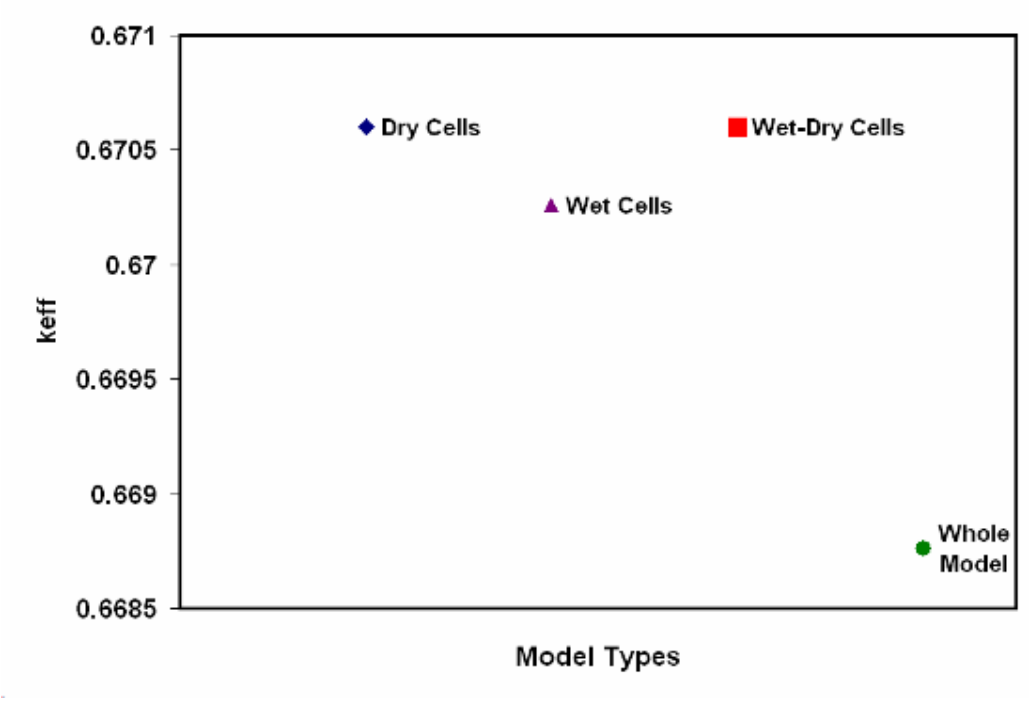

Figure 17: k_{eff} Values for the Most Reactive Configuration of each Model Type

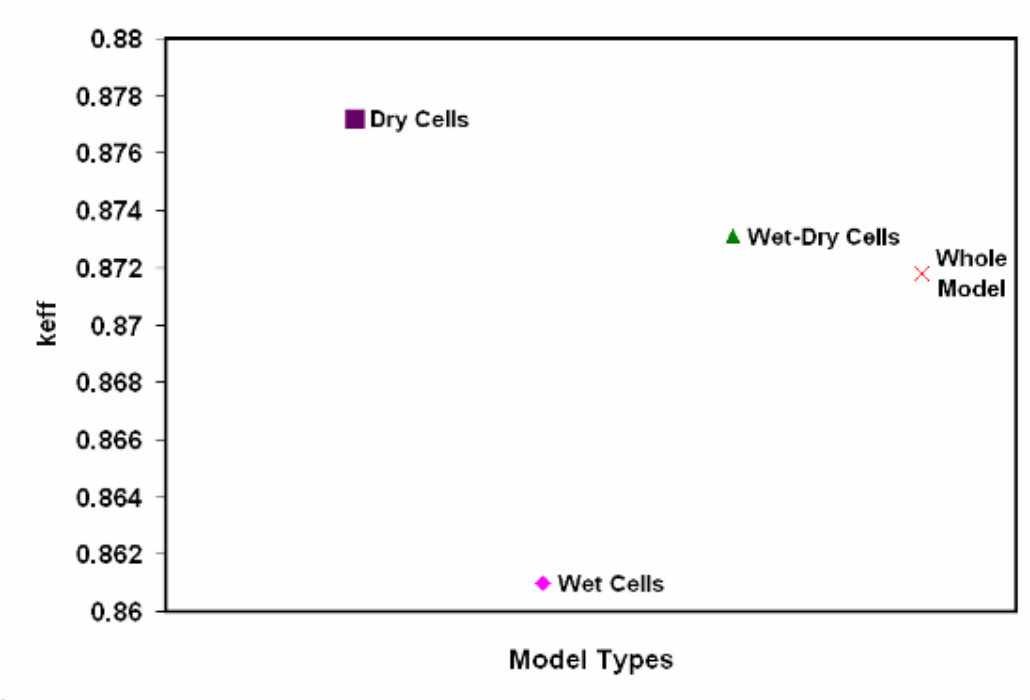

Figure 18: k_{eff} Values at Optimum Moderation for the Most Reactive Configuration of each Model Type

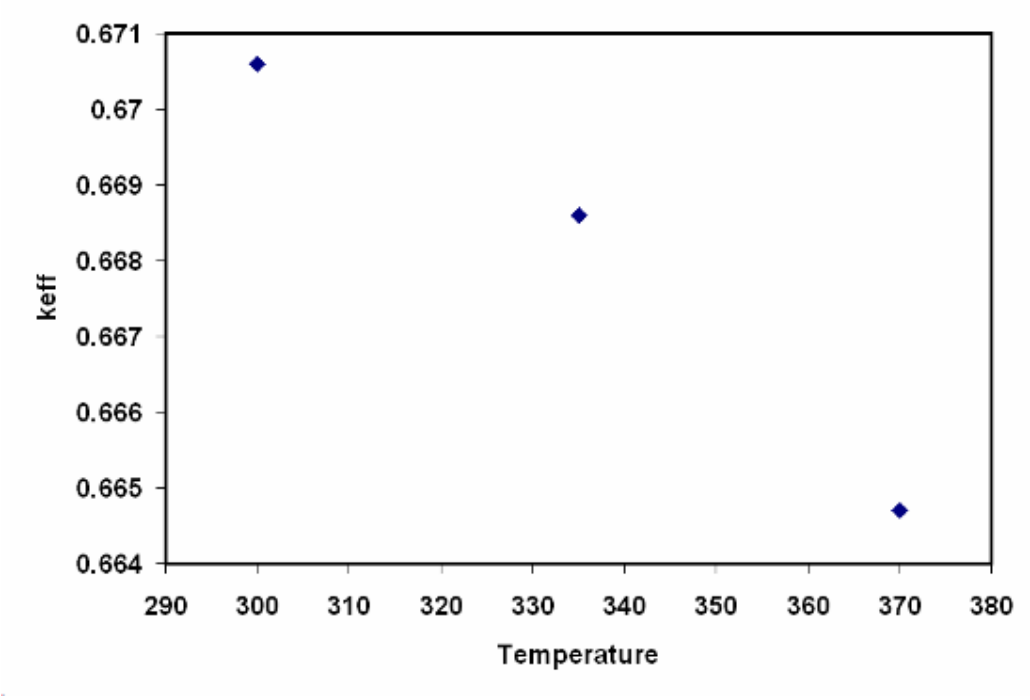

Figure 19: Maximum k_{eff} obtained at each Temperature Analysed

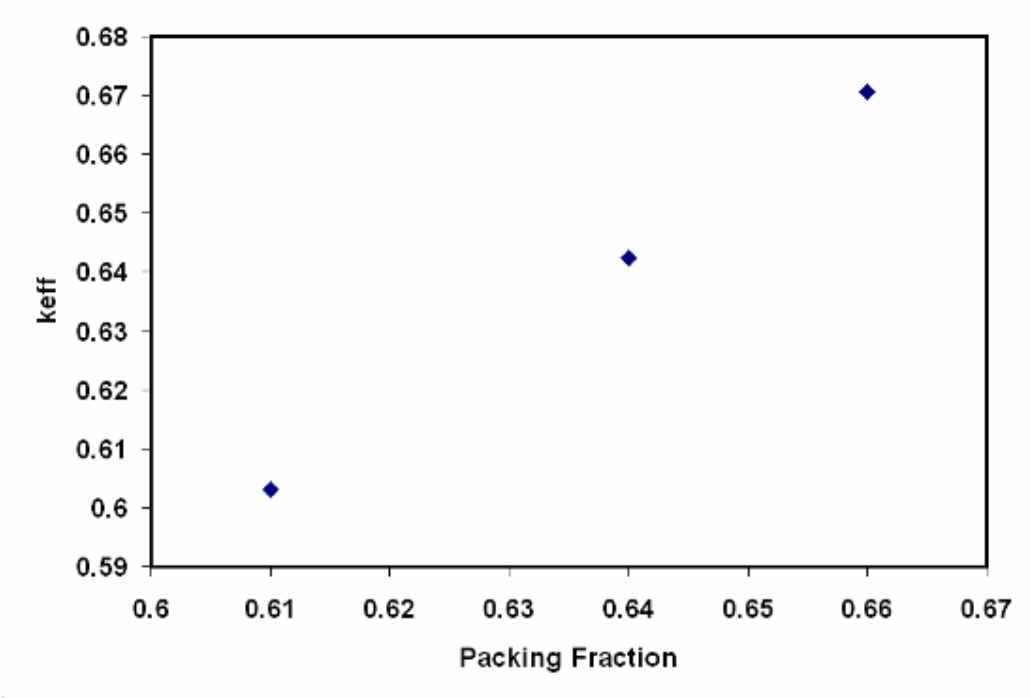

Figure 20: Maximum k_{eff} obtained for each Packing Fraction Analysed

5.1.9 Fresh Fuel Spheres (4.2 w/o Enriched)

Table 24: k_{eff} for the Most Reactive Configuration of Each Model Type when containing 4.2 w/o enriched Fresh Fuel

Most Reactive Configuration for Each Model Type	k_{eff}
Dry Cells	0.5258 (0.0010)
Wet Cells	0.52514 (0.00085)
Wet-Dry Cell	0.52597 (0.00091)
Whole Model	0.52614 (0.00086)

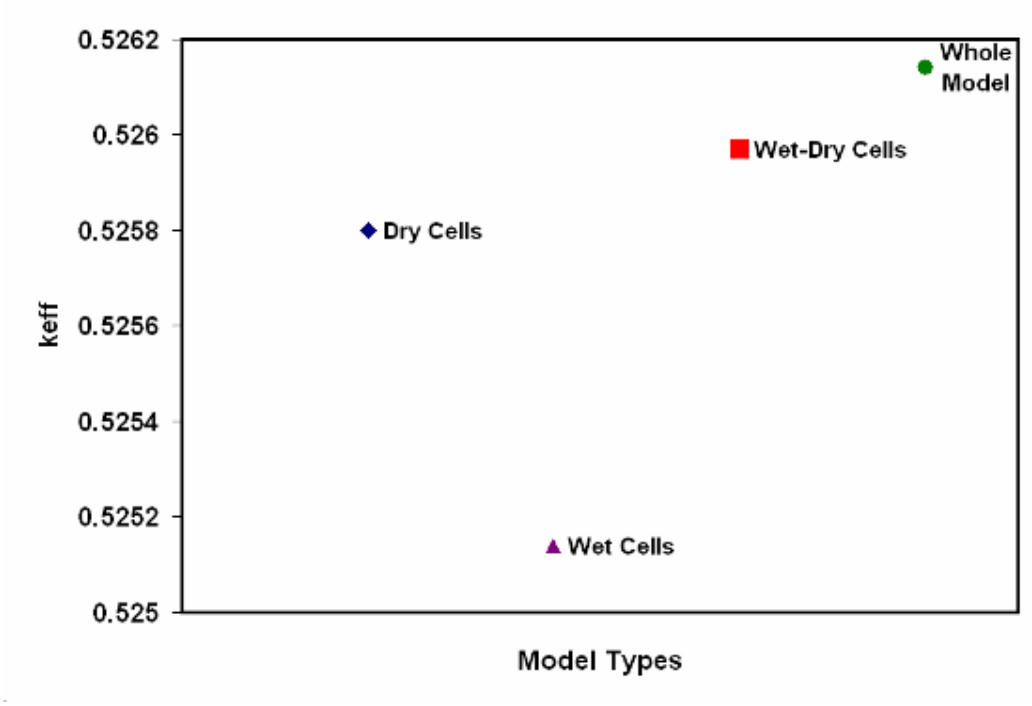

Figure 21: Maximum k_{eff} obtained for Most Reactive Configuration of each type of Model when filled with 4.2 w/o Enriched Fresh Fuel

5.1.10 Graphite Spheres interspersed within Fresh Fuel Spheres (4.2 w/o enriched)

Table 25: k_{eff} for Different Percentages of Graphite Spheres amongst 4.2 w/o enriched Fresh Fuel

Percentage of Graphite Spheres in each Storage Container	k_{eff}
0	0.52597 (0.00091)
6	0.50484 (0.00097)
8	0.49411 (0.00086)
10	0.48787 (0.00085)

5.1.11 Graphite Spheres interspersed within Used Fuel Spheres from the Most Reactive Core

Table 26: k_{eff} for Different Percentages of Graphite Spheres amongst Fuel Spheres from the Most Reactive Core

Percentage of Graphite Spheres in each Storage Container	k_{eff}
0	0.6706 (0.0011)
6	0.6449 (0.0012)
8	0.63449 (0.00078)
10	0.62805 (0.00093)

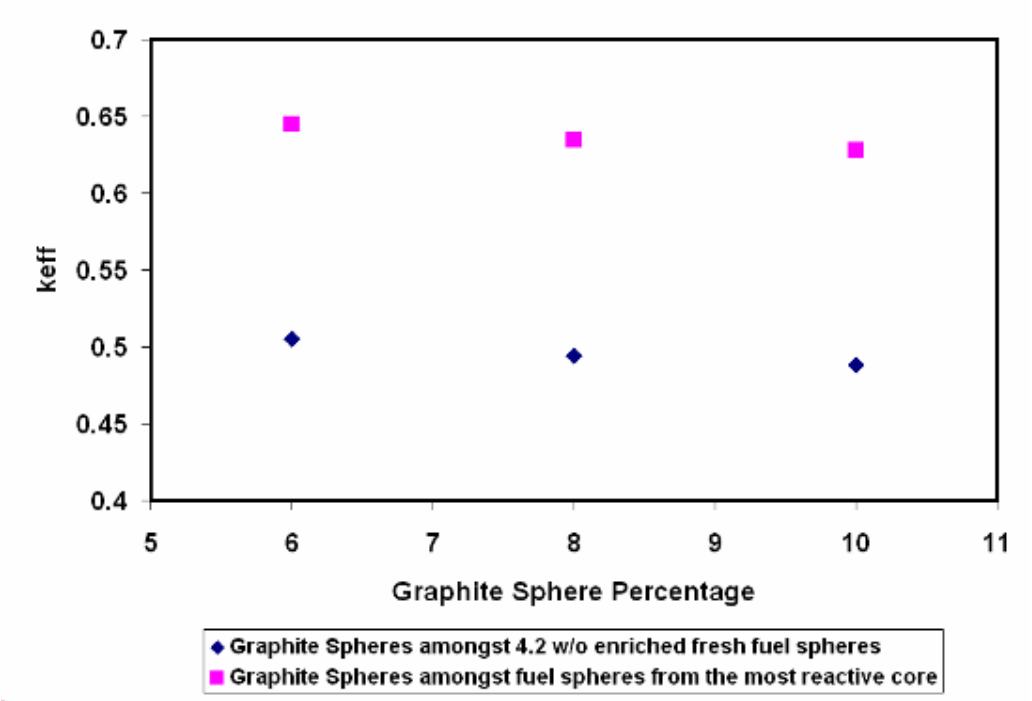

Figure 22: k_{eff} for Different Percentages of Graphite Spheres

5.1.12 Optimum Moderation of the Low Burnup Cluster Model

Table 27: k_{eff} for the Clusters in the Most Reactive Model Configuration at Varying Water Densities inside Containers (Temperature at 300 K and Packing Fraction at 0.66)

Water Density(g/cm^3)	k_{eff}
0.001	0.6320 (0.0016)
0.1	0.8398 (0.0017)
0.2	0.8929 (0.0015)
0.3	0.8985 (0.0015)
0.4	0.8816 (0.0015)
0.5	0.8511 (0.0013)
0.6	0.8204 (0.0011)
0.7	0.7866 (0.0010)
0.8	0.7576 (0.0011)
0.9	0.72402 (0.00097)
0.9982	0.6927 (0.0013)

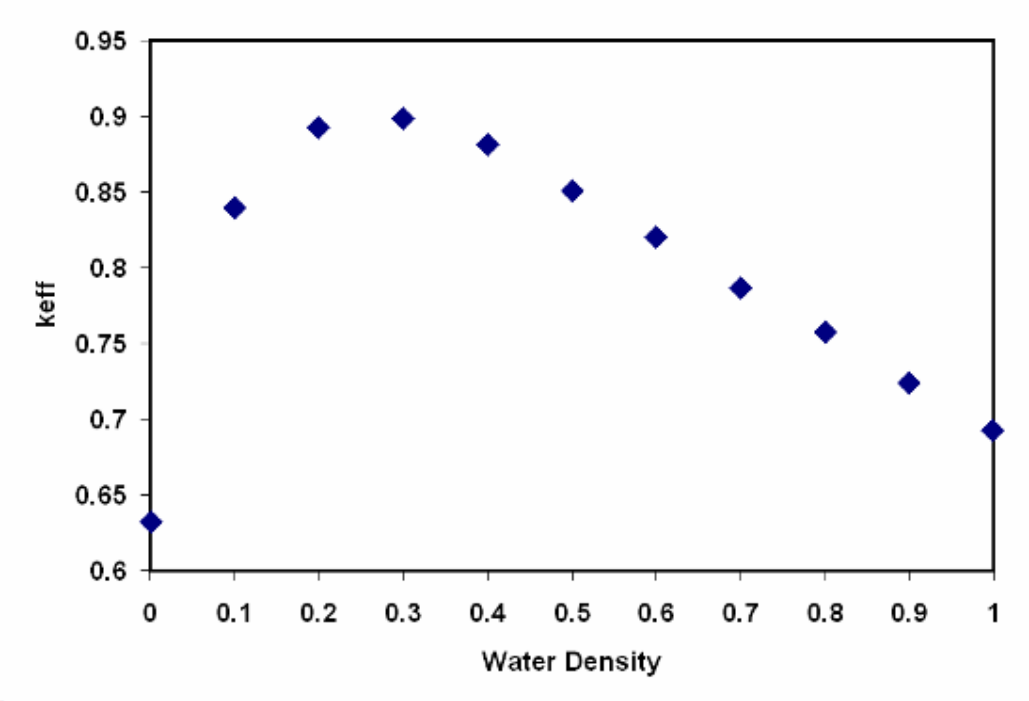

Figure 23: k_{eff} for the Clusters in the Most Reactive Model Configuration at Varying Water Densities

Table 28: k_{eff} of Fuel Spheres in a Storage Cell from 6 Burst Storage Containers at Varying Water Densities (Temperature of 300 K and a Packing Fraction of 0.61)

Water Density (g/cm^3)	k_{eff}
0.001	0.8008 (0.0012)
0.1	1.0849 (0.0013)
0.2	1.2511 (0.0014)
0.3	1.3399 (0.0011)
0.4	1.3890 (0.0013)
0.5	1.4200 (0.0016)
0.6	1.4354 (0.0012)
0.7	1.4373 (0.0017)
0.8	1.4332 (0.0014)
0.9	1.4255 (0.0013)
0.9982	1.4117 (0.0016)

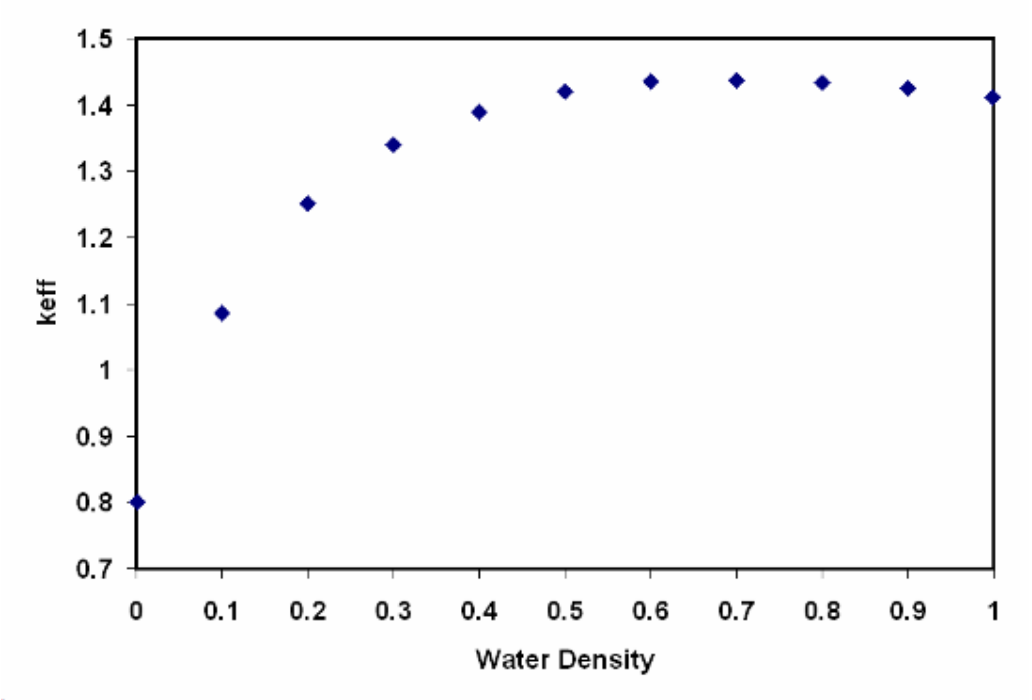

Figure 24: k_{eff} of Fuel Spheres in a Storage Cell from 6 Burst Storage Containers at Varying Water Densities (Temperature of 300 K and a Packing Fraction of 0.61)

5.2 DISCUSSION OF THE RESULTS

A large number of models were developed during the study in order to investigate the sensitivity of k_{eff} to changes in various parameters. It is interesting to note that a number of common trends were observed amongst the models, although the models ranged from a single storage cell to the whole spent storage facility.

The results reveal that for cases of water in the cells (outside the storage containers) for all the models at the various packing fractions and temperatures has the least reactivity. The introduction of air into the cells raises the reactivity significantly in all the models. This indicates that water in the cell decouples the storage containers neutronically. When water was introduced into the containers, it was found that the k_{eff} of a model with water inside and outside the containers has more or less the same value of k_{eff} as for a model with only water inside the containers. This implies that in those cases the importance of decoupling by the water in the cells (outside the containers) has been reduced due to water inside the containers. This could be due to several effects such as the neutron absorption by the water in the containers or spectrum changes. However the highest reactivity is observed for cases with water inside the containers implying that the absorption is far less than the increased moderation by the introduction of the water. The PBMR fuel with the heavy metal loading of 9 grams is under moderated and explains the relative large effect of adding water (k_{eff} increase from 0.6097 to 0.6696 for 1 Wet cell). With an optimal water concentration inside the container this increases to 0.8610).

For a given model with a fixed packing fraction, it was found that for temperatures, 300 K, 335 K and 370 K, the k_{eff} value decreases with increasing temperature as expected (showed in most of the cases or results fall within the calculation uncertainty).

All four of the model types had their maximum k_{eff} value for the same packing fraction of 0.66 and temperature of 300 K, as well as for the same modelled off-normal event (ingress of water into the storage containers) with the exception for the wet cell storage type (water ingress into the storage containers and cells). This is expected as the configurations that contain fuel spheres immersed directly in water should be more reactive at lower temperatures because of the resonance effects. The two dry-cell and the wet-dry storage types had the largest maximum k_{eff} and the whole model type the lowest.

The water inside and outside the container modelled event that had the highest k_{eff} from all the four model types had the water density inside the container varied to obtain the optimal moderation condition. Optimal moderation occurs in the water density region of 0.3 g/cm^3 for water inside the container.

The value of k_{eff} increases with the increase in packing fraction for a given model at a given temperature. This trend is consistent and occurs for all the models studied at all the different temperatures. The trend is as expected because the increase in the packing fraction allows more fissile material per unit volume, thereby increasing the reactivity.

The evaluation of the clustering of low burnup fuel spheres in the storage containers yield a k_{eff} value higher than for the other models but still far below the 0.95 value. It was also observed that optimum moderation also occurred for water density in the region of 0.3 g/cm^3. For conservatism in pebble fuel criticality calculations, clustering of low burnup pebbles should be considered. For the current design conservatively assuming all these clusters of low burnup fuel to be fresh was still critical safe. The effect is therefore a combination of replacing fuel of the average core in the most reactive case with fresh fuel and grouping these in clusters.

The analyses of the addition of pure graphite spheres into the fuel storage containers reveals that the reactivity decreases with increasing quantities of graphite indicating that the accidental loading of graphite spheres with fuel from the most reactive core into the containers does not pose a safety concern . The same trend was observed when increasing quantities of graphite were added to the containers filled with 4.2 w/o enriched fresh fuel spheres.

It can also be concluded that the storage cells are loosely coupled neutronically. The eigenvalue of storage cell pairs or individual cells does not differ significantly from that of the entire facility.

The investigation of the consequence of six storage containers bursting and releasing all the stored fuel spheres from the containers into a storage cell filled with water reveal that the configuration will go critical (k_{eff} > 1.0). It was assumed that three storage containers contained fuel from the most reactive core and the remaining three contained fresh 4.2 w/o

enriched fuel. This equated to filling the storage cell with almost 2 core worth of highly reactive fuel. The probability that the core will require a full-core offload at the point in the cycle of highest reactivity then followed closely by another full core offload of fresh start-up fuel can be considered to be beyond design basis. Furthermore, the amount of time needed to refill the core after the first offload would give the operators sufficient time to direct the second core offload into the other wet cell. In the unlikely event that above situation does occur, the probability of all the containers then bursting and being immersed in water should be extremely small. The results show that the above scenario is still critical safe provided that no water enters the cell after the containers have burst. For these reasons, a design change is not considered necessary.

6. CONCLUSION

The primary intention of this study was to investigate the safety of the proposed Used and Spent Fuel Storage Facility of the PBMR from the aspect of criticality. The indicator used to demonstrate the margins of subcriticality was the universally accepted Effective Neutron Multiplication Factor, k_{eff}. A criticality safety analyses performed on a system that yields a k_{eff} of less than or equal to 0.95 implies that the system is critical safe. Therefore, all mention of critical safe models in this study implies that the k_{eff} calculated for that particular system is equal or less than 0.95.

I am satisfied that this study bounds the range of plausible events and the important phenomena that affect criticality were investigated. The results obtained show that, for all design basis scenarios, the Effective Neutron Multiplication Factor will always be well below the 0.95 value, indicating that this proposed design is critical safe. The one configuration that indicated a criticality risk is considered both beyond design basis and easily preventable. Therefore, this study shows that the proposed design of the sphere storage system is adequate from the perspective of criticality safety.

It is always good practice that work done with respect to safety, especially criticality safety, should also be validated independently using the same code or another code to set up the models as done in this study and to compare the results obtained. Therefore, I suggest that future work as a result of this study could form part of a separate set of analyses, using a different code (like MCNP) to evaluate the safety of the storage facility from the criticality perspective. Verification of calculation techniques should also be done by comparing with experimental results. An experiment on a cold-critical facility (such as PROTEUS or ASTRA) to confirm a number of parameters in the design should also be considered. Additional future work should be done in the area of deformation of the storage containers and the load/unload mechanism as well as misplacement of the load/unload mechanism as these issues were not covered in this study.

7. BIBLIOGRAPHY

The following documents are referenced within this document.

[1] The DME, “National Response to South Africa’s Electricity Shortage”, Department: Minerals and Energy, Republic of South Africa, January 2008.

[2] Information from Energy Intensive Users Group, ”South Africa’s Electricity Supply/Demand Balance – 2006 to 2021”, Energize, June 2006.

[3] Matzner, D., “PBMR Project Status and the Way Ahead”, 2nd International Topical Meeting on High Temperature Reactor Technology, Beijing, China, September 22-24, 2005.

[4] Goluoglu, S., Williams M. L., ”Modeling Doubly Heterogeneous Systems in SCALE”, Submitted to the American Nuclear Society 2005 Winter Meeting “Talk About Nuclear Differently: A Good Story Untold”, Washington D.C, November 13-17, 2005.

[5] Drijfhout, F., “SSS Criticality Analysis Input Data”, Doc. No. FHDI-000220-229/1, Rev. D, Westinghouse, South Africa, Centurion, 2008.

[6] http://www.iaea.org/Publications/Factsheets/English/ines.pdf

[7] Goluoglu, S., “Analysis of a Computational Benchmark for a High-Temperature Reactor Using Scale”, Oak Ridge National Laboratory, Oak Ridge, Tennessee.

[8] Snoj, L., Ravnik, M., ”Effect of Packing Fractions Variations on Reactivity in Pebble-Bed Reactor”, International Conference: Nuclear Energy for New Europe 2004”, Portoroz, Slovenia, September 6-9, 2004

[9] Lee, J S (IAEA Officer), “Operation and Maintenance of Spent Fuel Storage and Transportation Casks/Containers” IAEA TECDOC-1532, International Atomic Energy Agency, Vienna, January 2007.

[10] SCALE: A Modular Code System for Performing Standardized Computer Analyses for Licensing Evaluation, ORNL/TM-2005/39, Version 5.1, Vols. I–III, November 2006. Available from Radiation Safety Information Computational Center at Oak Ridge National Laboratory as CCC-732.

[11] Venter, J., Haley, R., Bowden R, L., “K-Effective as a Measure of Criticality Safety”, Nuclear Technologies plc, Cheshire, United Kingdom.

[12] Reitsma, F., Stoker C, C., “PBMR Used Fuel Storage Criticality for Most Reactive Core Loading”, The 8th International Conference on Nuclear Criticality Safety, St Petersburg, Russia, May 28 – June 1, 2007.

[13] Van Heerden, G., Gxumisa, N., “Design and SAR-2 Reactor Model Input for the VSOP, TINTE and MCNP Codes – Geometrical and Material Property Data”, Doc. No. 022028, Rev. 1A, Pebble Bed Modular Reactor Company, Centurion, August 2008.

[14] http://en.wikipedia.org/wiki/Rhombic_dodecahedron

8. APPENDIX: INPUT FOR THE SPHERE STORAGE SYSTEM (WHOLE MODEL AT TEMPERATURE OF 300 K WITH A PACKING FRACTION OF 0.61. WATER IS PRESENT ONLY IN THE WET CELLS, AIR IN THE DRY CELLS AND BETWEEN ALL THE FUEL SPHERES)

```
=csas26     parm=(centrm)
Sphere Storage System (Whole Model)
V6-238
read comp
' fuel kernel
  u-234 1 0 1.8069e-5 300 end
  u-235 1 0 1.2133e-3 300 end
  u-236 1 0 1.7747e-4 300 end
  u-238 1 0 2.0451e-2 300 end
  np-237 1 0 6.5079e-6 300 end
  pu-239 1 0 1.0596e-4 300 end
  pu-240 1 0 4.6801e-5 300 end
  pu-241 1 0 3.4344e-5 300 end
  pu-242 1 0 1.4186e-5 300 end
  o 1 0 4.6152e-2 300 end

' buffer
  c 2 den=1.05 1 300 end
' inner pyrolytic carbon
  c 3 den=1.9 1 300 end

'silicon carbide
  atom-sic 4 3.18 2 14000 1 6000 1 1 300 end
' outer pyrolytic carbon
  c 5 den=1.9 1 300 end

'graphite matrix
  c 6 den=1.74 1 300 end
'pebble coating(cladding)
  c 7 den=1.72 1 300 end

'water between pebbles
  h2o 8 den=0.9982 1 300 end
'steel container
  ss304 9 1 300 end
```

```
'air
  atom-air 11 1.204E-3 3 6000 0.0126 7014 76.508 8016 23.4793 1 300 end

'Concrete
  reg-concrete 12 1 300 end

end comp

read celldata
  doublehet right_bdy=white fuelmix=10 end
  gfr=0.025 1 coatt=0.0095 2 coatt=0.004 3 coatt=0.0035 4 coatt=0.004 5
  matrix=6 numpar=15000 end grain
  pebble sphtriangp right_bdy=white hpitch=3.2002 8 fuelr=2.5 cladr=3.0 7 end
  centrm data
    ixprt=1 isn=8 nprt=2
  end centrm
end celldata

read geom
  unit 1
    sphere 20 2.5
    sphere 30 3.0
    dodecahedron 40 3.2002
    media 10 1 20
    media 7 1 30 -20
    media 11 1 40 -30
  boundary 40

  unit 2
    dodecahedron 20 3.2002
    media 11 1 20
  boundary 20

  unit 3
    cylinder 1 44.0 926.4 -1050.4 origin x=0.0 y=0.0 z=0.0
    array 1 1 place 17 17 1 0.0 0.0 -1052.3
  boundary 1
  unit 4
    cylinder 1 46.0 926.4 881.9 origin x=0.0 y=0.0 z=0.0
```

media 9 1 1

cylinder 2 46.0 841.9 771.9 origin x=0.0 y=0.0 z=0.0

media 9 1 2

cylinder 3 46.0 731.9 661.9 origin x=0.0 y=0.0 z=0.0

media 9 1 3

cylinder 4 46.0 621.9 551.9 origin x=0.0 y=0.0 z=0.0

media 9 1 4

cylinder 5 46.0 511.9 441.9 origin x=0.0 y=0.0 z=0.0

media 9 1 5

cylinder 6 46.0 401.9 331.9 origin x=0.0 y=0.0 z=0.0

media 9 1 6

cylinder 7 46.0 291.9 221.9 origin x=0.0 y=0.0 z=0.0

media 9 1 7

cylinder 8 46.0 181.9 111.9 origin x=0.0 y=0.0 z=0.0

media 9 1 8

cylinder 9 46.0 71.9 1.9 origin x=0.0 y=0.0 z=0.0

media 9 1 9

cylinder 10 46.0 -38.1 -108.1 origin x=0.0 y=0.0 z=0.0

media 9 1 10

cylinder 11 46.0 -148.1 -218.1 origin x=0.0 y=0.0 z=0.0

media 9 1 11

cylinder 12 46.0 -258.1 -328.1 origin x=0.0 y=0.0 z=0.0

media 9 1 12

cylinder 13 46.0 -368.1 -438.1 origin x=0.0 y=0.0 z=0.0

media 9 1 13

cylinder 14 46.0 -478.1 -548.1 origin x=0.0 y=0.0 z=0.0

media 9 1 14

cylinder 15 46.0 -588.1 -658.1 origin x=0.0 y=0.0 z=0.0

media 9 1 15

cylinder 16 46.0 -698.1 -768.1 origin x=0.0 y=0.0 z=0.0

media 9 1 16

cylinder 17 46.0 -808.1 -878.1 origin x=0.0 y=0.0 z=0.0

media 9 1 17

cylinder 18 46.0 -918.1 -988.1 origin x=0.0 y=0.0 z=0.0

media 9 1 18

cylinder 19 46.0 -1028.1 -1050.4 origin x=0.0 y=0.0 z=0.0

media 9 1 19

hole 3 origin x=0.0 y=0.0 z=0.0

cylinder 20 46.1 926.4 -1050.4 origin x=0.0 y=0.0 z=0.0

media 11 1 20 -1 -2 -3 -4 -5 -6 -7 -8 -9 -10 -11 -12 -13 -14 -15 -16 -17 -18 -19

boundary 20

global unit 5

cylinder 1 84.0 926.4 -1050.4 origin x=-203.1 y=-134.0 z=0.0

cylinder 2 85.6 928.0 -1052.0 origin x=-203.1 y=-134.0 z=0.0

cylinder 3 84.0 926.4 -1050.4 origin x=-203.1 y=134.0 z=0.0

cylinder 4 85.6 928.0 -1052.0 origin x=-203.1 y=134.0 z=0.0

cylinder 5 84.0 926.4 -1050.4 origin x=-471.1 y=-134.0 z=0.0

cylinder 6 85.6 928.0 -1052.0 origin x=-471.1 y=-134.0 z=0.0

cylinder 7 84.0 926.4 -1050.4 origin x=-471.1 y=134.0 z=0.0

cylinder 8 85.6 928.0 -1052.0 origin x=-471.1 y=134.0 z=0.0

cylinder 9 84.0 926.4 -1050.4 origin x=-739.1 y=-134.0 z=0.0

cylinder 10 85.6 928.0 -1052.0 origin x=-739.1 y=-134.0 z=0.0

cylinder 11 84.0 926.4 -1050.4 origin x=-739.1 y=134.0 z=0.0

cylinder 12 85.6 928.0 -1052.0 origin x=-739.1 y=134.0 z=0.0

cylinder 13 84.0 926.4 -1050.4 origin x=-1145.3 y=-134.0 z=0.0

cylinder 14 85.6 928.0 -1052.0 origin x=-1145.3 y=-134.0 z=0.0

cylinder 15 84.0 926.4 -1050.4 origin x=-1145.3 y=134.0 z=0.0

cylinder 16 85.6 928.0 -1052.0 origin x=-1145.3 y=134.0 z=0.0

cylinder 17 84.0 926.4 -1050.4 origin x=-1413.3 y=-134.0 z=0.0

cylinder 18 85.6 928.0 -1052.0 origin x=-1413.3 y=-134.0 z=0.0

cylinder 19 84.0 926.4 -1050.4 origin x=-1413.3 y=134.0 z=0.0

cylinder 20 85.6 928.0 -1052.0 origin x=-1413.3 y=134.0 z=0.0

cylinder 21 84.0 926.4 -1050.4 origin x=-1681.3 y=-134.0 z=0.0

cylinder 22 85.6 928.0 -1052.0 origin x=-1681.3 y=-134.0 z=0.0

cylinder 23 84.0 926.4 -1050.4 origin x=-1681.3 y=134.0 z=0.0

cylinder 24 85.6 928.0 -1052.0 origin x=-1681.3 y=134.0 z=0.0

cylinder 25 84.0 926.4 -1050.4 origin x=173.1 y=-134.0 z=0.0

cylinder 26 85.6 928.0 -1052.0 origin x=173.1 y=-134.0 z=0.0

cylinder 27 84.0 926.4 -1050.4 origin x=173.1 y=134.0 z=0.0

cylinder 28 85.6 928.0 -1052.0 origin x=173.1 y=134.0 z=0.0

cylinder 29 84.0 926.4 -1050.4 origin x=441.1 y=-134.0 z=0.0

cylinder 30 85.6 928.0 -1052.0 origin x=441.1 y=-134.0 z=0.0

cylinder 31 84.0 926.4 -1050.4 origin x=441.1 y=134.0 z=0.0

cylinder 32 85.6 928.0 -1052.0 origin x=441.1 y=134.0 z=0.0

cylinder 33 84.0 926.4 -1050.4 origin x=709.1 y=-134.0 z=0.0

cylinder 34 85.6 928.0 -1052.0 origin x=709.1 y=-134.0 z=0.0

cylinder 35 84.0 926.4 -1050.4 origin x=709.1 y=134.0 z=0.0

cylinder 36 85.6 928.0 -1052.0 origin x=709.1 y=134.0 z=0.0

cylinder 37 84.0 926.4 -1050.4 origin x=1055.3 y=-134.0 z=0.0

cylinder 38 85.6 928.0 -1052.0 origin x=1055.3 y=-134.0 z=0.0
cylinder 39 84.0 926.4 -1050.4 origin x=1055.3 y=134.0 z=0.0
cylinder 40 85.6 928.0 -1052.0 origin x=1055.3 y=134.0 z=0.0
cylinder 41 84.0 926.4 -1050.4 origin x=1323.3 y=-134.0 z=0.0
cylinder 42 85.6 928.0 -1052.0 origin x=1323.3 y=-134.0 z=0.0
cylinder 43 84.0 926.4 -1050.4 origin x=1323.3 y=134.0 z=0.0
cylinder 44 85.6 928.0 -1052.0 origin x=1323.3 y=134.0 z=0.0
cylinder 45 84.0 926.4 -1050.4 origin x=1591.3 y=-134.0 z=0.0
cylinder 46 85.6 928.0 -1052.0 origin x=1591.3 y=-134.0 z=0.0
cylinder 47 84.0 926.4 -1050.4 origin x=1591.3 y=134.0 z=0.0
cylinder 48 85.6 928.0 -1052.0 origin x=1591.3 y=134.0 z=0.0
cylinder 49 84.0 926.4 -1050.4 origin x=1937.5 y=-134.0 z=0.0
cylinder 50 85.6 928.0 -1052.0 origin x=1937.5 y=-134.0 z=0.0
cylinder 51 84.0 926.4 -1050.4 origin x=1937.5 y=134.0 z=0.0
cylinder 52 85.6 928.0 -1052.0 origin x=1937.5 y=134.0 z=0.0
cylinder 53 84.0 926.4 -1050.4 origin x=2205.5 y=-134.0 z=0.0
cylinder 54 85.6 928.0 -1052.0 origin x=2205.5 y=-134.0 z=0.0
cylinder 55 84.0 926.4 -1050.4 origin x=2205.5 y=134.0 z=0.0
cylinder 56 85.6 928.0 -1052.0 origin x=2205.5 y=134.0 z=0.0
cylinder 57 84.0 926.4 -1050.4 origin x=2473.5 y=-134.0 z=0.0
cylinder 58 85.6 928.0 -1052.0 origin x=2473.5 y=-134.0 z=0.0
cylinder 59 84.0 926.4 -1050.4 origin x=2473.5 y=134.0 z=0.0
cylinder 60 85.6 928.0 -1052.0 origin x=2473.5 y=134.0 z=0.0
cylinder 61 84.0 926.4 -1050.4 origin x=2819.7 y=-134.0 z=0.0
cylinder 62 85.6 928.0 -1052.0 origin x=2819.7 y=-134.0 z=0.0
cylinder 63 84.0 926.4 -1050.4 origin x=2819.7 y=134.0 z=0.0
cylinder 64 85.6 928.0 -1052.0 origin x=2819.7 y=134.0 z=0.0
cylinder 65 84.0 926.4 -1050.4 origin x=3087.7 y=-134.0 z=0.0
cylinder 66 85.6 928.0 -1052.0 origin x=3087.7 y=-134.0 z=0.0
cylinder 67 84.0 926.4 -1050.4 origin x=3087.7 y=134.0 z=0.0
cylinder 68 85.6 928.0 -1052.0 origin x=3087.7 y=134.0 z=0.0
cylinder 69 84.0 926.4 -1050.4 origin x=3355.7 y=-134.0 z=0.0
cylinder 70 85.6 928.0 -1052.0 origin x=3355.7 y=-134.0 z=0.0
cylinder 71 84.0 926.4 -1050.4 origin x=3355.7 y=134.0 z=0.0
cylinder 72 85.6 928.0 -1052.0 origin x=3355.7 y=134.0 z=0.0

cuboid 73 -77.5 -864.7 -350.0 -400.0 1172.0 -1072.0 origin x=0.0 y=0.0 z=0.0
cuboid 74 -1019.7 -1806.9 -350.0 -400.0 1172.0 -1072.0 origin x=0.0 y=0.0 z=0.0
cuboid 75 -38.5 -903.7 349.0 -499.0 1172.0 -1171.0 origin x=0.0 y=0.0 z=0.0
cuboid 76 -980.7 -1845.9 349.0 -499.0 1172.0 -1171.0 origin x=0.0 y=0.0 z=0.0

cuboid 77 -37.5 -904.7 350.0 -500.0 1172.0 -1172.0 origin x=0.0 y=0.0 z=0.0
cuboid 78 -979.7 -1846.9 350.0 -500.0 1172.0 -1172.0 origin x=0.0 y=0.0 z=0.0
cuboid 79 37.5 844.7 -350.0 -400.0 1172.0 -1072.0 origin x=0.0 y=0.0 z=0.0
cuboid 80 919.7 1726.9 -350.0 -400.0 1172.0 -1072.0 origin x=0.0 y=0.0 z=0.0
cuboid 81 1801.9 2609.1 -350.0 -400.0 1172.0 -1072.0 origin x=0.0 y=0.0 z=0.0
cuboid 82 2684.1 3491.3 -350.0 -400.0 1172.0 -1072.0 origin x=0.0 y=0.0 z=0.0
cuboid 83 37.5 844.7 350.0 -500.0 1172.0 -1172.0 origin x=0.0 y=0.0 z=0.0
cuboid 84 919.7 1726.9 350.0 -500.0 1172.0 -1172.0 origin x=0.0 y=0.0 z=0.0
cuboid 85 1801.9 2609.1 350.0 -500.0 1172.0 -1172.0 origin x=0.0 y=0.0 z=0.0
cuboid 86 2684.1 3491.3 350.0 -500.0 1172.0 -1172.0 origin x=0.0 y=0.0 z=0.0
cuboid 87 3566.3 -1921.9 500.0 -650.0 1322.0 -1322.0 origin x=0.0 y=0.0 z=0.0

array 1 1 place 17 17 1 -203.1 -134.0 -1052.3
media 9 1 2 -1
hole 4 origin x=-203.1 y=-134.0 z=0.0

array 1 3 place 17 17 1 -203.1 134.0 -1052.3
media 9 1 4 -3
hole 4 origin x=-203.1 y=134.0 z=0.0

array 1 5 place 17 17 1 -471.1 -134.0 -1052.3
media 9 1 6 -5
hole 4 origin x=-471.1 y=-134.0 z=0.0

array 1 7 place 17 17 1 -471.1 134.0 -1052.3
media 9 1 8 -7
hole 4 origin x=-471.1 y=134.0 z=0.0

array 1 9 place 17 17 1 -739.1 -134.0 -1052.3
media 9 1 10 -9
hole 4 origin x=-739.1 y=-134.0 z=0.0

array 1 11 place 17 17 1 -739.1 134.0 -1052.3
media 9 1 12 -11
hole 4 origin x=-739.1 y=134.0 z=0.0

array 1 13 place 17 17 1 -1145.3 -134.0 -1052.3
media 9 1 14 -13
hole 4 origin x=-1145.3 y=-134.0 z=0.0

array 1 15 place 17 17 1 -1145.3 134.0 -1052.3
media 9 1 16 -15
hole 4 origin x=-1145.3 y=134.0 z=0.0

array 1 17 place 17 17 1 -1413.3 -134.0 -1052.3
media 9 1 18 -17
hole 4 origin x=-1413.3 y=-134.0 z=0.0

array 1 19 place 17 17 1 -1413.3 134.0 -1052.3
media 9 1 20 -19
hole 4 origin x=-1413.3 y=134.0 z=0.0

array 1 21 place 17 17 1 -1681.3 -134.0 -1052.3
media 9 1 22 -21
hole 4 origin x=-1681.3 y=-134.0 z=0.0

array 1 23 place 17 17 1 -1681.3 134.0 -1052.3
media 9 1 24 -23
hole 4 origin x=-1681.3 y=134.0 z=0.0

array 1 25 place 17 17 1 173.1 -134.0 -1052.3
media 9 1 26 -25
hole 4 origin x=173.1 y=-134.0 z=0.0

array 1 27 place 17 17 1 173.1 134.0 -1052.3
media 9 1 28 -27
hole 4 origin x=173.1 y=134.0 z=0.0

array 1 29 place 17 17 1 441.1 -134.0 -1052.3
media 9 1 30 -29
hole 4 origin x=441.1 y=-134.0 z=0.0

array 1 31 place 17 17 1 441.1 134.0 -1052.3
media 9 1 32 -31
hole 4 origin x=441.1 y=134.0 z=0.0

array 1 33 place 17 17 1 709.1 -134.0 -1052.3
media 9 1 34 -33
hole 4 origin x=709.1 y=-134.0 z=0.0

array 1 35 place 17 17 1 709.1 134.0 -1052.3
media 9 1 36 -35
hole 4 origin x=709.1 y=134.0 z=0.0

array 1 37 place 17 17 1 1055.3 -134.0 -1052.3
media 9 1 38 -37
hole 4 origin x=1055.3 y=-134.0 z=0.0

array 1 39 place 17 17 1 1055.3 134.0 -1052.3
media 9 1 40 -39
hole 4 origin x=1055.3 y=134.0 z=0.0

array 1 41 place 17 17 1 1323.3 -134.0 -1052.3
media 9 1 42 -41
hole 4 origin x=1323.3 y=-134.0 z=0.0

array 1 43 place 17 17 1 1323.3 134.0 -1052.3
media 9 1 44 -43
hole 4 origin x=1323.3 y=134.0 z=0.0

array 1 45 place 17 17 1 1591.3 -134.0 -1052.3
media 9 1 46 -45
hole 4 origin x=1591.3 y=-134.0 z=0.0

array 1 47 place 17 17 1 1591.3 134.0 -1052.3
media 9 1 48 -47
hole 4 origin x=1591.3 y=134.0 z=0.0

array 1 49 place 17 17 1 1937.5 -134.0 -1052.3
media 9 1 50 -49
hole 4 origin x=1937.5 y=-134.0 z=0.0

array 1 51 place 17 17 1 1937.5 134.0 -1052.3
media 9 1 52 -51
hole 4 origin x=1937.5 y=134.0 z=0.0

array 1 53 place 17 17 1 2205.5 -134.0 -1052.3
media 9 1 54 -53
hole 4 origin x=2205.5 y=-134.0 z=0.0

array 1 55 place 17 17 1 2205.5 134.0 -1052.3
media 9 1 56 -55
hole 4 origin x=2205.5 y=134.0 z=0.0

array 1 57 place 17 17 1 2473.5 -134.0 -1052.3
media 9 1 58 -57
hole 4 origin x=2473.5 y=-134.0 z=0.0

array 1 59 place 17 17 1 2473.5 134.0 -1052.3
media 9 1 60 -59
hole 4 origin x=2473.5 y=134.0 z=0.0

array 1 61 place 17 17 1 2819.7 -134.0 -1052.3
media 9 1 62 -61
hole 4 origin x=2819.7 y=-134.0 z=0.0

array 1 63 place 17 17 1 2819.7 134.0 -1052.3
media 9 1 64 -63
hole 4 origin x=2819.7 y=134.0 z=0.0

array 1 65 place 17 17 1 3087.7 -134.0 -1052.3
media 9 1 66 -65
hole 4 origin x=3087.7 y=-134.0 z=0.0

array 1 67 place 17 17 1 3087.7 134.0 -1052.3
media 9 1 68 -67
hole 4 origin x=3087.7 y=134.0 z=0.0

array 1 69 place 17 17 1 3355.7 -134.0 -1052.3
media 9 1 70 -69
hole 4 origin x=3355.7 y=-134.0 z=0.0

array 1 71 place 17 17 1 3355.7 134.0 -1052.3
media 9 1 72 -71
hole 4 origin x=3355.7 y=134.0 z=0.0

media 12 1 73
media 12 1 74
media 12 1 79
media 12 1 80

```
media 12 1 81
media 12 1 82
media 8 1 75 -73 -2 -4 -6 -8 -10 -12
media 8 1 76 -74 -14 -16 -18 -20 -22 -24
media 9 1 77 -75 -73 -2 -4 -6 -8 -10 -12
media 9 1 78 -76 -74 -14 -16 -18 -20 -22 -24
media 11 1 83 -79 -26 -28 -30 -32 -34 -36
media 11 1 84 -80 -38 -40 -42 -44 -46 -48
media 11 1 85 -81 -50 -52 -54 -56 -58 -60
media 11 1 86 -82 -62 -64 -66 -68 -70 -72
media 12 1 87 -77 -75 -73 -2 -4 -6 -8 -10 -12 -78 -76 -74 -14 -16 -18 -20 -22 -24 -83 -79 -26 -28 -30
     -32 -34 -36 -84 -80
-38 -40 -42 -44 -46 -48 -85 -81 -50 -52 -54 -56 -58 -60 -86 -82 -62 -64 -66 -68 -70 -72

boundary 87
end geom

read array gbl=1 ara=1 typ=dodecahedral nux=33 nuy=33 nuz=462
fill
1089*2
34*2 30*1 3*2 30*1 28Q33 68*2
68*2 29*1 4*2 29*1 27Q33 68*2
34*2 30*1 3*2 30*1 28Q33 68*2
68*2 29*1 4*2 29*1 27Q33 68*2
34*2 30*1 3*2 30*1 28Q33 68*2
68*2 29*1 4*2 29*1 27Q33 68*2
34*2 30*1 3*2 30*1 28Q33 68*2
68*2 29*1 4*2 29*1 27Q33 68*2
34*2 30*1 3*2 30*1 28Q33 68*2
68*2 29*1 4*2 29*1 27Q33 68*2
34*2 30*1 3*2 30*1 28Q33 68*2
68*2 29*1 4*2 29*1 27Q33 68*2
34*2 30*1 3*2 30*1 28Q33 68*2
68*2 29*1 4*2 29*1 27Q33 68*2
34*2 30*1 3*2 30*1 28Q33 68*2
68*2 29*1 4*2 29*1 27Q33 68*2
34*2 30*1 3*2 30*1 28Q33 68*2
68*2 29*1 4*2 29*1 27Q33 68*2
34*2 30*1 3*2 30*1 28Q33 68*2
68*2 29*1 4*2 29*1 27Q33 68*2
```

34*2 30*1 3*2 30*1 28Q33 68*2

68*2 29*1 4*2 29*1 27Q33 68*2

34*2 30*1 3*2 30*1 28Q33 68*2

68*2 29*1 4*2 29*1 27Q33 68*2

34*2 30*1 3*2 30*1 28Q33 68*2

68*2 29*1 4*2 29*1 27Q33 68*2

34*2 30*1 3*2 30*1 28Q33 68*2

68*2 29*1 4*2 29*1 27Q33 68*2

34*2 30*1 3*2 30*1 28Q33 68*2

68*2 29*1 4*2 29*1 27Q33 68*2

34*2 30*1 3*2 30*1 28Q33 68*2

68*2 29*1 4*2 29*1 27Q33 68*2

34*2 30*1 3*2 30*1 28Q33 68*2

68*2 29*1 4*2 29*1 27Q33 68*2

34*2 30*1 3*2 30*1 28Q33 68*2

68*2 29*1 4*2 29*1 27Q33 68*2

34*2 30*1 3*2 30*1 28Q33 68*2

68*2 29*1 4*2 29*1 27Q33 68*2

34*2 30*1 3*2 30*1 28Q33 68*2

68*2 29*1 4*2 29*1 27Q33 68*2

34*2 30*1 3*2 30*1 28Q33 68*2

68*2 29*1 4*2 29*1 27Q33 68*2

34*2 30*1 3*2 30*1 28Q33 68*2

68*2 29*1 4*2 29*1 27Q33 68*2

34*2 30*1 3*2 30*1 28Q33 68*2

68*2 29*1 4*2 29*1 27Q33 68*2

34*2 30*1 3*2 30*1 28Q33 68*2

68*2 29*1 4*2 29*1 27Q33 68*2

34*2 30*1 3*2 30*1 28Q33 68*2

68*2 29*1 4*2 29*1 27Q33 68*2

34*2 30*1 3*2 30*1 28Q33 68*2

68*2 29*1 4*2 29*1 27Q33 68*2

34*2 30*1 3*2 30*1 28Q33 68*2

68*2 29*1 4*2 29*1 27Q33 68*2

34*2 30*1 3*2 30*1 28Q33 68*2

68*2 29*1 4*2 29*1 27Q33 68*2

34*2 30*1 3*2 30*1 28Q33 68*2

68*2 29*1 4*2 29*1 27Q33 68*2

34*2 30*1 3*2 30*1 28Q33 68*2

68*2 29*1 4*2 29*1 27Q33 68*2

34*2 30*1 3*2 30*1 28Q33 68*2
68*2 29*1 4*2 29*1 27Q33 68*2
34*2 30*1 3*2 30*1 28Q33 68*2
68*2 29*1 4*2 29*1 27Q33 68*2
34*2 30*1 3*2 30*1 28Q33 68*2
68*2 29*1 4*2 29*1 27Q33 68*2
34*2 30*1 3*2 30*1 28Q33 68*2
68*2 29*1 4*2 29*1 27Q33 68*2
34*2 30*1 3*2 30*1 28Q33 68*2
68*2 29*1 4*2 29*1 27Q33 68*2
34*2 30*1 3*2 30*1 28Q33 68*2
68*2 29*1 4*2 29*1 27Q33 68*2
34*2 30*1 3*2 30*1 28Q33 68*2
68*2 29*1 4*2 29*1 27Q33 68*2
34*2 30*1 3*2 30*1 28Q33 68*2
68*2 29*1 4*2 29*1 27Q33 68*2
34*2 30*1 3*2 30*1 28Q33 68*2
68*2 29*1 4*2 29*1 27Q33 68*2
34*2 30*1 3*2 30*1 28Q33 68*2
68*2 29*1 4*2 29*1 27Q33 68*2
34*2 30*1 3*2 30*1 28Q33 68*2
68*2 29*1 4*2 29*1 27Q33 68*2
34*2 30*1 3*2 30*1 28Q33 68*2
68*2 29*1 4*2 29*1 27Q33 68*2
34*2 30*1 3*2 30*1 28Q33 68*2
68*2 29*1 4*2 29*1 27Q33 68*2
34*2 30*1 3*2 30*1 28Q33 68*2
68*2 29*1 4*2 29*1 27Q33 68*2
34*2 30*1 3*2 30*1 28Q33 68*2
68*2 29*1 4*2 29*1 27Q33 68*2
34*2 30*1 3*2 30*1 28Q33 68*2
68*2 29*1 4*2 29*1 27Q33 68*2
34*2 30*1 3*2 30*1 28Q33 68*2
68*2 29*1 4*2 29*1 27Q33 68*2
34*2 30*1 3*2 30*1 28Q33 68*2
68*2 29*1 4*2 29*1 27Q33 68*2
34*2 30*1 3*2 30*1 28Q33 68*2
68*2 29*1 4*2 29*1 27Q33 68*2
34*2 30*1 3*2 30*1 28Q33 68*2
68*2 29*1 4*2 29*1 27Q33 68*2

34*2 30*1 3*2 30*1 28Q33 68*2

68*2 29*1 4*2 29*1 27Q33 68*2

34*2 30*1 3*2 30*1 28Q33 68*2

68*2 29*1 4*2 29*1 27Q33 68*2

34*2 30*1 3*2 30*1 28Q33 68*2

68*2 29*1 4*2 29*1 27Q33 68*2

34*2 30*1 3*2 30*1 28Q33 68*2

68*2 29*1 4*2 29*1 27Q33 68*2

34*2 30*1 3*2 30*1 28Q33 68*2

68*2 29*1 4*2 29*1 27Q33 68*2

34*2 30*1 3*2 30*1 28Q33 68*2

68*2 29*1 4*2 29*1 27Q33 68*2

34*2 30*1 3*2 30*1 28Q33 68*2

68*2 29*1 4*2 29*1 27Q33 68*2

34*2 30*1 3*2 30*1 28Q33 68*2

68*2 29*1 4*2 29*1 27Q33 68*2

34*2 30*1 3*2 30*1 28Q33 68*2

68*2 29*1 4*2 29*1 27Q33 68*2

34*2 30*1 3*2 30*1 28Q33 68*2

68*2 29*1 4*2 29*1 27Q33 68*2

34*2 30*1 3*2 30*1 28Q33 68*2

68*2 29*1 4*2 29*1 27Q33 68*2

34*2 30*1 3*2 30*1 28Q33 68*2

68*2 29*1 4*2 29*1 27Q33 68*2

34*2 30*1 3*2 30*1 28Q33 68*2

68*2 29*1 4*2 29*1 27Q33 68*2

34*2 30*1 3*2 30*1 28Q33 68*2

68*2 29*1 4*2 29*1 27Q33 68*2

34*2 30*1 3*2 30*1 28Q33 68*2

68*2 29*1 4*2 29*1 27Q33 68*2

34*2 30*1 3*2 30*1 28Q33 68*2

68*2 29*1 4*2 29*1 27Q33 68*2

34*2 30*1 3*2 30*1 28Q33 68*2

68*2 29*1 4*2 29*1 27Q33 68*2

34*2 30*1 3*2 30*1 28Q33 68*2

68*2 29*1 4*2 29*1 27Q33 68*2

34*2 30*1 3*2 30*1 28Q33 68*2

68*2 29*1 4*2 29*1 27Q33 68*2

34*2 30*1 3*2 30*1 28Q33 68*2

68*2 29*1 4*2 29*1 27Q33 68*2

34*2 30*1 3*2 30*1 28Q33 68*2
68*2 29*1 4*2 29*1 27Q33 68*2
34*2 30*1 3*2 30*1 28Q33 68*2
68*2 29*1 4*2 29*1 27Q33 68*2
34*2 30*1 3*2 30*1 28Q33 68*2
68*2 29*1 4*2 29*1 27Q33 68*2
34*2 30*1 3*2 30*1 28Q33 68*2
68*2 29*1 4*2 29*1 27Q33 68*2
34*2 30*1 3*2 30*1 28Q33 68*2
68*2 29*1 4*2 29*1 27Q33 68*2
34*2 30*1 3*2 30*1 28Q33 68*2
68*2 29*1 4*2 29*1 27Q33 68*2
34*2 30*1 3*2 30*1 28Q33 68*2
68*2 29*1 4*2 29*1 27Q33 68*2
34*2 30*1 3*2 30*1 28Q33 68*2
68*2 29*1 4*2 29*1 27Q33 68*2
34*2 30*1 3*2 30*1 28Q33 68*2
68*2 29*1 4*2 29*1 27Q33 68*2
34*2 30*1 3*2 30*1 28Q33 68*2
68*2 29*1 4*2 29*1 27Q33 68*2
34*2 30*1 3*2 30*1 28Q33 68*2
68*2 29*1 4*2 29*1 27Q33 68*2
34*2 30*1 3*2 30*1 28Q33 68*2
68*2 29*1 4*2 29*1 27Q33 68*2
34*2 30*1 3*2 30*1 28Q33 68*2
68*2 29*1 4*2 29*1 27Q33 68*2
34*2 30*1 3*2 30*1 28Q33 68*2
68*2 29*1 4*2 29*1 27Q33 68*2
34*2 30*1 3*2 30*1 28Q33 68*2
68*2 29*1 4*2 29*1 27Q33 68*2
34*2 30*1 3*2 30*1 28Q33 68*2
68*2 29*1 4*2 29*1 27Q33 68*2
34*2 30*1 3*2 30*1 28Q33 68*2
68*2 29*1 4*2 29*1 27Q33 68*2
34*2 30*1 3*2 30*1 28Q33 68*2
68*2 29*1 4*2 29*1 27Q33 68*2
34*2 30*1 3*2 30*1 28Q33 68*2
68*2 29*1 4*2 29*1 27Q33 68*2
34*2 30*1 3*2 30*1 28Q33 68*2
68*2 29*1 4*2 29*1 27Q33 68*2

34*2 30*1 3*2 30*1 28Q33 68*2
68*2 29*1 4*2 29*1 27Q33 68*2
34*2 30*1 3*2 30*1 28Q33 68*2
68*2 29*1 4*2 29*1 27Q33 68*2
34*2 30*1 3*2 30*1 28Q33 68*2
68*2 29*1 4*2 29*1 27Q33 68*2
34*2 30*1 3*2 30*1 28Q33 68*2
68*2 29*1 4*2 29*1 27Q33 68*2
34*2 30*1 3*2 30*1 28Q33 68*2
68*2 29*1 4*2 29*1 27Q33 68*2
34*2 30*1 3*2 30*1 28Q33 68*2
68*2 29*1 4*2 29*1 27Q33 68*2
34*2 30*1 3*2 30*1 28Q33 68*2
68*2 29*1 4*2 29*1 27Q33 68*2
34*2 30*1 3*2 30*1 28Q33 68*2
68*2 29*1 4*2 29*1 27Q33 68*2
34*2 30*1 3*2 30*1 28Q33 68*2
68*2 29*1 4*2 29*1 27Q33 68*2
34*2 30*1 3*2 30*1 28Q33 68*2
68*2 29*1 4*2 29*1 27Q33 68*2
34*2 30*1 3*2 30*1 28Q33 68*2
68*2 29*1 4*2 29*1 27Q33 68*2
34*2 30*1 3*2 30*1 28Q33 68*2
68*2 29*1 4*2 29*1 27Q33 68*2
34*2 30*1 3*2 30*1 28Q33 68*2
68*2 29*1 4*2 29*1 27Q33 68*2
34*2 30*1 3*2 30*1 28Q33 68*2
68*2 29*1 4*2 29*1 27Q33 68*2
34*2 30*1 3*2 30*1 28Q33 68*2
68*2 29*1 4*2 29*1 27Q33 68*2
34*2 30*1 3*2 30*1 28Q33 68*2
68*2 29*1 4*2 29*1 27Q33 68*2
34*2 30*1 3*2 30*1 28Q33 68*2
68*2 29*1 4*2 29*1 27Q33 68*2
34*2 30*1 3*2 30*1 28Q33 68*2
68*2 29*1 4*2 29*1 27Q33 68*2
34*2 30*1 3*2 30*1 28Q33 68*2
68*2 29*1 4*2 29*1 27Q33 68*2
34*2 30*1 3*2 30*1 28Q33 68*2
68*2 29*1 4*2 29*1 27Q33 68*2

34*2 30*1 3*2 30*1 28Q33 68*2
68*2 29*1 4*2 29*1 27Q33 68*2
34*2 30*1 3*2 30*1 28Q33 68*2
68*2 29*1 4*2 29*1 27Q33 68*2
34*2 30*1 3*2 30*1 28Q33 68*2
68*2 29*1 4*2 29*1 27Q33 68*2
34*2 30*1 3*2 30*1 28Q33 68*2
68*2 29*1 4*2 29*1 27Q33 68*2
34*2 30*1 3*2 30*1 28Q33 68*2
68*2 29*1 4*2 29*1 27Q33 68*2
34*2 30*1 3*2 30*1 28Q33 68*2
68*2 29*1 4*2 29*1 27Q33 68*2
34*2 30*1 3*2 30*1 28Q33 68*2
68*2 29*1 4*2 29*1 27Q33 68*2
34*2 30*1 3*2 30*1 28Q33 68*2
68*2 29*1 4*2 29*1 27Q33 68*2
34*2 30*1 3*2 30*1 28Q33 68*2
68*2 29*1 4*2 29*1 27Q33 68*2
34*2 30*1 3*2 30*1 28Q33 68*2
68*2 29*1 4*2 29*1 27Q33 68*2
34*2 30*1 3*2 30*1 28Q33 68*2
68*2 29*1 4*2 29*1 27Q33 68*2
34*2 30*1 3*2 30*1 28Q33 68*2
68*2 29*1 4*2 29*1 27Q33 68*2
34*2 30*1 3*2 30*1 28Q33 68*2
68*2 29*1 4*2 29*1 27Q33 68*2
34*2 30*1 3*2 30*1 28Q33 68*2
68*2 29*1 4*2 29*1 27Q33 68*2
34*2 30*1 3*2 30*1 28Q33 68*2
68*2 29*1 4*2 29*1 27Q33 68*2
34*2 30*1 3*2 30*1 28Q33 68*2
68*2 29*1 4*2 29*1 27Q33 68*2
34*2 30*1 3*2 30*1 28Q33 68*2
68*2 29*1 4*2 29*1 27Q33 68*2
34*2 30*1 3*2 30*1 28Q33 68*2
68*2 29*1 4*2 29*1 27Q33 68*2
34*2 30*1 3*2 30*1 28Q33 68*2
68*2 29*1 4*2 29*1 27Q33 68*2
34*2 30*1 3*2 30*1 28Q33 68*2
68*2 29*1 4*2 29*1 27Q33 68*2

34*2 30*1 3*2 30*1 28Q33 68*2
68*2 29*1 4*2 29*1 27Q33 68*2
34*2 30*1 3*2 30*1 28Q33 68*2
68*2 29*1 4*2 29*1 27Q33 68*2
34*2 30*1 3*2 30*1 28Q33 68*2
68*2 29*1 4*2 29*1 27Q33 68*2
34*2 30*1 3*2 30*1 28Q33 68*2
68*2 29*1 4*2 29*1 27Q33 68*2
34*2 30*1 3*2 30*1 28Q33 68*2
68*2 29*1 4*2 29*1 27Q33 68*2
34*2 30*1 3*2 30*1 28Q33 68*2
68*2 29*1 4*2 29*1 27Q33 68*2
34*2 30*1 3*2 30*1 28Q33 68*2
68*2 29*1 4*2 29*1 27Q33 68*2
34*2 30*1 3*2 30*1 28Q33 68*2
68*2 29*1 4*2 29*1 27Q33 68*2
34*2 30*1 3*2 30*1 28Q33 68*2
68*2 29*1 4*2 29*1 27Q33 68*2
34*2 30*1 3*2 30*1 28Q33 68*2
68*2 29*1 4*2 29*1 27Q33 68*2
34*2 30*1 3*2 30*1 28Q33 68*2
68*2 29*1 4*2 29*1 27Q33 68*2
34*2 30*1 3*2 30*1 28Q33 68*2
68*2 29*1 4*2 29*1 27Q33 68*2
34*2 30*1 3*2 30*1 28Q33 68*2
68*2 29*1 4*2 29*1 27Q33 68*2
34*2 30*1 3*2 30*1 28Q33 68*2
68*2 29*1 4*2 29*1 27Q33 68*2
34*2 30*1 3*2 30*1 28Q33 68*2
68*2 29*1 4*2 29*1 27Q33 68*2
34*2 30*1 3*2 30*1 28Q33 68*2
68*2 29*1 4*2 29*1 27Q33 68*2
34*2 30*1 3*2 30*1 28Q33 68*2
68*2 29*1 4*2 29*1 27Q33 68*2
34*2 30*1 3*2 30*1 28Q33 68*2
68*2 29*1 4*2 29*1 27Q33 68*2
34*2 30*1 3*2 30*1 28Q33 68*2
68*2 29*1 4*2 29*1 27Q33 68*2
34*2 30*1 3*2 30*1 28Q33 68*2
68*2 29*1 4*2 29*1 27Q33 68*2

34*2 30*1 3*2 30*1 28Q33 68*2
68*2 29*1 4*2 29*1 27Q33 68*2
34*2 30*1 3*2 30*1 28Q33 68*2
68*2 29*1 4*2 29*1 27Q33 68*2
34*2 30*1 3*2 30*1 28Q33 68*2
68*2 29*1 4*2 29*1 27Q33 68*2
34*2 30*1 3*2 30*1 28Q33 68*2
68*2 29*1 4*2 29*1 27Q33 68*2
34*2 30*1 3*2 30*1 28Q33 68*2
68*2 29*1 4*2 29*1 27Q33 68*2
34*2 30*1 3*2 30*1 28Q33 68*2
68*2 29*1 4*2 29*1 27Q33 68*2
34*2 30*1 3*2 30*1 28Q33 68*2
68*2 29*1 4*2 29*1 27Q33 68*2
34*2 30*1 3*2 30*1 28Q33 68*2
68*2 29*1 4*2 29*1 27Q33 68*2
34*2 30*1 3*2 30*1 28Q33 68*2
68*2 29*1 4*2 29*1 27Q33 68*2
34*2 30*1 3*2 30*1 28Q33 68*2
68*2 29*1 4*2 29*1 27Q33 68*2
34*2 30*1 3*2 30*1 28Q33 68*2
68*2 29*1 4*2 29*1 27Q33 68*2
34*2 30*1 3*2 30*1 28Q33 68*2
68*2 29*1 4*2 29*1 27Q33 68*2
34*2 30*1 3*2 30*1 28Q33 68*2
68*2 29*1 4*2 29*1 27Q33 68*2
34*2 30*1 3*2 30*1 28Q33 68*2
68*2 29*1 4*2 29*1 27Q33 68*2
34*2 30*1 3*2 30*1 28Q33 68*2
68*2 29*1 4*2 29*1 27Q33 68*2
34*2 30*1 3*2 30*1 28Q33 68*2
68*2 29*1 4*2 29*1 27Q33 68*2
34*2 30*1 3*2 30*1 28Q33 68*2
68*2 29*1 4*2 29*1 27Q33 68*2
34*2 30*1 3*2 30*1 28Q33 68*2
68*2 29*1 4*2 29*1 27Q33 68*2
34*2 30*1 3*2 30*1 28Q33 68*2
68*2 29*1 4*2 29*1 27Q33 68*2
34*2 30*1 3*2 30*1 28Q33 68*2
68*2 29*1 4*2 29*1 27Q33 68*2

34*2 30*1 3*2 30*1 28Q33 68*2
68*2 29*1 4*2 29*1 27Q33 68*2
34*2 30*1 3*2 30*1 28Q33 68*2
68*2 29*1 4*2 29*1 27Q33 68*2
34*2 30*1 3*2 30*1 28Q33 68*2
68*2 29*1 4*2 29*1 27Q33 68*2
34*2 30*1 3*2 30*1 28Q33 68*2
68*2 29*1 4*2 29*1 27Q33 68*2
34*2 30*1 3*2 30*1 28Q33 68*2
68*2 29*1 4*2 29*1 27Q33 68*2
34*2 30*1 3*2 30*1 28Q33 68*2
68*2 29*1 4*2 29*1 27Q33 68*2
34*2 30*1 3*2 30*1 28Q33 68*2
68*2 29*1 4*2 29*1 27Q33 68*2
34*2 30*1 3*2 30*1 28Q33 68*2
68*2 29*1 4*2 29*1 27Q33 68*2
34*2 30*1 3*2 30*1 28Q33 68*2
68*2 29*1 4*2 29*1 27Q33 68*2
34*2 30*1 3*2 30*1 28Q33 68*2
68*2 29*1 4*2 29*1 27Q33 68*2
34*2 30*1 3*2 30*1 28Q33 68*2
68*2 29*1 4*2 29*1 27Q33 68*2
34*2 30*1 3*2 30*1 28Q33 68*2
68*2 29*1 4*2 29*1 27Q33 68*2
34*2 30*1 3*2 30*1 28Q33 68*2
68*2 29*1 4*2 29*1 27Q33 68*2
34*2 30*1 3*2 30*1 28Q33 68*2
68*2 29*1 4*2 29*1 27Q33 68*2
34*2 30*1 3*2 30*1 28Q33 68*2
68*2 29*1 4*2 29*1 27Q33 68*2
34*2 30*1 3*2 30*1 28Q33 68*2
68*2 29*1 4*2 29*1 27Q33 68*2
34*2 30*1 3*2 30*1 28Q33 68*2
68*2 29*1 4*2 29*1 27Q33 68*2
34*2 30*1 3*2 30*1 28Q33 68*2
68*2 29*1 4*2 29*1 27Q33 68*2
34*2 30*1 3*2 30*1 28Q33 68*2
68*2 29*1 4*2 29*1 27Q33 68*2
34*2 30*1 3*2 30*1 28Q33 68*2
68*2 29*1 4*2 29*1 27Q33 68*2

34*2 30*1 3*2 30*1 28Q33 68*2
68*2 29*1 4*2 29*1 27Q33 68*2
34*2 30*1 3*2 30*1 28Q33 68*2
68*2 29*1 4*2 29*1 27Q33 68*2
34*2 30*1 3*2 30*1 28Q33 68*2
68*2 29*1 4*2 29*1 27Q33 68*2
34*2 30*1 3*2 30*1 28Q33 68*2
68*2 29*1 4*2 29*1 27Q33 68*2
34*2 30*1 3*2 30*1 28Q33 68*2
68*2 29*1 4*2 29*1 27Q33 68*2
34*2 30*1 3*2 30*1 28Q33 68*2
68*2 29*1 4*2 29*1 27Q33 68*2
34*2 30*1 3*2 30*1 28Q33 68*2
68*2 29*1 4*2 29*1 27Q33 68*2
34*2 30*1 3*2 30*1 28Q33 68*2
68*2 29*1 4*2 29*1 27Q33 68*2
34*2 30*1 3*2 30*1 28Q33 68*2
68*2 29*1 4*2 29*1 27Q33 68*2
34*2 30*1 3*2 30*1 28Q33 68*2
68*2 29*1 4*2 29*1 27Q33 68*2
34*2 30*1 3*2 30*1 28Q33 68*2
68*2 29*1 4*2 29*1 27Q33 68*2
34*2 30*1 3*2 30*1 28Q33 68*2
68*2 29*1 4*2 29*1 27Q33 68*2
34*2 30*1 3*2 30*1 28Q33 68*2
68*2 29*1 4*2 29*1 27Q33 68*2
34*2 30*1 3*2 30*1 28Q33 68*2
68*2 29*1 4*2 29*1 27Q33 68*2
34*2 30*1 3*2 30*1 28Q33 68*2
68*2 29*1 4*2 29*1 27Q33 68*2
34*2 30*1 3*2 30*1 28Q33 68*2
68*2 29*1 4*2 29*1 27Q33 68*2
34*2 30*1 3*2 30*1 28Q33 68*2
68*2 29*1 4*2 29*1 27Q33 68*2
34*2 30*1 3*2 30*1 28Q33 68*2
68*2 29*1 4*2 29*1 27Q33 68*2
34*2 30*1 3*2 30*1 28Q33 68*2
68*2 29*1 4*2 29*1 27Q33 68*2
34*2 30*1 3*2 30*1 28Q33 68*2
68*2 29*1 4*2 29*1 27Q33 68*2

34*2 30*1 3*2 30*1 28Q33 68*2
68*2 29*1 4*2 29*1 27Q33 68*2
34*2 30*1 3*2 30*1 28Q33 68*2
68*2 29*1 4*2 29*1 27Q33 68*2
34*2 30*1 3*2 30*1 28Q33 68*2
68*2 29*1 4*2 29*1 27Q33 68*2
34*2 30*1 3*2 30*1 28Q33 68*2
68*2 29*1 4*2 29*1 27Q33 68*2
34*2 30*1 3*2 30*1 28Q33 68*2
68*2 29*1 4*2 29*1 27Q33 68*2
34*2 30*1 3*2 30*1 28Q33 68*2
68*2 29*1 4*2 29*1 27Q33 68*2
34*2 30*1 3*2 30*1 28Q33 68*2
68*2 29*1 4*2 29*1 27Q33 68*2
34*2 30*1 3*2 30*1 28Q33 68*2
68*2 29*1 4*2 29*1 27Q33 68*2
34*2 30*1 3*2 30*1 28Q33 68*2
68*2 29*1 4*2 29*1 27Q33 68*2
34*2 30*1 3*2 30*1 28Q33 68*2
68*2 29*1 4*2 29*1 27Q33 68*2
34*2 30*1 3*2 30*1 28Q33 68*2
68*2 29*1 4*2 29*1 27Q33 68*2
34*2 30*1 3*2 30*1 28Q33 68*2
68*2 29*1 4*2 29*1 27Q33 68*2
34*2 30*1 3*2 30*1 28Q33 68*2
68*2 29*1 4*2 29*1 27Q33 68*2
34*2 30*1 3*2 30*1 28Q33 68*2
68*2 29*1 4*2 29*1 27Q33 68*2
34*2 30*1 3*2 30*1 28Q33 68*2
68*2 29*1 4*2 29*1 27Q33 68*2
34*2 30*1 3*2 30*1 28Q33 68*2
68*2 29*1 4*2 29*1 27Q33 68*2
34*2 30*1 3*2 30*1 28Q33 68*2
68*2 29*1 4*2 29*1 27Q33 68*2
34*2 30*1 3*2 30*1 28Q33 68*2
68*2 29*1 4*2 29*1 27Q33 68*2
34*2 30*1 3*2 30*1 28Q33 68*2
68*2 29*1 4*2 29*1 27Q33 68*2
34*2 30*1 3*2 30*1 28Q33 68*2
68*2 29*1 4*2 29*1 27Q33 68*2

```
1089*2
end fill
end array

read bounds
  xfc=white
  zfc=white
  yfc=white
end bounds

read start
  nst=1 xsm=3491.3 xsp=-1846.9 ysm=350.0 ysp=-500.0 zsm=1172.0 zsp=-1172.0
end start

read plot
  lpi= 10 scr=yes
  ttl='Sphere Storage System, at elevation z=-300.0'
  xul=-1922.0 yul=501.0 zul=-300.0
  xlr=3567.0 ylr=-651.0 zlr=-300.0
  uax=1 vdn=-1
  pic=mat nax=10000
  end plt0

  lpi= 10 scr=yes
  ttl='Sphere Storage System, cross-section at Y=-134.0'
  xul=-1922.0 yul=-134.0 zul=1333.0
  xlr=3567.0 ylr=-134.0 zlr=-1333.0
  uax=1 wdn=-1
  pic=mat nax=10000
  end plt1

  lpi= 10 scr=yes
  ttl='Sphere Storage System, cross-section at x=-203.1'
  xul=-203.1 yul=-651.0 zul=1333.0
  xlr=-203.1 ylr=501.0 zlr=-1333.0
  vax=1 wdn=-1
  pic=mat nax=10000
  end plt2

  lpi= 10 scr=yes
```

```
 ttl='Sphere Storage System, at elevation z=750.0'
 xul=-1922.0 yul=501.0 zul=750.0
 xlr=3567.0 ylr=-651.0 zlr=750.0
 uax=1 vdn=-1
 pic=mat nax=10000
 end plt3

 lpi= 10 scr=yes
 ttl='Sphere Storage System, at elevation z=801.0'
 xul=-1922.0 yul=501.0 zul=801.0
 xlr=3567.0 ylr=-651.0 zlr=801.0
 uax=1 vdn=-1
 pic=mat nax=10000
 end plt4

 lpi= 10 scr=yes
 ttl='Sphere Storage System, cross-section at x=173.1'
 xul=173.1 yul=-651.0 zul=1333.0
 xlr=173.1 ylr=501.0 zlr=-1333.0
 vax=1 wdn=-1
 pic=mat nax=10000

 end plt5

end plot

end data

end
```